ADDIS ABABA UNIVERSITY
ADDIS ABABA INSTITUTE OF TECHNOLOGY
SCHOOL OF ELECTRICAL AND COMPUTER ENGINEERING

Analysis of the functional variation of cascaded amplifier when replaced with their spintronics equivalents

A thesis Submitted to Addis Ababa Institute of Technology, School of Graduate Studies, Addis Ababa University

In Partial Fulfillment of the Requirement for the Degree of Masters of Science in Electrical Engineering (microelectronics Engineering)

Student name: Ermias Tewabe

Advisor: Dr. Getachew Alemu

Date: July 2019

Addis Ababa, Ethiopia

ADDIS ABABA UNIVERSITY
ADDIS ABABA INSTITUTE OF TECHNOLOGY
SCHOOL OF ELECTRICAL AND COMPUTER ENGINEERING

Analysis of the functional variation of cascaded amplifier when replaced with their spintronics equivalents

By

Ermias Tewabe

APPROVED BY BOARD OF EXAMINERS

____________________ __________________

Chairman Signature

Dr. Getachew Alemu __________________

Advisor Signature

____________________ __________________

Internal Examiner Signature

____________________ __________________

External Examiner Signature

Declaration

I, the undersigned, declare that this thesis is my original work, has not been presented for a degree in this or other universities, all sources of materials used for this thesis work have been fully acknowledged.

Name: Ermias Tewabe
Signature: _______________

Place: Addis Ababa Institute of Technology (AAiT), Addis Ababa University, Addis Ababa, Ethiopia.
Date: _______________

This thesis has been submitted for examination with my approval as a university advisor.

Advisor: Dr. Getachew Alemu

Signature: _________________

Date: ___________________

Acknowledgments

I would like to thank my advisor, Dr. Getachew Alemu, for his constant support and encouragement. Even though this thesis has been continually expanded and updated from what had been expected to do initially, the idea of spintronics was first initiated by him. Last but not least, I really also appreciate instructors and friends in microelectronics stream.

Abstract

Spintronics is a new technology that employs the spin degrees of freedom of carriers instead of electrons' charge for storing and processing data. Either by using spins alone or by adding the spin degrees of freedom to the more established semiconductor technology, it is possible to enhance the functionality of the device greatly.

In this thesis, two major things have been done. In part one, after studying literature reviews which were done on spin transistors, magnetic bipolar transistor models are proposed, Three quite different magnetic bipolar transistors are developed by incorporating magnetic impurities in all three regions. And the energy band edges of semiconductor device in the presence of magnetic impurities are calculated. In part two, the proposed spin transistors models are validated by employing on some application areas (Cascaded amplifier). The performances of magnetic bipolar transistors (i.e., using one of the models of spin transistors and the proposed ones) for multistage amplifiers are analyzed. In order to simplify the equivalent circuit for AC analysis, simplified re model for low frequency is used. And hybrid-π model is used for high frequency. Since each parameters in re model and hybrid-π model are function of spin polarization of carriers, the equivalent circuit models used in this thesis work quite well for spin based transistor.

In this thesis it is able to come up with quite different types of magnetic bipolar transistors in which spin of carriers are the main controlling inputs. It is shown that the device's parameters are function of the spin of electrons and holes, and the injected spin electrons in the emitter and collector. Contrary to the conventional bipolar transistor, the magnetic bipolar transistor models are capable of controlling current amplification factor and the density of minority of carries through spins of electrons and holes. As a result, the performances of cascaded amplifier are improved compared to the performances of the conventional transistor.

Keywords: spin transistor, spin, polarization of electron, magnetic bipolar transistor

Table of Contents

Contents

List of Figures

List of Tables

List of Abbreviations and symbols

2DEG	2 Dimension electron
3D	Three Dimensional
AC	Alternating Current
AF	Antiferromagnet
AMR	Anisotropic magnetoresistance effect
$Cd_{0.95}Mn_{0.05}Se$	Compound of cadmium, manganese and selenium
CrO_2	Chromium oxide
DMS	Dilute magnetic semiconductor
DOS	Density of states
FM1	Source ferromagnetic electrode
FM2	drain ferromagnetic electrode
GMR	Giant magnetoresistance
LnSb	Indium antimonida
MBT	Magnetic bipolar transistor
MFET	magnetic field effect transistor
MgO	magnesium oxide
MM	Magnetic metal
MRAM	magnetic random access memory
NM	non-ferromagnetic
SFET	spin field effect transistor
Spin-FET	spin field effect transistor
ZnO	Zinc oxide

Chapter One

Introduction

1.1 Background

During the last 50 years, the world saw a significant revolution on a digital logic of electronics from the earliest transistors to the powerful microprocessor in desktop computers. Most electronic devices have used circuits that represent data as binary digits represented by the presence or absence of electric charge [1]. The uses of transistors have grown since its invention in December 1947, into a multibillion dollar market. Life today is dependent on heavily on the capability of a few million transistors to process and to store data [2]. It is clear that an integrated circuit contain around one billion transistors, each smaller than 100nm in size, i.e., a five hundred times smaller than the diameter of a human hair. At the outset of the 21st century, the crossing of this symbolic 100 nm threshold ushered the era of nanotechnology [3], [4], [5].

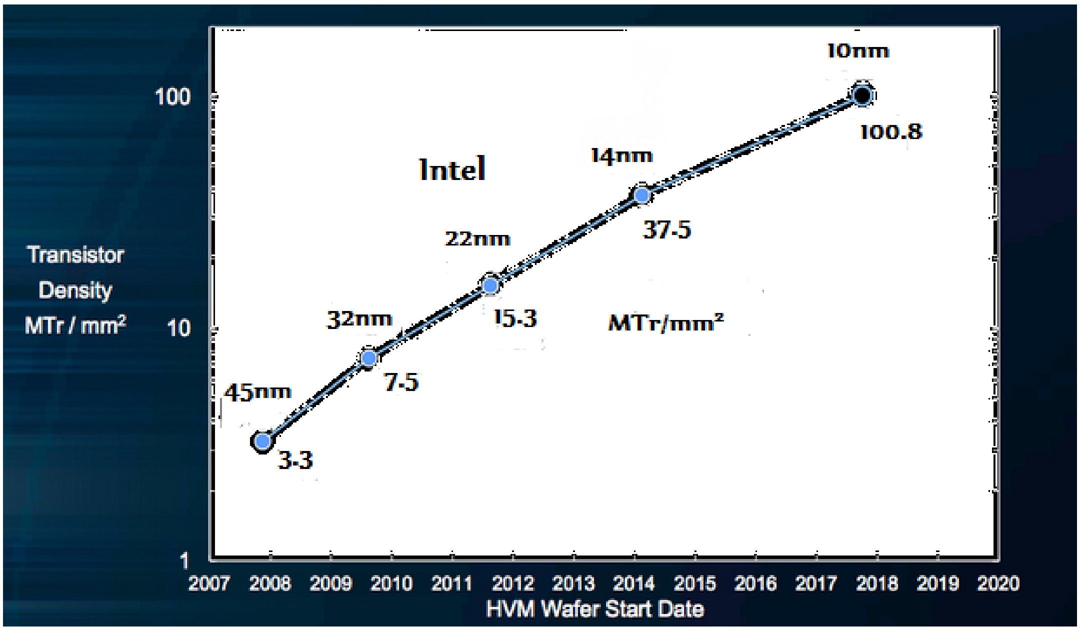

Figure 1.1: (Image: Intel) Ten years ago, the state-of-the-art for Intel was 3.3 million transistors per square millimeter [30].

The miniaturization of devices has led to more reliable, less bulky and high speed performance devices. Moore predicted the relentless progress of micro-electronics by his popular law which state that microprocessors will double in power every 18 months as electronic devices shrink and more logic is packed into every chip (shown in Figure 1.1) [1], [6].

Due to the miniaturization of semiconductor devices, the integrated circuits' computational power shows rapid decrease and decrease in speed. As the channel length continues on reducing, the downsizing of the channel length has become the main challenge. In the future, it is expected the gate length to be 5nm. As a result leakage current will be too high for the whole chip. From this trend, it looks that Moor's law is running out of momentum. But, due to constantly introduction of innovative changes in technological processes, the miniaturization of devices continues and Moor's law successfully continues. This is because the problems associated with miniaturization are reduced. [2], [4].

One of the solutions to circumvent these limitations is the modification of the existing structure that will help in extending their scalability. For instance, using double gate instead of single gate in conventional MOSFET in which the additional gate is used to control channel potential gate bias [2], [6]. The other alternative is to use new materials and technologies to replace the existing silicon based technologies. For instance, nanowires, Carbon nanotube transistor, single electron tunneling (SET) and graphene nanotube transistors are proposed to replace the silicon MOSFET [7]. There are a number of ways to minimize the off chip power by using such as double gate-metal oxide semiconductor field effect transistor (DG-MOSFET), fin-field effect transistor (fin-FET) and Si-nanowire MOSFET. Dual material surrounding gate (DMG) is also another technique to improve the carrier transport efficiency. Carbon nanotube field effect transistor (CNTFET) is another approach in nanodevice which has higher performance and lower power consumption. However the problem with all the aforementioned techniques is volatility [2].

But it is well understood that miniaturization of the size of semiconductor devices will reach a fundamental barrier. The fundamental physical laws of semiconductor electronics prevent them further reduction of sizes. But researchers and scientists noted that the miniaturization of devices has the concept of quantum mechanics which was developed in the last century-where ideas such as wave like behavior is more pronounced for electrons. And electron spin is a quantum phenomenon. As result many expert agree that spintronics with combined nanotechnology will minimize the challenges related with miniaturization [1]. Developing a novel device based on spin of electron is also an alternative way to solve the limitations of using silicon based devices. Developing new spin based devices or spin based devices which can work in coordination with the existing silicon based devices, will enhance the device performance, and will also serve as an additional controlling input mechanism.

In summary, in order to keep up with this continuing miniaturization, it is appropriate to

come up with devices based on the quantum properties of the electron. In short, for this reason and intending to enhance the multi-functionality of devices, researchers came up with another property of electron known as spin [1], [2], [6].

1.2 Basic spin electronics concepts

Spin electronics devices are based on the quantum properties of electrons whose characteristics are basically determined by the spin of the electrons in the atom in contrary to the conventional semiconductor electronics devices whose characteristics are dependent on the charge of electrons. The gradual development of spin electronics' technology from 1985 onwards is presented in Table 1.1.

	Lateral spin transport devices	*Semiconductor spintronics*	*Metallic magnetic multilayers*
-1985	*Spin injection into metals*		
1985 – 1990			*Interlayer exchange coupling(IEC)* *Giant Magnetoresistance(GMR)*
1990 – 1995		*Ferromagnetism in dilute magnetic semiconductor*	*Tunneling magnetoresistance(TMR)*
1995 -2000	*Carbon nanotube spin valve*	*Long spin coherence in semiconductors* *Spin injection into semiconductors*	*Hard drive based on GMR* *Spin torque*
2000 – 2005	*Lateral metal spin valve and spin precession* *Electrostatic gate control of spin transport*	*Electrical control of magnetism* *Spin hall effect in semiconductors*	*Enhanced spin injection via MgO barriers*
2005 -2010	*Spin hall effect in metals* *Spin Hall effect detected at room temperature.*	*Hanle effect in semiconductor spin valve*	*MRAM based on TMR* *Magnetic Superatoms*
2010-2015	*Graphene-based Spintronics switch*		
2015-2019		*Low-current solid-state spintronic device* *Graphene-based room-temperature spin field-effect transistor*	

Table 1.1: Timeline [10],[45]

In the fundamental spin electronics structure proposed by Datta, S., and B. Das, in 1990 [11], spin FET is sandwiched between two ferromagnetic materials as shown in the Figure 1.2.

Contrary to the conventional field effect transistor, the source and drain in spin FET is ferromagnetic material. The drain current reaches maximum value when the spin orientation is parallel to the magnetization of electrodes and injection.

Material which exhibits unique magnetic behavior known as ferromagnetic material. Iron, nickel and cobalt are some of known good examples. Ferromagnetic materials exhibit a long-range ordering phenomenon at the atomic level which causes the unpaired electron spins to line up parallel with each other in a region called a domain. A small external imposed magnetic field can cause the magnetic domains to line up with each other and the material is said to magnetized. Semiconductor material is neither a good conductor nor a good insulator. The conductivity of those elements with four valence electrons in the carbon group is not as good as the conductors but still better than the insulators, and they are given the name semiconductors [9], [11], [13] .

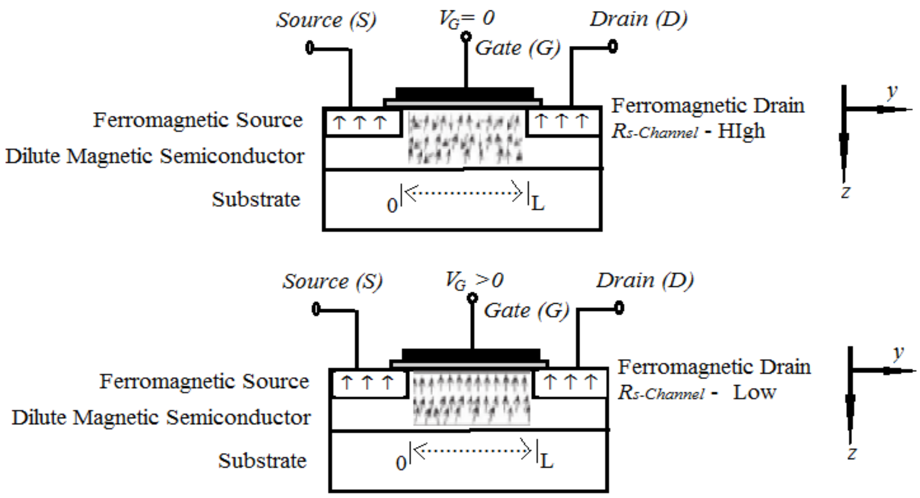

Figure 1.2: Schematic representation of the spin field effect transistor [12]

When the gate terminal voltage applies, the electric field induces Rashba spin-orbit interaction. And this interaction controls the spin polarized s electrons which shown is in Figure 1.3a. Figure 1.3b illustrates the situation when the gate voltage is zero [6], [9].

1.3 Giant Magnetoresistance

GMR refers to a large change in resistance (typically 10 to 20%) when the devices are subjected to a magnetic field, compared with a maximum sensitivity of a few percent for other types of magnetic sensors. When the magnetic moments of the ferromagnetic layers are parallel, the spin dependent scattering of carriers is minimized, and the material has its lowest resistance. When the ferromagnetic layers are anti-aligned, the spin-dependent scattering of the carriers is maximized, and the material has its highest resistance. Before Giant Magnetoresistance (GMR) came into existence, there was an effect called Aniso-magnetoresistance effect (AMR). In 1857, the British physicist Lord Kelvin reported “that iron, when subjected to a magnetic force, acquire an increase resistance to the conduction of electricity along and a diminution of resistance to the conduction of electricity across, the line of magnetization” this effect was known as Anisotropic magnetoresistance (AMR). AMR can be used to detect changes of magnetization, and it was a basis of hard drive read sensors before GMR invention. But, the magnitude of AMR effect is small [2], [5], [13], [14].

The "giant magnetoresistive" (GMR) effect was discovered in the late 1980s by two European scientists working independently: Peter Gruenberg of the KFA research institute in Julich, Germany, and Albert Fert of the University of Paris-Sud. They saw very large resistance changes 6 percent and 50 percent, respectively in materials comprised of alternating very thin layers of various metallic elements. Figure 1.3 shows the implementation of GMR as a read head in storage media [2], [6], [10].

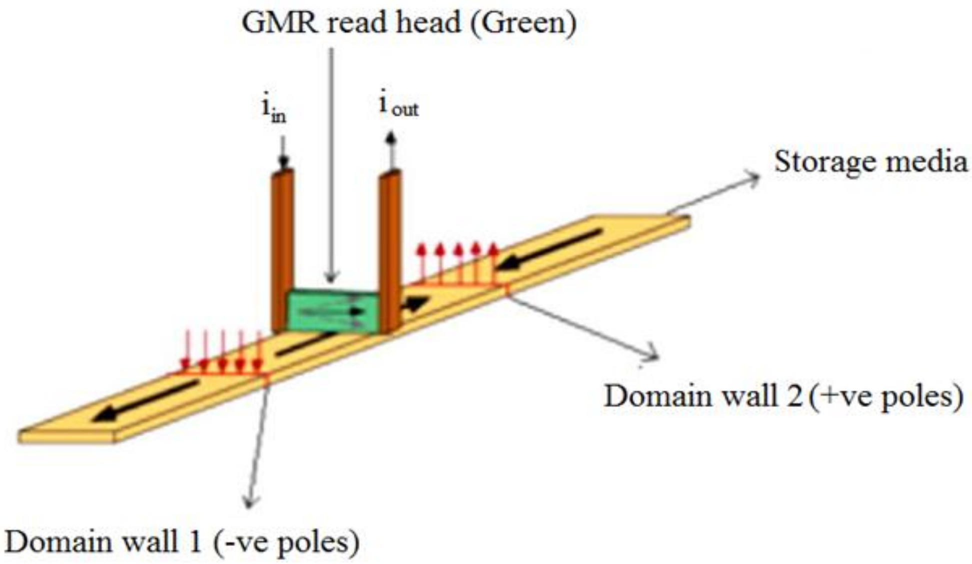

Figure 1.3: A schematic representation of GMR read head that passes over the storage media [2]

1.4 Half Metal

The efficiency of the magnetoelectronic effect is more pronounced as the density of states are more spin polarized (i.e., the more N↑ deviate from N↓) at the Fermi energy (Figure 1.4).

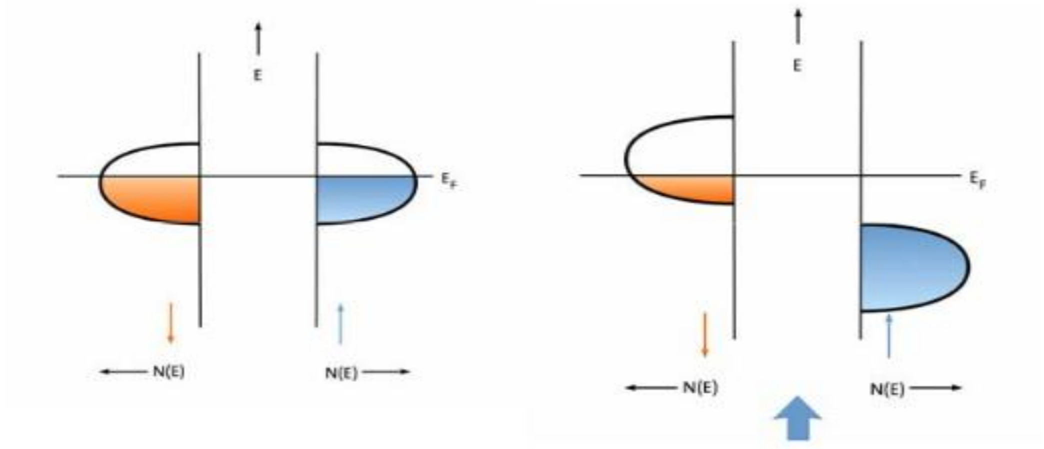

Figure 1.4: Schematic illustration of the density of states for non-magnetic (Left) and ferromagnetic CrO2 (right) [15]

As it can be seen in the figure 1.4, for the ferromagnetic case (right), the spin down electrons (orange) are placed in a metallic band, while the spin up electrons (blue) Show an electronic structure that is typical for an insulator. The net spin polarization shown by a thick blue arrow [15], [19].

1.5 Spin Polarization

Theoretically, spin polarization can be calculated by the following relation [25],

$$P_n = s/n = (n\uparrow - n\downarrow)/(n\uparrow + n\downarrow) \quad (1.1)$$

Where $n\uparrow$ is spin up electron and $n\downarrow$ is spin down electron

The energy level diagram for spin up and spin down of normal metal and ferromagnetic material is depicted in Figure 1.5. Since the spin up and spin down electrons in the normal metal are non-magnetic material equal, their energy state will remain equal and lie above the Fermi energy level (shown in Figure 1.5a). When either of spins completely dominates, their energy states will lie above and below the Fermi energy level as shown respectively in Figure 1.5b and Figure 1.5c.

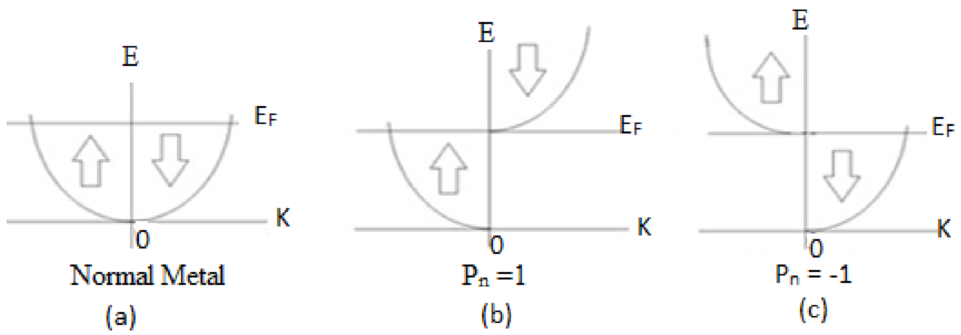

Figure 1.5: Energy level (E-K) diagram using SW model [2]

If $n\downarrow = 0$; $P_n = 1$ in this case spin polarization is 100% because only majority spins are dominant which is depicted in Figure 1.5. Such material referred to as ferromagnetic half metal or Heusler alloys. If $n\uparrow = 0$; $P_n = -1$, if $n\uparrow=n\downarrow$; $P_n = 0$ (only for paramagnetic or normal metal) [2].

Using Stoner-Wohlfarth (SW), the model of ferromagnet is shown in Figure 1.6. When the spin up and spin down present as majority and minority in specific material, the trends of energy of states is shown in Figure 1.6a and Figure 1.6b respectively. While Figure 1.6c shows a half metal in which either of the spins dominates completely.

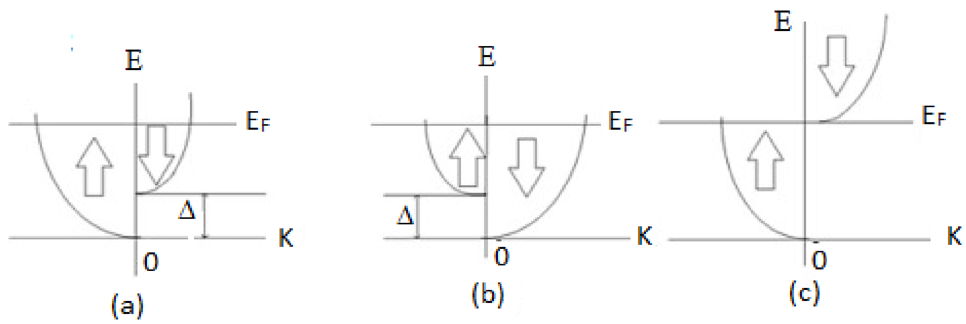

Figure 1.6: E-K diagram for ferromagnet and half metal at absolute 0 K. [2]

Source ferromagnetic electrode (FM1) polarized the injected electrons, and the polarized electron drain into the semiconductor channel. The electric field is applied perpendicularly by gate voltage as the spin polarized current flowing in the channel. 2-Dimension electron gas (2DEG) is created by the current in the semiconductor; as a result spin precession occurs. The spin orbit modulation is modulated by gate induced electric field, transforming into an effective magnetic field (the Rashba mechanism). The length of the channel, the material of the semiconductor and the gate voltage affects the spin orientation of the arriving electrons. Depending on the orientation of FM2 (drain) magnetization, the spin orientation will either parallel or antiparallel to the source electrode [2], [11], [13].

1.6 Ferromagnetic Semiconductor

Ferromagnetic semiconductors are noted for their potential advantage in integrating additional functionality to the semiconductor device by employing spin degree of freedom. Recently, it is noted for successful doping of iron in semiconductor which shows ferromagnetism at room temperature. Ferromagnetic semiconductor can be used in application areas such as spin transistor [20].

A dilute magnetic semiconductor (DMS) is a semiconductor alloy in which a small amount of (less than 10%) magnetic ion is doped to non-magnetic semiconductor materials. The first magnetic was introduced in III-V DMS, but they are working below 200K temperature [20], [21], [22], [23], [24].

1.7 Spin Injection

Electrical spin injection is an excellent way of generating non-equilibrium spin in non-magnetic material. When current flows from ferromagnetic material to metal, non-equilibrium spin will develop as a result of spin polarized carriers presence in ferromagnetic region as shown in Figure 1.7 [25].

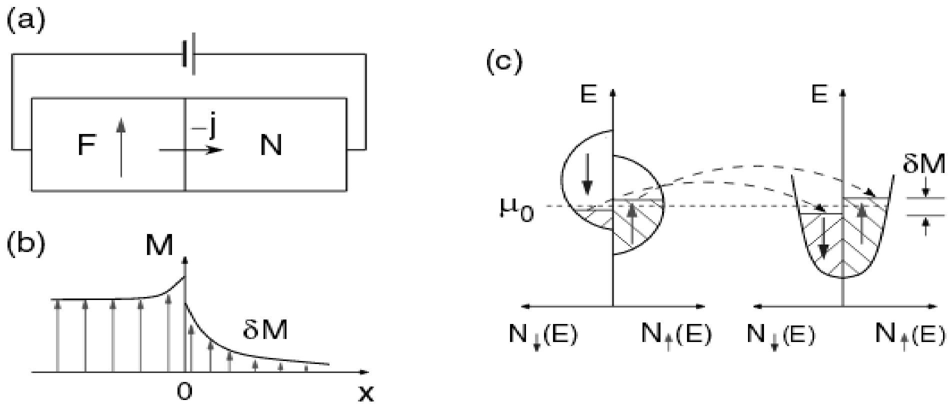

Figure 1.7: Pedagogical illustration of the concept of electrical spin injection from a ferromagnet (F) into a normal metal (N). [25]

Figure 1.7a shows the schematic device geometry in which it depicts the possibility of spin injection from ferromagnetic material to normal, and the intensity of injected spin carriers into normal metal is reach highest at the proximity of the junction which is shown in Figure 1.7b. The energy of states in the normal metal and the ferromagnetic material is clearly shown in Figure 1.7c.

Aronov and Pikus are the first to propose the idea of creating non-equilibrium electrons spins in semiconductor by passing a current through a ferromagnetic contact. The process of spin polarized electrons injecting from ferromagnet to non-magnetic semiconductor was the main challenge. The conductivity mismatch between metallic ferromagnetic and the semiconductor was another challenge [6], [10], [26].

1.8 Statement of the problem

The reduction of the size of transistor in the integrated circuit helps the device to be Compact, more efficient, and help to have better speed. But the continuing reduction of the size of the transistor is more problematic as heat make devices to perform inefficiently; in addition, leakage current is another concern when devices compacted together in a chip. Last but not least, quantum effect will interfere with normal operation as the miniaturization of devices continues. As a result, there is a need to develop a mechanism as a way out of this deadlock. Hence spintronics devices are the best choice to circumvent these pitfalls. The beginning of this long journey can be start by incorporating spins of carriers into the conventional devices namely transistors. In order to alleviate the problem at hand, researchers have been conducting researches on spintronics for the last few decades. Even though the researches which have been carried out in the spin based bipolar transistor are few, there are researches which need further study which have not been covered by earlier researchers. Besides, the developed spin based models haven't been validated fully by analyizing the performances of the parameters of a device. Indirectly, up to now; the performances of the developed spin based devices have not been anlayzed by applying on some application areas.

1.9 Objectives

1.9.1 General Objective

The general objective of this thesis is to investigate the functional variation of cascaded amplifier when replaced with spin cascaded amplifier.

1.9.2 Specific objectives

- To study spin transistor
- To model magnetic bipolar transistor models
- To calculate the perturbed energy due to the interaction between the spin of magnetic impurities and spin of carriers
- To validate the proposed models by applying on spin cascaded amplifier.
- To compare and contrast spin cascaded amplifier and conventional one using the outcome
- To obtain the calculated parameters of the magnetic bipolar transistors and cascaded amplifier
- To simulate the output response of the cascaded amplifier.

1.10 Methodology

The methodologies used to carry out the thesis are:

- Studying different literature reviews on spin transistors.
- Performing a mathematical modelling of magnetic bipolar transistors
- Applying the proposed transistor model on some application areas (multistage amplifiers)
- Obtain the calculated parameters as function of polarization of carriers using MATLAB software.
- Simulate the output responses of performances of cascaded amplifier using LTspice software.

The flow chart which shows the methodologies used in this thesis is shown in Figure 1.8.

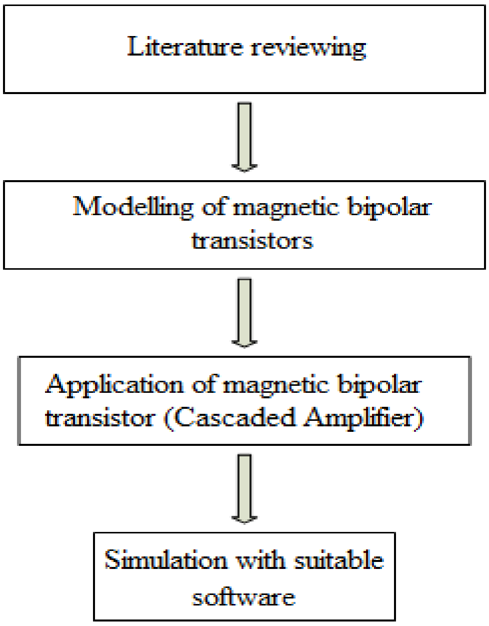

Figure 1.8: Methodologies employed for this thesis

1.11 Scope of the Thesis and Limitation

1.11.1 Scope of the Thesis

This thesis examined the potential advantages of one of the spin transistors with respect to conventional transistors. Spin transistor model is proposed and this spin transistor is applied on some application areas. Different parameters of spin based multistage amplifier are evaluated. The output response of different parameters is done by using by different electrical software.

1.11.2 Limitation

In this thesis, it is a bit difficult to obtain enough reference which have done on magnetic bipolar transistors

1.12 Contribution of the Thesis

Spintronics is a new technology and its development in device level are still in its infant stage, and hence researches have been undergoing more or less in theoretical level. The development of magnetic bipolar transistor will add additional controlling mechanism to the existing conventional device. In addition, the increased amount of output attributed to spin will be beneficial in some application areas.

1.13 Thesis Organization

In Chapter One, brief introduction of spintronics is done. Giant magnetoresistance (GMR), spin valve and the like are also included, and this chapter comprises also an overview of the work to be done in this thesis. In Chapter Two, literature review is discussed briefly. Chapter Three presents the proposed spin transistor's models. In addition, application of spin transistor is done on multistage amplifier. Chapter four presents all the result of output response of the different parameters which was carried out using different electrical software. Besides, all relevant discussion pertinent to the obtained result is done. Chapter five discusses the conclusion and recommended future works.

Chapter Two

Literature Review

A research which was done on spin transistor is a magnetic field effect transistor (MFET) by R. N. Gurzhi et al. shown in Figure 2.1. They proposed a magnetic field effect transistor that exhibit a giant negative magnetoresistance by generating spin polarized current. The device consists of a nonmagnetic conductive channel (wire or strip) sandwiched by a grounded magnetic shell [27].

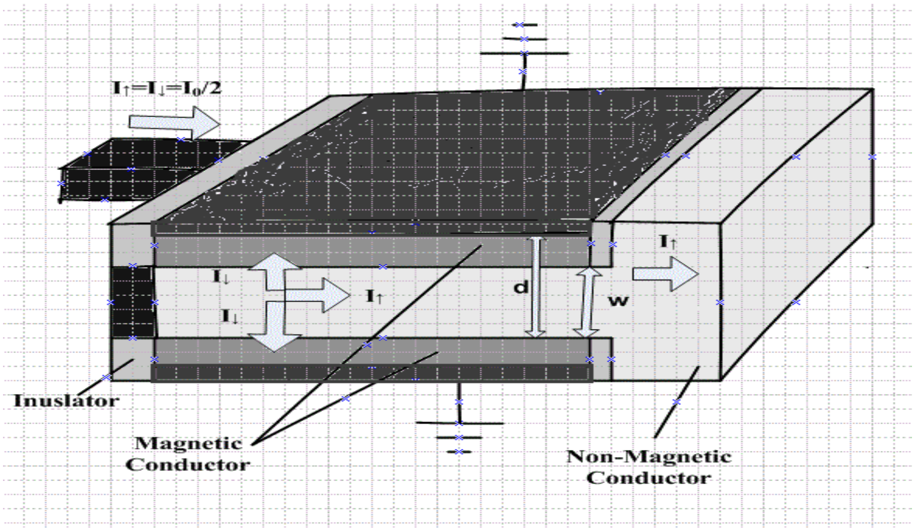

Figure 2.1: A schematic of the spin guide [27]

The principle of operation lies on the fact that the withdrawal of one component of spin from the channel result in spin polarized current in the non-magnetic channel. In contrast to conventional one, this magnetic field effect transistor control electric current flow by magnetic field. When current flows parallel to the non-magnetic metal (NM)/ magnetic metal (MM) interface away from the channel entrance, a difference between spin up and spin down current will develop. One of spin component will leave non-magnetic channel for magnetic shell. With high probability, the electrons dissipate at the ground without returning back to the channel. As a result, a polarized electric current will be generated in the channel. The current in the channel is:

$$I\uparrow\downarrow= \frac{2I_0}{\mathrm{w}}\sum_n \frac{\alpha_N\ \cosh[k_n\,(L-x)}{\mathrm{w}\cosh(k_n\,\mathrm{L})} *(\langle f_n^+\rangle\ _w^2\ \pm \frac{\langle f_n^+\rangle_w \langle f_n^+\rangle_w}{2} \tag{2.1}$$

where

$$f^{\pm}\ =\ \begin{cases} c_N^{\pm}\cos(k_N^{\pm}\mathrm{z}), & |\mathrm{z}|\ <\ \mathrm{w}/2, \\ c_M^{\pm}\sin\left[k_M^{\pm}\left(\frac{\mathrm{d}}{2}-\mathrm{z}\right)\right], & |\mathrm{z}| > \mathrm{w}/2, \end{cases} \tag{2.2}$$

$$\kappa^{+}_{M,N}=k,\quad \kappa^{-}_{M,N}=\sqrt{k^2-\lambda^{-2}_{M,N}},\tag{2.3}$$

where L is spin-guide length, $\sigma_{\uparrow,\downarrow}$ are the corresponding conductivities, k_n is damping parameter, the diffusion length $\lambda_{M,N}$ is the characteristic length-scale for equilibration of the spin subsystems in the magnetic (M) and nonmagnetic (N) regions, respectively.

Simulation of spin field effect transistor was done by Ratheash Thakaekshmi and Alok Rastogi [9]. They conducted this research theoretically using transistor based on magnetic impurity doped with Zno (Zno is zinc oxide). They modeled theoretically a switched change in the channel charge. Finally using MATLAB software, they simulated range of channel parameters; spin modulation relative to sensors, the electron mobility and the doping concentration for the spin switched changes in the electron conductance. Their results show that induction of spin-polarized electron channel through Rashba field can be considered a viable device structure for a spin-FET. Studies on magnetic bipolar transistor need to be carried out thoroughly.

The other research which was done on magnetic bipolar transistor was by M. E. Flatte et al. [28], where the base region is doped with magnetic impurities and injected unpolarized electron in the emitter region (shown in Figure 2.2). The main aim of this research was to generate 100% spin polarized current injection into nonmagnetic semiconductor.

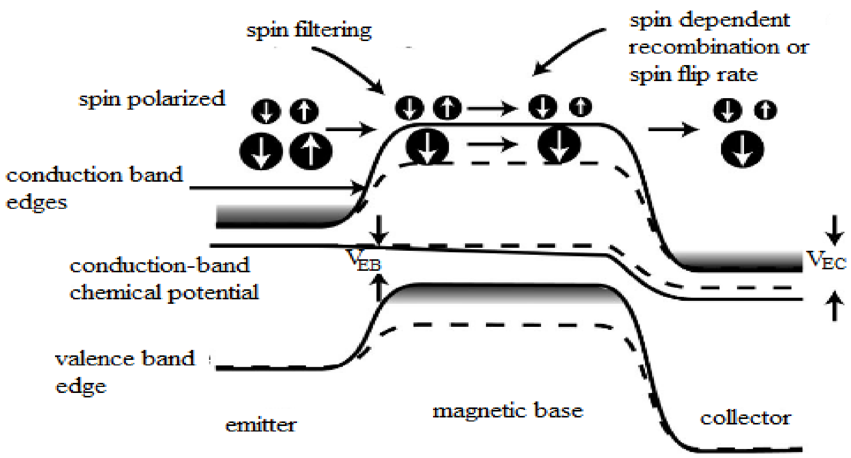

Figure 2.2: n-p↑-n transistor [28]

They obtained analytic solution for simplified of negligible spin relaxation and drift field in the base using the following equations:

$$E v_{\uparrow}\frac{\partial n_{\uparrow}}{\partial z} + D_{\uparrow}\frac{\partial^2 n_{\uparrow}}{\partial z^2} = \frac{n_{\uparrow}}{\tau_{\uparrow\downarrow}} - \frac{n_{\downarrow}}{\tau_{\uparrow\downarrow}} + \frac{n_{\uparrow}}{\tau_{R\uparrow}}\tag{2.4}$$

$$E v_{\downarrow}\frac{\partial n_{\downarrow}}{\partial z} + D_{\downarrow}\frac{\partial^2 n_{\downarrow}}{\partial z^2} = \frac{n_{\downarrow}}{\tau_{\uparrow\downarrow}} - \frac{n_{\uparrow}}{\tau_{\uparrow\downarrow}} + \frac{n_{\downarrow}}{\tau_{R\downarrow}} \quad (2.5)$$

The emitter current density for spin direction s is:

$$J_{Es} = \left(\frac{-\,q\,D_{Bs}n_{Bso}}{(L_{Bs}\sinh(w/L_{Bs})}\right)\left[\left(e^{-\frac{qV_{EB}}{kT}} - 1\right)\cosh\left(\frac{w)}{L_{Bs}}\right) - \left(e^{-\frac{qV_{cb)}}{kT}} - 1\right)\right] - \frac{qD_E p_{Eo}\ )}{L_E}\left[e^{-\frac{qV_{cb)}}{kT}} - 1\right] \quad (2.6)$$

The collector current is

$$J_{Cs} = \left(\frac{-\,q\,D_{Bs}n_{Bso}}{(L_{Bs}\sinh(\frac{w)}{L_{Bs}})}\right)\left[\left(e^{-q\frac{V_{EB})}{kT}} - 1\right) - \left(e^{-\frac{qV_{cb)}}{kT}} - 1\right)\cosh\left(\frac{w)}{L_{Bs}}\right)\right] - \frac{qD_C p_{Co}}{L_c}\left[e^{-\frac{qV_{cb)}}{kT}} - 1\right] \quad (2.7)$$

where w is the width of the base, V_{BE} is voltage between emitter and base, V_{CB} is voltage between collector and base, L_s is diffusion length, n_{Bso} is the equilibrium density of spins. This research didn't investigate the influence of magnetic impurities in other regions (base and collector). And it wouldn't analyzed the effects when injected electrons are applied in other regions. Lastly, the changes come from as result of interaction of spin of electrons of magnetic atoms and carries was not dealt with.

R.R. Pela and et al. [12] studied magnetic bipolar transistor theoretically and compared the result with conventional bipolar transistor. They simulated the characteristics curves, and they compare and contrast the current amplification factor, the open loop gain, the hybrid

parameter and the cut off frequency. As a result, they obtained additional functionality of bipolar junction transistor due to spin-charge coupling. It is clear that this research studied limited parameters of a transistor; in addition, it lacks validating on application areas.

Another research which was done by Ansil Kumar et al. [29] is a spin-valve transistor. They developed a spin valve transistor which shows high sensitivity at low field. With an external magnetic field, they managed to change the relative orientation of magnetic layer in spin valve. The emitter diode is forward biased and collector diode is reverse biased. The emitter diode has a barrier height of nearly 0.85ev and the collector diode nearly 0.75ev in which a forward biasing of emitter injects hot electron into spin-valve. This transistor was analyzed by inserting spin valve in the base region, investigation of magnetic doped regions in the transistor were not treated.

One of the interesting researches which were done on magnetic bipolar transistor (MBT) was by Fabian et al. [31] (shown in Figure 2.3). The goal of this research was to show the possibility of electrical spin injection into semiconductor based transistor. In addition the research was aimed to show whether the current amplification of the transistor could be tuned by spin or not. They calculated density of minority electrons in the base as:

$$n_{ob} = \frac{n_i^2}{N_{ab}\sqrt{((1-\alpha_{ob}^2))}} \tag{2.8}$$

In addition they calculated the density of minority of electrons n_{be} and spin s_{be} in the base emitter junction as:

$$n_{be} = n_0 \exp\frac{v_{bc}}{kT}\,[1+\alpha_{0b}\,\alpha_e] \tag{2.9}$$

$$s_{be} = n_0 \exp\frac{v_{bc}}{kT}\,[\alpha_{0b}+\alpha_e] \tag{2.10}$$

Where α_{0b} is equilibrium spin polarization in the base, α_e is non-equilibrium spin polarization in the emitter, n_i is intrinsic carrier density and N_{ab} is acceptor in the base.

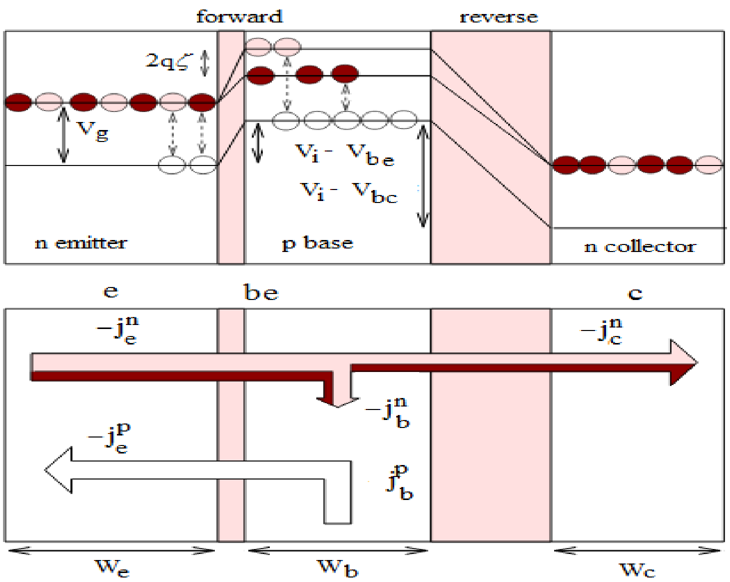

Figure 2.3: Scheme of an npn transistor with magnetic base [31]

In this research they showed the possibility of spin injection successfully through MBTs, and in addition they showed how current amplification factor easily controlled by both the injected source and the equilibrium spin.

The flip sides of this research are as follows: first this transistor model dealt with only one region of the transistor (base) which was doped with magnetic impurities. Hence the influence of other regions when doped with magnetic impurities was not investigated. Second, external injection of polarized electron was studied by applying only in emitter region. The significance of injected electrons in other regions was not studied. Third, this research assumed only electrons as spin polarized in the base region and as result the impact of polarized holes weren't considered.

Chapter Three
Modeling of magnetic bipolar transistors

3.1 Modeling of magnetic bipolar transistors

In this thesis, magnetic bipolar transistor models are mathematically proposed, and they will be presented separately in detail below. All these proposed models are intended to work for any magnetic material and it should be remembered that we are not using any specific magnetic material doping. But we used spin polarization of carriers $P_c = \tan 2q\psi_c/k_BT$ as a variable which represent each magnetic material. The splitting of energy bands $2q\psi$ in the semiconductor is attributed to the presence of magnetic material. The cause of this splitting can be to the exchange interaction or Zeeman Effect. The later resulted from g factor (for instance LnSb has g factor of 50 and $Cd_{0.95}Mn_{0.05}Se$ is 50) [17], [18], [31], [33]. Below we how we used the spin polarization of carriers as a variable to represent all types of magnetic material.

3.1.1 Type 1 Proposed magnetic bipolar transistor

In this type of transistor, we have three regions similar to the conventional transistor one, but emitter and base are considered to be magnetic which is doped with suitable magnetic material $2q\psi_c$, and the collector is semiconductor material which is shown Figure 3.1.

This transistor has the following features:

- The emitter and base are magnetic and the collector is semiconductor material.
- In the emitter only holes assumed spin polarized
- In the base only electrons are assumed spin polarized
- There is an injected spin polarized electrons in the emitter

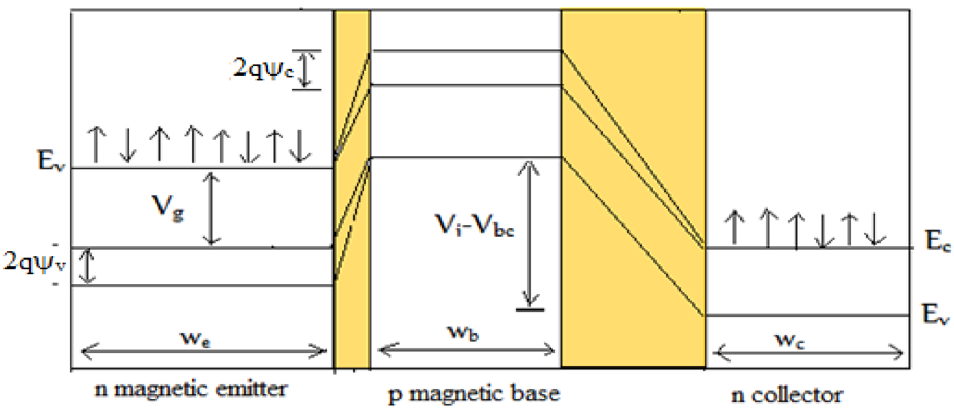

Figure 3.1: npn transistor with magnetic base and emitter

Here, it is assumed that electrons in the base are only spin polarized and holes are ignored for simplicity. Similarly, holes are only considered polarized in the emitter region. As a result splitting of conduction band in the base and valence band in the emitter are expected. This splitting could be attributed to Zeeman effects or to exchange type which is resulted from exchange coupling in ferromagnetic semiconductor. The amount of energy splitting in conduction and valence bands are $2q\psi_c$ and $2q\psi_v$ respectively [31]. Additionally, there is external injected spin polarized electrons in the emitter using by optical excitation or electrical method [42]. The main goal of this research is to obtain additional controlling mechanism (notably, spin) for the device's parameters (for instance, current amplification factor) in addition to charge of electron.

Density of electrons and holes in the base and emitter regions are calculated. Equation for density of electrons in the base emitter junction which is resulted from spin and charge of carriers is developed. Since holes are assumed spin polarized in the emitter, splitting of energy band happened only in valence band. Using the following two equations [25], [32], density of equilibrium holes and electrons in the base and emitter can be evaluated.

$$n_\lambda = \frac{\mathrm{Nc}}{2} \exp\left(\frac{E_{c\lambda} - \mu_{n\lambda})}{\mathrm{kT}}\right)) \quad (3.1.1)$$

$$p_\lambda = \frac{\mathrm{Nv}}{2} \exp\left(\frac{\mu_{p\lambda} - E_{v\lambda})}{\mathrm{kT}}\right) \quad (3.1.2)$$

where,

$$E_{c\lambda} = E_o - q\Phi - \lambda q\psi_c$$

$$E_{v\lambda} = E_{vo} - q\Phi - \lambda q\psi_v$$

λ stands for ↓ or↑, Φ - built in potential in the junction, E_c -Conduction energy, μ -Chemical potential, and ψ_c is conduction splitting energy.

From above equation, we can write density of spin electron as:

$$n_\uparrow = \frac{\mathrm{Nc}}{2} \exp\left(\frac{Eco - q\Phi - \uparrow q\psi_c - \mu_{n\uparrow}}{\mathrm{kT}}\right) \quad (3.1.1a)$$

$$n_\downarrow = \frac{\mathrm{Nc}}{2} \exp\left(\frac{Eco - q\Phi - \downarrow q\psi_c - \mu_{n\downarrow}}{\mathrm{kT}}\right) \quad (3.1.2a)$$

The spin polarization of carriers is defined by [25]:

$$P = s/n = \frac{(n\uparrow - n\downarrow)}{(n\uparrow + n\downarrow)} \quad (3.1.3)$$

where *s* and *n* are number of spin of carries and electrons respectively.

Using Equation (3.1.1a), (3.1.2a) and (3.1.3), spin polarization of equilibrium electrons in the base is:

$$P_{ob} = \tanh \frac{q\psi_c}{kT} \tag{3.1.4}$$

Again using Equation (3.1.1a) and (3.1.2a), we can show density of hole in the emitter as:

$$p_{oe} = \frac{n_i^2}{N_{De}} \cosh\frac{q\psi_v}{kT} \tag{3.1.5}$$

(Its derivation is shown in Appendix B: (1))

From Equation (3.1.5) we understand that the density of minority of holes is dependent on splitting energy ψ_v. And it is clear that $\cosh\frac{q\psi_v}{kT}$ has positive value for any value of ψ_v. The density of holes in the conventional and researchers' work is given by [31], [40]:

$$p_{oe} = \frac{n_i^2}{N_{De}}$$

Since, $\cosh \frac{q\psi_v}{kT} = \frac{1}{\sqrt{(1-P_{oh}^2)}}$

where n_i is intrinsic carrier density and N_{De} is donor in the emitter, k is Boltzman constant, T is temprature and P_{oh} is equilibrium spin polarization of holes and given by $P_{oh} = \tanh\frac{q\psi_v}{kT}$.

Equation (3.1.5) can be expressed as:

$$p_{oe} = \frac{n_i^2}{N_{De}} \frac{1}{\sqrt{(1-P_{oh}^2)}} \tag{3.1.5a}$$

From trigonometry we have the relation:

$$\cosh x = \frac{1}{\sqrt{(1-(\tanh)^2 x)}}$$

Similarly using Equation (3.1.1a) and (3.1.2a), we can write equation that represents density of electrons in the base:

$$n_{ob} = \frac{n_i^2}{N_{ab}} \cosh \frac{q\psi_c}{kT} \tag{3.1.6}$$

where N_{ab} is acceptor in the base.

Here we can see that the density of minority of electrons is dependent on the splitting energy ψ_c.

The conventional value of density of minority of electron is given by [31], [40]:

$$n_{ob} = \frac{n_i^2}{N_{ab}}$$

The density of holes in the base emitter junction is:

$$p_e = \frac{n_i^2}{N_{De}\sqrt{(1-P_{oe}^2)}} \exp\left(\frac{qV_{be}}{kT}\right)$$

where vbe is biasing voltage between base and emitter.

Spin polarization is given by:

$$P= \frac{\tanh\frac{(\delta\mu\_)}{kT} + P_{ob}}{1 + P_{ob}\tanh\frac{(\delta\mu\_)}{kT}} \tag{3.1.7}$$

Equation (3.1.7) can be derived as follows:

$$n_{be}= n= n_{ob}\ exp(\frac{(qV_{be})}{kT})$$

Or alternatively, we can write [25]:

$$n_{\lambda}= n_{\lambda ob}\ exp(\frac{(q(\delta\phi) + \delta\mu_{n\lambda})}{kT}) \tag{3.1.8}$$

$$n_{\uparrow}= n_{ob\uparrow}\ \exp(\frac{(q(\delta\phi) + \delta\mu_{n\uparrow})}{kT}) \tag{3.1.8a}$$

$$n_{\downarrow}= n_{ob\downarrow}\ \exp(\frac{q(\delta\phi) + \delta\mu_{n\downarrow}}{kT}) \tag{3.1.8b}$$

Rearranging equations (3.1.8a) and (3.1.8b), we can get the following equations:

$$n= exp\ \frac{(\Phi + \mu+)}{kT}[n_o\cosh(\mu-) + s_o\sinh(\mu-)]\quad) \tag{3.1.19}$$

$$s= exp\ \frac{(\Phi + \mu+)}{kT}\ [n_o\sinh(\mu-)+ s_o\cosh(\mu-)] \tag{3.1.10}$$

where

$$\mu\pm = \frac{((\mu\downarrow \pm \mu\downarrow))}{2}$$

And remembering the definition of spin (in Equation (3.1.3)), we have:

P= s/n, the spin polarization of non-equilibrium electron is:

$$P= \frac{tanh(\mu-) + P_{ob}}{1 + P_{ob}\ tanh\mu-)}$$

(Full derivation is shown in Appendix B: (2)

Using Equations (3.1.7) and (3.1.9), it is possible to show density of electrons in the base emitter junction as:

$$n_{be} = n_{0b}\exp(\frac{qV_{be}}{kT})\ (1 + P_{ob}\frac{P_e+ P_{oe}}{1-P_{oe}P_e}) \tag{3.1.11}$$

where P_{ob} is equilibrium spin polarization in the base and P_e is non-equilibrium spin polarization of injected in the emitter (It is shown in the Appendix (3)).

Here the density of minority of electrons in the base emitter junction is a function of equilibrium spin polarization in the base and non-equilibrium injected spin polarization in the emitter. As we can see when the injected spin polarization in the emitter P_e and spin polarization of equilibrium electrons in the base P_{ob} have the same sign (if their spin directions are parallel), the density of minority electrons in the base emitter junction become high. And the converse is also true.

The density of minority of electrons in the base emitter junction in the conventional transistor is given by [31], [40]:

$$n_{be} = n_{0b} \exp(\frac{qV_{be}}{kT})$$

The presence of spin polarized holes in the emitter result in slight difference in the magnitude of the density of electrons in the base emitter region with respect to the result obtained in the researchers' model. The density of minority of electron in the base emitter junction in the researchers' model is calculated as [31]:

$$n_{be} = n_{0b} \exp(\frac{qV_{be}}{kT}) (1 + P_{ob}P_e)$$

The density of spin of electrons in the base emitter junction is calculated using Equation (3.1.8) and (3.1.9) as:

$$s_{be} = \frac{n_i^2\left(\cosh\left(\frac{q\psi_c}{kT}\right)\right)}{N_{ab}} \left[\frac{(P_e - P_{0e})}{1 - P_{oe}P_e} + P_{0b}\right] \exp(\frac{qV_{be}}{kT})$$

The density of electron in the base collector region is calculated as:

$$n_{bc} = \frac{(n_i^2)}{N_{ab}} \cosh\frac{q\psi_c}{\mathrm{kT}} \exp\frac{v_{bc}}{kT} \tag{3.1.12}$$

(This is shown in the Appendix B (4))

The density of minority of electrons in the base collector region in the conventional and researchers' model is ignored as result of its negligible value.

The emitter and collector currents are given by [25], [32] (their derivations are shown in the Appendix B (**5**)):

$$J_e = \frac{qD_n}{L_n} [n_{be}(\coth\frac{w_b}{L_n}) - n_{bc} \sinh(\frac{w_b}{L_n})] + [\frac{qD_p}{L_p} (p_{be}) (\coth\frac{w_e}{L_p}] \tag{3.1.13}$$

$$J_c = \frac{qD_n}{L_n}[n_{be} \frac{1}{\sinh\frac{w_b}{L_n}} - n_{bc}(\frac{(\cosh\frac{w_b}{L_n})}{\sinh\frac{w_c}{L_p}})] - [\frac{qD_p}{L_p} p_{bc} (\coth\frac{w_c}{L_p})] \tag{3.1.14}$$

By substituting the density of minority carriers into Equations (3.1.13) and (3.1.14), we can obtain emitter and collector current which represent for magnetic transistor model. The base current j_b is $J_b = j_e - j_b$ and the current amplification factor β is defined by:

$$\beta = \frac{jc}{\mathrm{jb}} \tag{3.1.15}$$

$$\beta = \frac{1}{\left(\cosh\frac{w_b}{L_n} - 1\right) + \frac{D_p L_n N_{ab}\left(\coth\frac{w_e}{L_p}\right)}{D_n L_p N_{De}\left(\coth\frac{w_b}{L_n}\right)} \frac{\sqrt{(1-P_{ob}^2)}}{(1+P_{ob}(\frac{P_e+P_{oe}}{1-P_e P_{oe}})\sqrt{(1-P_{oe}^2)}}} \quad (3.1.15a)$$

where D_n and D_P are electron and hole diffusivities respectively, L_n and L_p are electron and hole diffusion lengths respectively, and w_b is nominal width of the base.

From this result, we can understand that the current amplification factor is controlled by spin of holes and electrons. By holding one of the spin polarization of carriers constant, and varying the other, we can see the exact effect. This result can be seen clearly in the result and discussion chapter. The current amplification factor for conventional bipolar transistor has a value of [31], [40] :

$$\beta = \frac{1}{\left(\cosh\frac{w_b}{L_n} - 1\right) + \frac{D_p L_n N_{ab}\left(\coth\frac{w_e}{L_p}\right)}{D_n L_p N_{De}\left(\coth\frac{w_b}{L_n}\right)}} \quad (3.1.16)$$

The current amplification factor in the researchers' model is only managed to be controlled by spin of electrons and electron of charges. But in this model, we managed the current amplification factor to be controlled by spin of holes as well. The current amplification factor calculated by the researchers' model is [31]:

$$\beta = \frac{1}{\left(\cosh\frac{w_b}{L_n} - 1\right) + \frac{D_p L_n N_{ab}\left(\coth\frac{w_e}{L_p}\right)}{D_n L_p N_{De}\left(\coth\frac{w_b}{L_n}\right)} \frac{\sqrt{(1-P_{ob}^2)}}{(1+P_{ob}P_e}} \quad (3.1.17)$$

3.1.2 Type 2 proposed magnetic bipolar transistor

In this type of model, the base and the emitter are magnetic and the collector is semiconductor material as shown in Figure 3.2.

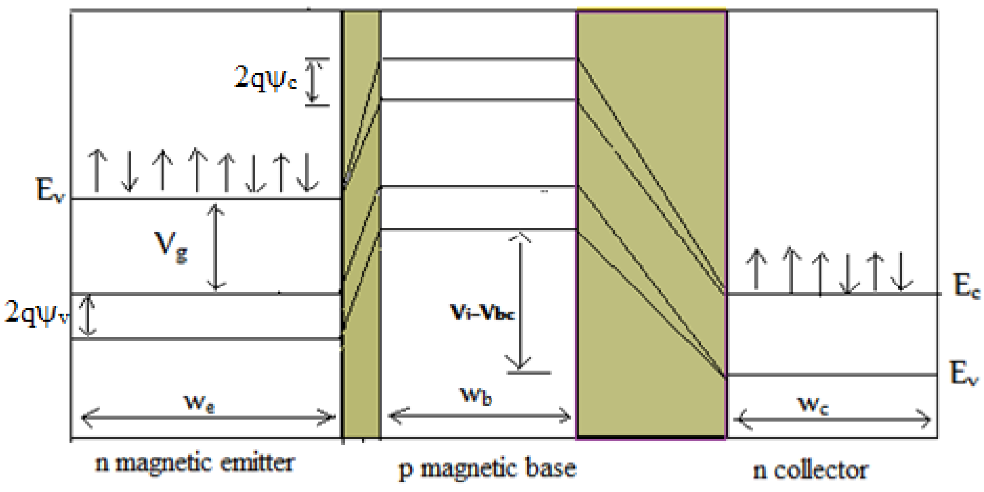

Figure 3.2: npn transistor with both emitter and base are magnetic

Generally, this transistor model has the following features:

- the emitter and the base are magnetic, and the collector is semiconductor material
- the holes are assumed spin polarized in the emitter
- both electron and hole are assumed to be spin polarized in the base
- there is an injected spin polarized electrons in the emitter

The main goal of this research is to increase the efficiency of the bipolar transistor by employing the spins of electrons and holes. In addition it is also intended to have an additional input controlling mechanism, notably spins beside charge of electrons. It is assumed that electrons and holes are spin polarized in the base, and holes are only spin polarized in the emitter. As a result, the conduction and valence bands split in the base and valence band in the emitter. The density of electrons and holes in the base-emitter and base-collector junction is calculated. Subsequently, the emitter and collector currents' equations are also determined.

Using Equation (3.1.1a) and (3.1.2a), the density of electrons in the base is calculated as:

$$n_{ob} = \frac{n_i^2\left(\cosh\left(\frac{q\psi_c}{kT}\right)\right)\cosh\left(\frac{q\psi_v}{kT}\right)}{N_{ab}} \qquad (3.1.18)$$

where $q\psi_c$ is conduction band splitting, and $q\psi_v$ is valence band splitting.

(All derivations are shown in Appendix B: (1))

Or, n_{ob} can be expressed as:

$$n_{ob} = \frac{n_i^2}{N_{ab}\sqrt{(1-P_{ob}^2)}\sqrt{(1-P_{obh}^2)}} \qquad (3.1.18a)$$

where P_{ob} and P_{obh} are equilibrium spin polarization of electrons and holes in the base respectively.

From Equation (3.1.18), we can see that the density of minority electrons shows significant changes as result of the spin polarization of holes and electrons in the base compared to both the density of electrons in the researchers' model [31] and conventional bipolar transistor's values. Since the cosine hyperbolic function $\cosh(\frac{q\psi_v}{kT})$ is positive for any value, the density of electrons increases. The density of minority of electron in the researchers' model is [31]:

$$n_{ob} = \frac{n_i^2\cosh\left(\frac{q\psi_c}{kT}\right)}{N_{ab}}$$

And the density of minority of electron in the base in the conventional bipolar transistor is [31], [40]:

$$n_{ob} = \frac{n_i^2}{N_{ab}}$$

Using Equations (3.1.7) and (3.1.9), the density of electrons in the base emitter junction can be calculated as:

$$n_{be} = \frac{n_i^2\left(\cosh\left(\frac{q\psi_c}{kT}\right)\right)\cosh\left(\frac{q\psi_v}{kT}\right)}{N_{ab}} \left(1 + P_{ob}\frac{P_e - P_{oe}}{1 - P_{oe}P_e}\right) \exp\left(\frac{qV_{be}}{kT}\right) \tag{3.1.19}$$

where P_{oe} is polarization of equilibrium holes in the emitter region, P_e is polarization of injected electron in the emitter and P_{ob} is polarization of equilibrium electrons in the base region.
(Its full derivation is shown in the appendix B)

As we can see the density of minority of electrons in the base emitter junction is dependent on both equilibrium and non-equilibrium spin polarization. The density of minority of electrons in the base emitter junction in this type of model is increased due to the presence of hyperbolic function $\left(\cosh\left(\frac{q\psi_c}{kT}\right)\right)$ (resulted from spin polarization of carriers) and spin polarization of in injected electrons in the emitter P_e. The density of minority of electrons in the base emitter junction in the conventional transistor is:

$$n_{be} = \frac{n_i^2}{N_{ab}} \exp\left(\frac{qV_{be}}{kT}\right)$$

Compared to the researchers' model [31], the density of electrons in the base emitter junction in this type of model is increases due to the same reason explained before. And the density of minority of electrons in base emitter junction in the researchers' model [31] is:

$$n_{be} = \frac{n_i^2\left(\cosh\left(\frac{q\psi_c}{kT}\right)\right)}{N_{ab}} \left(1 + P_oP_e\right) \exp\left(\frac{qV_{be}}{kT}\right)$$

The density of spin carriers in base emitter region is calculated as:

$$s_{be} = \frac{n_i^2\left(\cosh\left(\frac{q\psi_c}{kT}\right)\right)\cosh\left(\frac{q\psi_v}{kT}\right)}{N_{ab}} \left[\frac{(P_e - P_{0e})}{1 - P_{oe}P_e} + P_{0b}\right] \exp\left(\frac{qV_{be}}{kT}\right) \tag{3.1.20}$$

It is clear that the density of spin carriers in the conventional bipolar transistor is zero. On the other hand, the density of spins in the base emitter junction in the researchers' model is [31]:

$$s_{be} = \frac{n_i^2\left(\cosh\left(\frac{q\psi_c}{kT}\right)\right)}{N_{ab}} \left[P_e + P_{0b}\right] \exp\left(\frac{qV_{be}}{kT}\right)$$

The density of spin of electrons is a function of spin polarization of electrons in the base, spin polarization of injected electrons in the emitter and spin polarization of holes in the emitter. On the other hand, the density of electrons in the base-collector junction is given by:

$$n_{bc} = \frac{n_i^2\left(\cosh\left(\frac{q\psi_c}{kT}\right)\right)\cosh\left(\frac{q\psi_v}{kT}\right)}{N_{ab}} \ \exp \frac{qV_{bc}}{kT} \tag{3.1.21}$$

The density of spin carriers in the base collector region is :

$$s_{bc} = \frac{n_i^2\left(\cosh\left(\frac{q\psi_c}{kT}\right)\right)\cosh\left(\frac{q\psi_v}{kT}\right)}{N_{ab}} \ P_{0b} \exp \frac{qv_{bc}}{kT} \tag{3.1.22}$$

The density of electrons and spin in the base collector regions are ignored in the conventional bipolar transistor and researchers' model [31] because of its small magnitude.

The density of equilibrium holes in emitter is:

$$p_{oe} = \frac{n_i^2}{N_{De}\sqrt{(1 - P_{oe}^2)}} \tag{3.1.23}$$

The density of holes increases as the result of spin polarization of holes in the emitter P_{oe} compared to both the conventional bipolar transistor's value and researchers' value which has the value of [31], [40]:

$$p_{oe} = \frac{n_i^2}{N_{De}}$$

The density of holes in base-emitter junction is:

$$p_e = \frac{n_i^2}{N_{De}\sqrt{(1 - P_{oe}^2)}} \exp\left(\frac{qV_{be}}{kT}\right) \tag{3.1.24}$$

The density of equilibrium holes in collector is:

$$p_{oc} = \frac{n_i^2}{N_{Dc}} \tag{3.1.25}$$

The density of holes in base collector junction is:

$$p_c = p_{oc} \exp \frac{qV_{bc}}{kT} \tag{3.1.26}$$

In the conventional bipolar transistor and researchers' model [31], the density of minority of holes in the base collector region is ignored due to its small magnitude.

Using Equations (3.1.13), (3.1.14) and (3.1.15), we can calculate the current amplification factor. Since the electron and hole currents emanating from collector region are very small, we can write the current amplification factor as:

$$\beta = \frac{1}{\left(\cosh\frac{w_b}{L_n} - 1\right) + \frac{D_p L_n N_{ab}\left(\coth\frac{w_e}{L_p}\right)}{D_n L_p N_{De}\left(\coth\frac{w_b}{L_n}\right)} \frac{\sqrt{(1-P_{ob}^2)}\sqrt{(1-P_{obh}^2)}}{(1+P_{ob}(\frac{P_e+P_{oe}}{1-P_eP_{oe}})\sqrt{(1-P_{oe}^2)}}} \tag{3.1.27}$$

The current amplification factor obtained in this model is quite different from the conventional bipolar transistor and researchers' model value. The current amplification factor in the model developed in the researchers' is [31]:

$$\beta = \frac{1}{\left(\cosh\frac{w_b}{L_n} - 1\right) + \frac{D_p L_n N_{ab}\left(\coth\frac{w_e}{L_p}\right)}{D_n L_p N_{De}\left(\coth\frac{w_b}{L_n}\right)} \frac{\sqrt{(1-P_{ob}^2)}}{(1+P_{ob}P_e}}$$

And the current amplification factor in the conventional transistor is [40], [33]:

$$\beta = \frac{1}{\left(\cosh\frac{w_b}{L_n} - 1\right) + \frac{D_p L_n N_{ab}\left(\coth\frac{w_e}{L_p}\right)}{D_n L_p N_{De}\left(\coth\frac{w_b}{L_n}\right)}}$$

The disparity between the current amplification factors of the two comes as a result of incorporation of spin of electrons in the researchers' model [31].

3.1.3 Type 3 proposed magnetic bipolar transistor with all regions magnetic

This transistor model type with all regions assumed magnetic which is shown in Figure 3.3 has the following features:

1. All regions (collector, base and emitter) are magnetic
2. There is an injected spin polarized electrons in both emitter and collector regions
3. Electrons are assumed spin polarized in the base region
4. Holes are assumed spin polarized in the emitter and collector regions

Using Equation (3.1.1a) and (3.1.2a), the density of minority of electrons in the base is calculated as:

$$n_{ob} = \frac{n_i^2}{N_{De}\sqrt{(1-P_{ob}^2)}} \tag{3.1.28}$$

The density of minority of electrons in this type of model is similar to the density of minority of electrons calculated in the model (in Equation (3.1.6)) where only emitter and base are magnetic, and electrons are only assumed spin polarized. As a result the explanation which was done earlier (in section 3.1.1) could also apply here. Using Equation (3.1.7) and (3.1.9), the density of electrons in the base emitter region is calculated as:

$$n_{be} = \frac{n_i^2}{N_{De}\sqrt{(1-P_{ob}^2)}} \left(1 + P_{ob} \frac{(P_e - P_{oe})}{(1-P_{oe}P_e)}\right) \exp \frac{v_{be}}{kT} \tag{3.1.29}$$

The derivation is shown in Appendix B: (3)

Similarly, the density of minority of electrons in the base emitter junction obtained in this model has similar effect with the one explained in the model (in Equation (3.1.11)) where emitter and base are magnetic material, and electrons are only assumed spin polarized.

The density of spin carriers in base emitter region is calculated as:

$$s_{be} = \frac{n_i^2}{N_{De}\sqrt{(1-P_{ob}^2)}} \left[\frac{(P_e - P_{0e})}{1-P_{oe}P_e} + P_{0b}\right] \exp\frac{v_{be}}{kT} \tag{3.1.30}$$

The density of minority of spin carriers in the conventional bipolar transistor is zero. In comparison to the researchers' model [31], the density of spin of electrons in the base emitter junction has the same effect with the one obtained in the model where emitter and base are only magnetic, and electrons are only assumed spin polarized (in Equation (3.1.19)).

In the same way, using Equations (3.1.1a) and (3.1.2a), the density of holes in the emitter is:

$$p_{oe} = \frac{n_i^2}{N_{De}\sqrt{(1-P_{oe}^2)}} \tag{3.1.31}$$

The same explanation can be done here like the one we did on the density of holes obtained in the model type 1 (in Equation (3.1.5)).

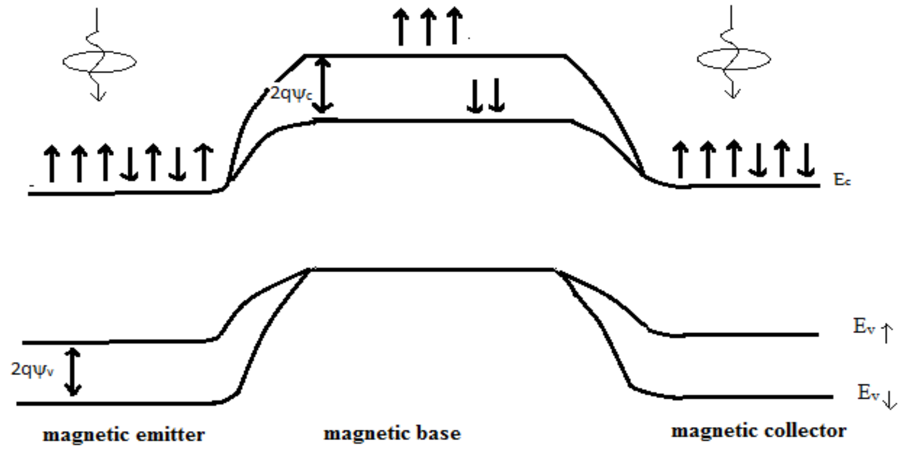

Figure 3.3: Magnetic npn transistor with all regions are magnetic semiconductor materials

The density of holes in the base emitter is [31], [40]:

$$p_e = p_{oe} \exp\left(\frac{qV_{be}}{kT}\right) \tag{3.1.32}$$

Using Equation (3.1.1a) and (3.1.2a), the density of holes in the collector is:

$$p_{oc} = \frac{n_i^2}{N_{De}\sqrt{(1-P_{oc}^2)}} \tag{3.1.33}$$

where P_{oc} is spin polarization of holes in the collector region.

The density of holes in the base collector junction is small and it is ignored in the conventional bipolar transistor and researchers' model [31]. Using Equation (3.1.7) and (3.1.9), the density of electron in the base collector junction is:

$$n_{bc} = \frac{n_i^2}{N_{De}\sqrt{(1-P_{ob}^2)}}\left(1+P_o\frac{P_c-P_{0c}}{1-P_{0c}P_c}\right)\exp\left(\frac{qV_{bc}}{kT}\right) \tag{3.1.34}$$

where P_c is non-equilibrium spin polarization injected in the collector.
(The derivation is shown in Appendix B: (4))

The magnitude of density of minority of electrons in the base collector junction is a function of spin polarized equilibrium electrons and non-equilibrium injected spin polarized electrons in the collector. In the conventional bipolar transistor and researchers' model, the density of minority of electrons in the base collector junction is ignored for its negligible value, which has an equation of [40], [32]:

$$n_{bc} = n_{ob}\left(\exp\left(\frac{qV_{bc}}{kT}\right)\right)$$

Using Equation (3.1.8) and (3.1.9), the density of spin carriers in the base collector region is calculated as:

$$s_{bc} = \frac{n_i^2}{N_{De}\sqrt{(1-P_{ob}^2)}}\left[\frac{P_c-P_{0c}}{1-P_{0c}P_c}+P_{0b}\right]\exp\left(\frac{qV_{bc}}{kT}\right)$$

(Shown in Appendix B: (3))

The density of spin in the base collector region in the conventional bipolar transistor and researchers' model [31] is zero.

3.2 Calculation of energy band edges using perturbation theory

The energy band edge of semiconductor in the presence of magnetic impurities is approximated by using ordinary perturbation theory. The calculation is done for non-degenerate and degenerate energy states.

The first order correction to the band energy is:

$$E_n^{(1)} = -(1/2N)\int \exp(inr) * \exp(-inr)\{\int \sum_R M_{exch}\,\delta(r-R)[(S^+_R\,\psi^\dagger{\downarrow}(r)\,\psi{\uparrow}(r) + S^-_R\,\psi^\dagger{\uparrow}(r)\,\psi{\downarrow}(r) + (S^z_R - \langle S^z\rangle)[\psi^\dagger{\uparrow}(r)\,\psi{\uparrow}(r) - \psi^\dagger{\downarrow}(r)\,\psi{\downarrow}(r)]]\,dr\}dr \tag{3.2.1}$$

Thus the first correction is calculated as:

$$E_n^{(1)} = -\frac{M_{exch}}{2VN}[(S^z_R - \langle S^z\rangle)\ (N_n{\uparrow} - N_n{\downarrow})] \tag{3.2.2}$$

All calculations are shown in the appendix.

The second order perturbation using equation is calculated as:

$$E_n^{(2)} = \frac{M^2_{exchR}}{4(VN)^2} \sum_n \frac{[(S_R^{(z)} - \langle S^z \rangle)]^2 \delta(n-m)\,[n^2{\uparrow} - 2\,n{\uparrow}n{\downarrow} + n^2{\downarrow}]}{(E_n^{(0)} - E_m^{(0)})} \qquad (3.2.3)$$

where $S^z_R = x\langle S^z_R\rangle = xSB_s(y)$, x is mole fraction of magnetic moles, $B_s(y)$ is Brillouin function and S is spin quantum number

$y = (g_L\mu_B SB)/(kT)$, g is g factor of electron, μ_B is Bohr magneton, k is Boltzman constant and T is temperature.

Therefore the energy band with perturbed state is:

$$E = E_0 + \hbar^2k^2/2m^* + E_n^{(1)} + E_n^{(2)}$$

Degenerate energy states (For two fold degeneracy)is represented by the equation [34], [36], [37]:

$$E^1_{\pm} = ½\,[W_{aa} + W_{bb} \pm \sqrt{\{(W_{aa} - W_{bb})^2 + 4/W_{ab}/^2\}}] \qquad (3.2.4)$$

where ,

$$W_{aa} = \langle \phi_a / H_1 / \phi_a \rangle,\ W_{bb} = \langle \phi_b / H_1 / \phi_b \rangle,\ W_{ab} = \langle \phi_a / H_1 / \phi_b \rangle$$

$$E^1_{\pm} = \frac{M^2_{exchR}}{2VN}(S^z_R - \langle S^z \rangle)\{[n_a{\uparrow} - n_a{\downarrow}] + [n_b{\uparrow} - n_b{\downarrow}] \pm \sqrt{(n^2_a{\uparrow} - n^2_b{\uparrow}) + (n^2_a{\downarrow} - n^2_b{\downarrow}) + 2\delta(b-a)\,[n^2_a{\uparrow} + n^2_a{\downarrow} + 2n_{a,}{\uparrow}\, n_a{\downarrow}]}\} \qquad (3.2.5)$$

(It is shown in Appendix B: (**6**))

Thus the energy with correction is:

$$E = E_0 + \hbar^2k^2/2m^* + E^{(1)}_{\pm}$$

3.3 Application of Spin Transistor

3.3.1 Cascaded Spin Amplifier

Using the proposed magnetic bipolar transistor's model (including both researchers' [31] and the proposed ones), different performances are investigated which includes: input impedance, output impedance, voltage gain, current gain, current amplification factor, electrons and holes generation current, density of electrons in the base and emitter current. Since a mathematical model was developed section 3.1, the effect of doping of magnetic material is visible in the splitting of energy bands. As a result, it is not necessary for now to depend on the doping concentration of a specific magnetic material. Since the splitting energy is taken as a variable, it is possible to use any magnetic material and determine its influence. Three stage cascaded amplifier is shown in Figure 3.4.

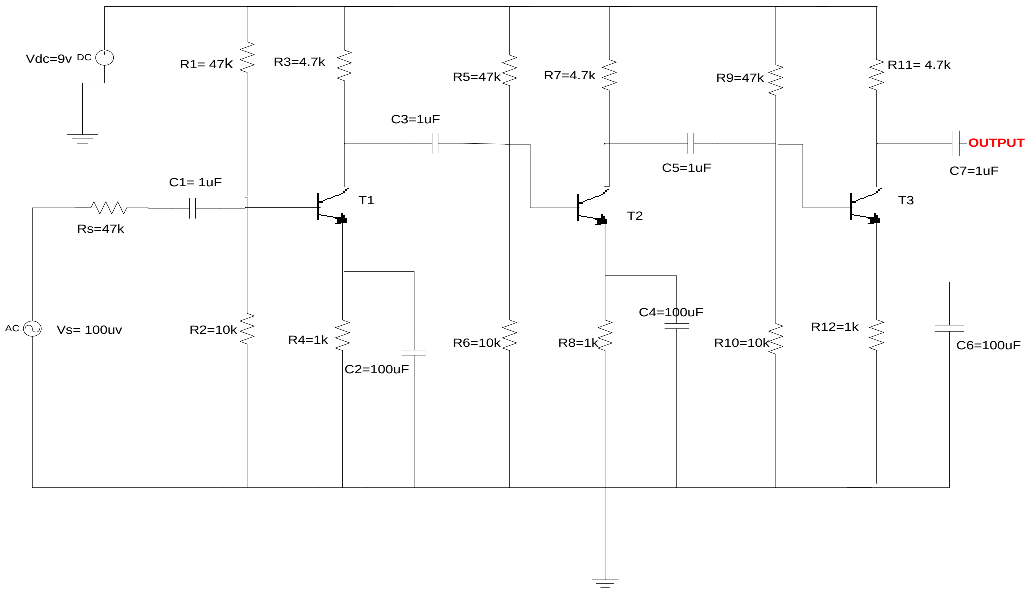

Figure 3.4: common emitter cascaded amplifier using Microsoft Office Visio

Current amplification factor of 132 for conventional bipolar transistor is calculated by substituting the following parameters [31]:

$L_p = L_s = 10um$, $L_n = 30um$, $\alpha_{ob} = 0.9$, $W_e = W_c = 2um$, $W_b = 1.5um$, $n_i = 1.5 * 10^{10}\ cm^3$,
$N_e = 10^{17}\ cm^3$, $N_b = 10^{16}\ cm^3$, $N_c = 10^{15}\ cm^3$, D_n=100, $D_p = 10cm^2/s$, Area=$17um^2$ and

$V_{be} = 0.5$ v, $V_{bc} = 0$ v

It should be clear that the same parameters are used to calculate for both conventional bipolar transistor and for the proposed magnetic bipolar transistor. In order to show how magnetic material and injected spin polarized electrons are integrated into the transistor, mathematical model was developed which is covered in chapter 3. As it is explained in chapter 3, the injected spin polarized electrons are mathematically incorporated into the device. Even though transistor's regions are not doped with magnetic material, its effect is visible in the variable spin polarization of electrons and holes. This is because the splitting of energy bands is caused by presence of magnetic impurities in the region. This splitting energy is about $2q\psi$ [31], and from chapter 3 the spin polarization is defined as $P_{ob}= \tanh(2q\psi/k_BT)$. It is also remembered from chapter 3 that this spin polarization is used as a variable to determine different parameters including current amplification factor. Hence it is clear that the type of magnetic material will only prevail in the magnitude of spin polarization of carriers. This is because the strength of spin splitting will depend on the g factor of the magnetic material. As a result, the exact type of magnetic material used is not important.

In order to analyse the small signal AC analysis for transistor, AC equivalent circuit is needed. And for low frequency, the simplified re model is used; and for high frequency hybrid-π is used. The hybrid-π can work quite well for low frequencies as well. Since the parameters of re model and hybrid-π are functions of spin of carriers, the equivalent AC models used for spin based devices in this thesis will work quite well. Bearing this in mind, different parameters of cascaded amplifier calculated as:

Input Impedance

$$R_{in\_tot} = \left(\frac{4.7*10^8*r_e*\beta}{[(57*10^3)r_e*\beta + (4.7*10^8)].} + j\frac{1.59*10^5}{f}\right) \tag{3.3.4}$$

where f is frequency, β is current amplification and r_e is emitter resistance

Output Impedance

$$Z_o = V_o / \beta * i_b = (r_o // R_{11})\, I_b\beta / \beta I_b = r_0 // R_{11} \cong r_{11} \tag{3.3.5}$$

Voltage Gain

$$A_{v\,(tot)} = \frac{R1 // R2}{Rs + R1 // R2} * A_{v1} * A_{v2} * A_{v3} = \frac{3.4 * 10^9 * \beta*\beta}{(2.2 * 10^3 + 0.738 * \beta * r_e)^2 (r_e)} \qquad 3.3.6)$$

Current Gain

Assuming V_s = 100uv

$$A_i = [8.24 * 10^3/(8.24 * 10^3 + \beta re)] * (\beta^3) \tag{3.3.7}$$

3.3.2 High frequency model hybrid-π common emitter model

In section 3.3.1, low frequency small signal analysis using simplified re model was considered. In this section using more advanced equivalent circuit model for high frequency, small signal analysis is investigated. After calculating each parasitic resistances and capacitances values of hybrid-π model, the performances of cascaded amplifier are analyzed. The hybrid-π model is shown in Figure 3.5. In order to calculate the hybrid-π parameters, evaluation of hybrid parameters are needed.

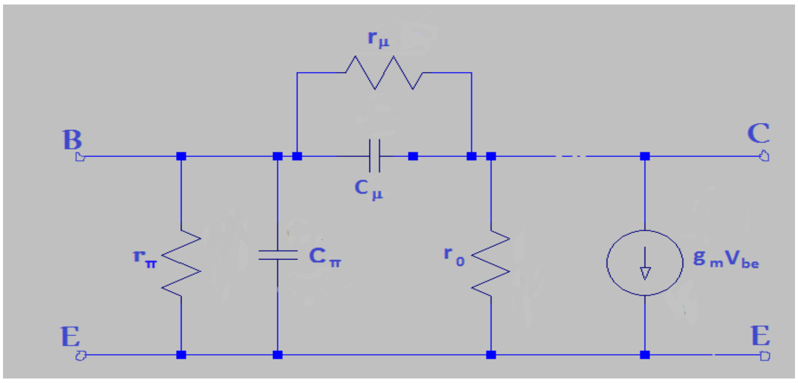

Figure 3.5: the hybrid-π model for the common emitter configuration

$$h_{ie}= \partial V_{be}/\partial I_b|_{Vce=constant} = 1/(\partial I_b/\partial V_{be})|_{Vce=constant} = V_T\beta/I_C = 26*10^{-3}\beta/I_C$$

$$h_{fe}=\partial I_c/\partial I_b |_{VCE= constant} \cong \beta_{dc} = \beta$$

To calculate h_{re} and h_{oe}, V_{be} and V_{ce} should be determined. Using Thevenin theorem to single stage of Figure 3.4, the base emitter voltage obtained as $V_b = V_sR_Bh_{ie}/((R_s + R_B)[R_S//R_B + h_{ie}])$

where V_T is thermal voltage ($26*10^{-3}$V), $Rs//R_B$ signifies as Rs parallel with R_B and similarly R_B is parallel combination of R_1 and R_2.

$$h_{re}= \partial V_{be}/\partial V_{ce}|_{Ib= constant} \cong V_sR_B V_T \beta/I_c^2/(R_s + R_B)[R_S//R_B + V_T\beta/I_C]R_c= [8.2*10^{-11} \beta/I^2_C] / [7*10^3 + 26*10^{-3}\beta/I_C]$$

$$h_{oe}= \partial I_c/\partial V_{CE}|_{Ib= constant} \cong 1/R_c = 2.12*10\text{-}4 \text{ Siemens}$$

It is clear that the hybrid parameters are function of current amplification factor β and collector current. And from section 3.1, current amplification factor and collector current are function of spin polarization of carriers.

Resistance values for the hybrid-π parameters calculated below.

$$g_m= \partial I_c/\partial V_{be}|_{Vce=constant} \cong -I_C/V_T = -38.4I_c \text{ (with } I_C= I_S \exp(qV_{EB}/KT))$$

$$r_\pi = \partial V_{be}/\partial VI_b|_{Vce=constant} = H_{fe}/g_m \cong \beta_{dc} (V_T)/ I_c = 26*10^{-3}\beta/I_C$$

$$r_\mu= r_\pi/h_{re}= \{(\beta V_T/ I_C)((R_s + R_B)[R_S//R_B + V_T\beta/I_C]Rs\} /(V_sR_B V_T \beta/I^2_c)) = [182Ic + 6.76*10^{-4}\beta] / [8.2*10^{-11}]= 2.2*10^{12} Ic + 8.24*10^6 \beta$$

$$r_o= 1/\{ 1/R_c - (\beta /r_\mu)\}= 1/\{2.12*10^{-4} - [\beta/(2.2*10^{12}I_C + 8.24*10^6\beta)]\}$$

Here also it can be seen that the parasitic resistances are function of current amplification β and collector current Ic. In other words the parasitic resistances are function of spin polarization of carriers.

Calculation of hybrid-π capacitances [43],[44] will be conducted below.

$$C_{\mu}= C_{JBC0}/(1- V_{BC}/V_{bibc})^{1/MJBC}$$

where V_{BC} is reverse biasing voltage, V_{bibc} is built in voltage in the base collector junction, MJC is grading coefficient for base collector junction, C_{JBC0} is the capacitance without biasing. Hence;

$$C_{JBC0}= Area^{*} \ sqrt(K_s\epsilon_0 q/2V_{bi})(N_B N_C/(N_B+ N_C))$$

where K_s is dielectric constant of semiconductor material (K_s= 11.7 for silicon), Area=17.2*10^{-6} , N_B and N_C are doping content in the base and collector respectively. And V_{BC} is given by [44]:

$$V_{inbc}= V_T \ln(N_C N_B/n_i^2)$$

The grading coefficient M_{JBC} lies between 0.3 and 0.5, and we will choose around 0.4. Hence,

$$C_{\mu} = C_{JBC0}= 1.86*10^{-12}F, V_{bibc}=0.64V$$

As a result the base collector junction capacitor C_{JBC} is [44]:

$$C_{JBC}= 1.86*10^{-12}$$

C_{π}= base emitter junction Capacitance + diffusion capacitance (Cd)

$$C_d= Q_B/V_{BE}|_{Qpoint}=W^2/2D_B*I_C/VT = 4.33*10^{-13}*I_C$$

where W is width of the base, QB is charge accumulated in the base, and D_B is diffusion coefficient.

The base emitter junction capacitance C_{JBE} is given by [43], [44]:

$$C_{JB0}= Area^{*} \ sqrt(K_s\epsilon_0 q/2V_{bi})(N_B N_C/(N_B+ N_C))$$

$$C_{\pi}= C_{JBE0}/ (1- V_{BE}/V_{bi})^{1/MJBE}$$

With M_{JBE}= 0.4, V_{BE}= 0.5V (the forward biasing voltage which is used to calculate the parameters of the transistor):

$$V_{bibe}= V_T \ln(N_E N_B/n_i^2)= 0.76V$$

$$C_{JBE0} = Area^{*} \ sqrt((K_s\epsilon_0 q/2V_{bi})(N_B NE/(N_B+ N_E))= 5.4*10^{-12}$$

$$C_{JBE}= C_{JBC0}/(1- V_{BE}/V_{bibe})1/M_{JBE}= 8.4*10^{-12}$$

$$C_{\pi}= 8.4*10^{-12} + 4.33*10^{-13}*I_C$$

Now the performances of the cascaded amplifier for high frequency of small signal will be investigated.

where C_{JBE0} capacitance between base and emitter at zero biasing, V_{bibe} is built in voltage between base and emitter

Input impedance

$$R_{in} = [1/(X_{C\mu}//r_\mu) + 1/(X_{C\pi}//r_\pi) + 1/(R_B)]^{-1} + X_c$$

$$(X_{C\mu}//r_\mu) = \{(2.2*10^{12}\ Ic + 8.24*10^6\ \beta)/(2\pi f(1.86*10^{-12}))\}/\ \{sqrt[(2.2*10^{12}\ Ic + 8.24*10^6\ \beta)^2 + 1.36*10^{10}/f^2\}$$

$$= [1.88*10^{23} IC/f + 7*10^{17}]/\ sqrt[(2.2*10^{12}\ Ic + 8.24*10^6\ \beta)^2 + 7.32*10^{21}/f^2]$$

$$(X_{C\pi}//r_\pi) = \{[26*10^{-3}\beta/I_C]/\ [(5.2*10^{-11} + 2.7*10^{-12} IC)]\}/\ \{sqrt[(26*10^{-3}\beta/I_C)^2 + (1/[5.27*10^{-11} + 2.7*10^{-12}\ I_C)^2/f^2]\}$$

$$Xc = 1/2\pi f\ (1*10\text{-}6) = 1.59*10^5/f$$

where f is frequency

Output impedance

$$R_{out} = R_o//\ R_c = \{4.7*10^3/[2.12*10^{-4} - [\beta/(2.2*10^{12} I_C + 8.24*10^6\beta)]]\}/\ \{(1/[2.12*10^{-4} - (\beta/(2.2*10^{12} I_C + 8.24*10^6\beta)]\ ) + 4.7*10^3\}$$

To calculate the output impedance, it will be suffice to substitute the current amplification factor β and collector current Ic.

Voltage gain

$$A_V = \ = [sqrt(\ 38*10^{18} + (4.39*10^{31}/f^{2)})]\ [[38.4I_c\ -\{sqrt[(26*10^{-3}\beta/I_C)^2 + (1/[5.27*10^{-11} + 2.7*10^{-12}\ I_C)^2/f^2]\}/\ \{4.7*10^3/[2.12*10^{-4} - [\beta/(2.2*10^{12} I_C + 8.24*10^6\beta)]]\}]^3$$

Current gain

$$A_{Is} = i_{b1}/i_s = R_B/\ ((r_\pi//X_{C\pi}) + R_B)$$

$$A_I = [R_B/\ ((r_\pi\ //\ X\ _\pi) + R_B)]\ [(g_{m1}-(1/r_{\mu1}//Xc_{\mu1}))\}/\{[(1/r_{\pi1}//XC_{\pi1}) + 1/(r_{\mu1}//X_{C\mu1})]^{-1}]^3$$

where r_π // X_π is resistor r_π parallel to capacitive reactance of X_π and g_m is transconductance.

The result of this investigation is fully analysed in chapter 4 in section 4.1.2 using MATLAB software.

Chapter Four
Result and Discussion

In chapter three, magnetic bipolar transistors were proposed and their performances on multistage amplifier were investigated. In this chapter, the obtained results are discussed. In section 4.1 the output response is investigated using MATLAB software. In section 4.2, simulation is conducted using LTspice and Hspice software.

4.1 Output responses using MATLAB software

4.1.1 Result obtained for low frequency re model small signal analysis using MATLAB software

In Figure 4.1, the density of electrons in the base is shown as function of polarization of electron in the base. We are using values for polarization of electron in the base in the range from -1 to 1. When we say -1, we are referring electrons are 100% polarized as spin down; i.e., there is no spin up polarized electron. Similarly, 1 implies that all electrons are polarized as spin up. When the value of polarization of electron lies between -1 and 1 (different from zero), it signifies that spin up electrons present predominantly as majority in the range between 0 and 1. Similarly, spin down electrons become majority in the range between -1 and 0.

Here in the plots, the abbreviations represents as follows:

P_{oe} –spin polarization of holes in the emitter

P_{obh} – spin polarization of holes in the base

P_{ob} – spin polarization of electrons in the base

P_e – injected non-equilibrium spin polarized electrons in the emitter

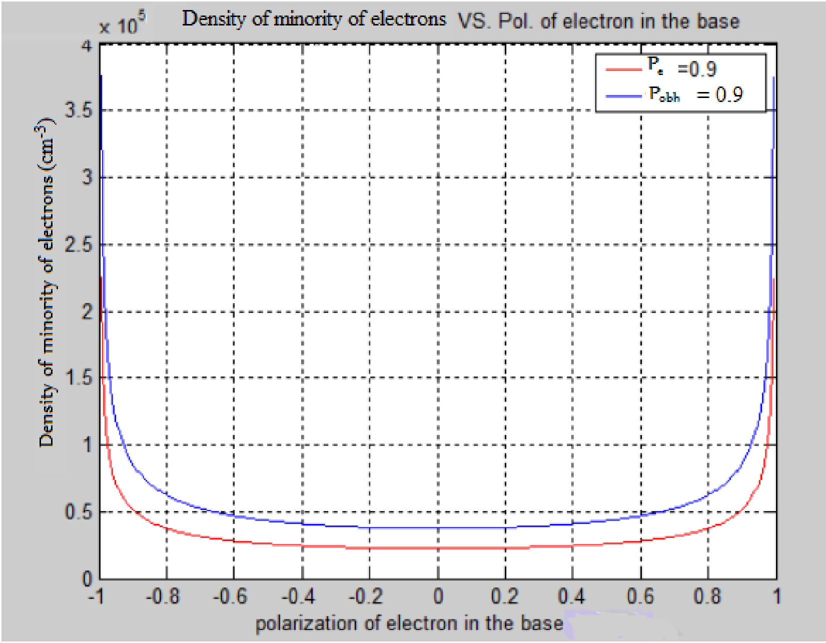

Figure 4.1: density of equilibrium electrons in the base versus polarization of equilibrium electron in the base

In Figure 4.1,

- The red line represents when base magnetic with injected spin electrons in the base set to P_e= 0.9, and only electrons are assumed spin polarized (this was done by researchers [31]).
- The blue line represents when base and emitter are magnetic, and electrons and holes are assumed spin polarized in the base with P_{obh}=0.9.

From the Figure 4.1, the density of electrons is highly dependent on electron's spin polarization. When the spin polarization of electrons set to zero, the value of density of electrons gives us the conventional transistor's density of electrons value. The density of electrons in the base rises significantly due to the presence of magnetic impurities in both emitter and base regions (which is shown in blue line). The number of spin polarized holes in the base due to spin splitting of energy bands help in increasing the density of electrons in the base. It should be clear that the emitter and collector currents are mainly function of density of carriers. Hence as the density of electrons increases, the currents will also increases. Similarly the current amplification factor deviates from the conventional value. As a result the variation of density of electrons has significant impact on the performances of the transistor.

The emitter current density as function of spin polarization of electrons in the base is shown Figure 4.2.

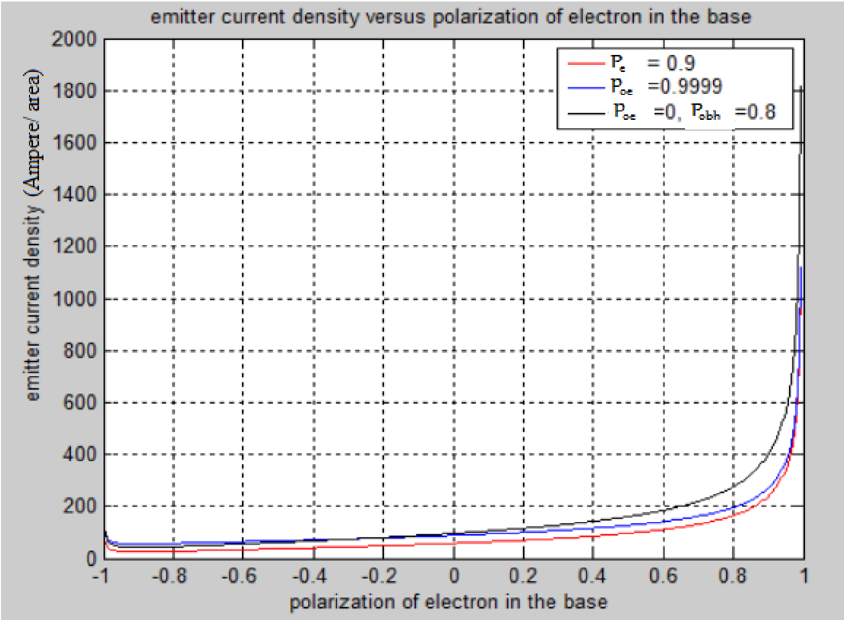

Figure 4.2: emitter current density versus polarization of equilibrium electron in the base.

In Figure 4.2,

- The red line represents when base magnetic with spin injection electrons in the emitter set to P_e =0.9, and only electrons are assumed spin polarized (this was done by researchers [31]).
- The black line represents when base and emitter are magnetic with the spin polarization of holes in the base set to P_{obh}= 0.8 and holes in the emitter set to P_{oe}=0, and both electrons and holes are assumed spin polarized.
- The blue line represents when is base and emitter are magnetic, and only electrons are assumed spin polarized with the spin polarization of holes in the emitter set to P_{oe}= 0.999.

From the Figure 4.2, we noted that as the spin up electrons becoming more and more predominantly majority, the emitter current density (black color line) rises up significantly in the model where base and emitter are magnetic (additionally electrons and holes are spin polarized) compared to the emitter current (the red color line) in the model where only the base are magnetic. So we noted that as far as the density of carriers' increases, the emitter current will also increases correspondingly. And since the number density of holes and electrons are dramatically rises up in the model where magnetic impurities employed, emitter current will also similarly shows increment in its magnitude as well.

Amplification is one of the main functions of bipolar transistor, and current amplification factor is the decisive parameter in voltage and current gain. In Figure 4.3, current amplification factor versus spin polarization of electrons is shown.

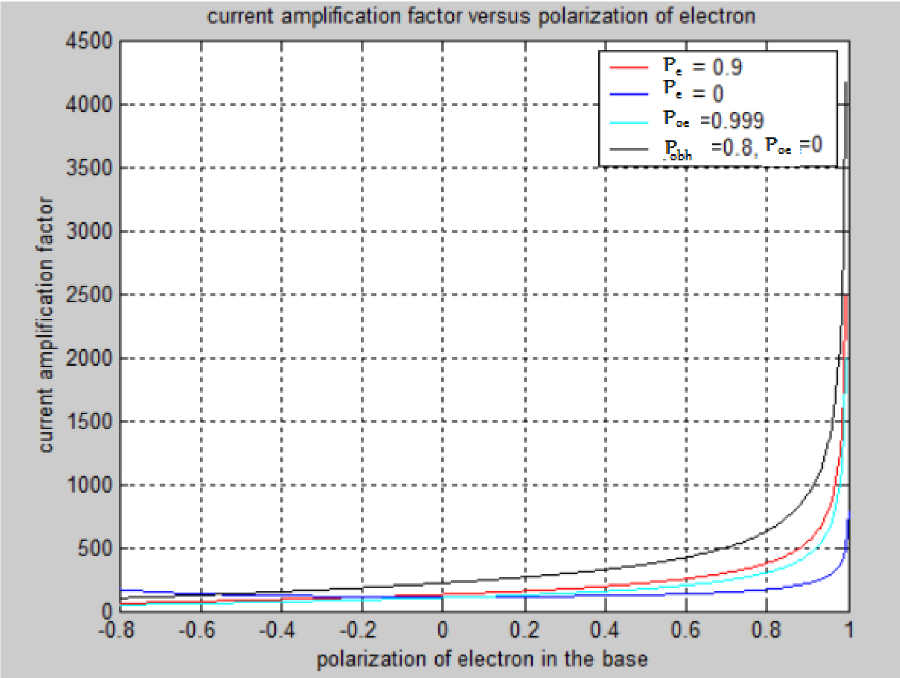

Figure 4.3: - current amplification factor versus base equilibrium electron's polarization.

In Figure 4.3,

- The red line represents when base is magnetic, and only electrons are assumed spin polarized in the base and with spin injection of electrons in the emitter set to P_e=0.9 (this was done by researchers [31]).
- The blue line represents when base is magnetic, and injected spin polarized electrons are ignored (P_e = 0).
- The black line represents when base and emitter are magnetic with the spin polarization of holes in the base set to P_{obh}= 0.8 and holes in the emitter set to P_{oe}=0 , and both electrons and holes are assumed spin polarized in the base.
- The light green line represents when base and emitter are magnetic with spin polarization of holes in the emitter set to P_{oe} =0.999, and only electrons are assumed spin polarized in the base.

Figure 4.3 shows how spins of carriers are used as a controlling input mechanism for current amplification factor of a transistor. When polarization of spin of electrons is zero, current amplification factor has the value of around 132 which corresponds to the conventional transistor value (when the emitter current is taken as 1mA). When the polarization of spin of electrons is increasing gradually, the current amplification factor gets larger and larger. As we can see the current amplification factor (the black line) has comparatively larger values in the model where the base and emitter are magnetic (Both electrons and holes are spin polarized in the base).

The 3D view of current amplification factor as a function of polarization of electrons and holes in the base is shown in Figure 4.4.

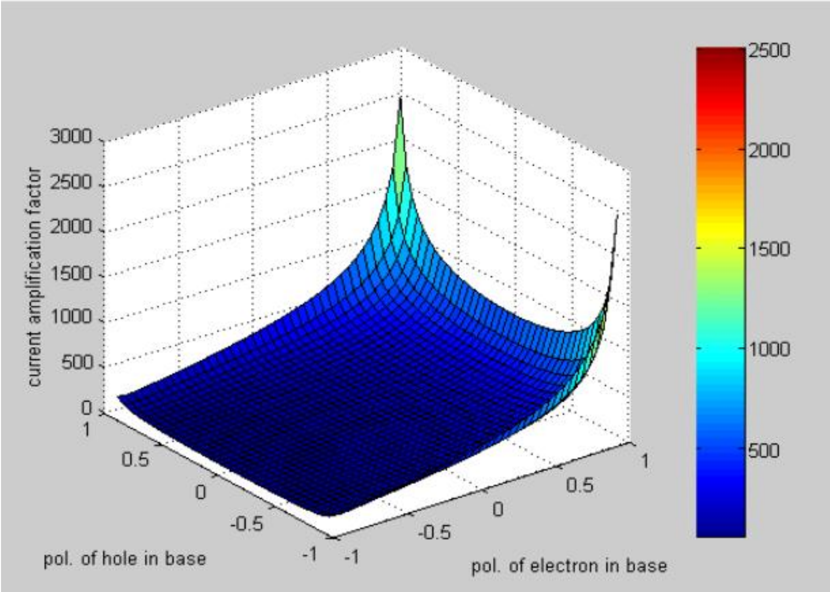

Figure 4.4: 3D view of current amplification factor

In Figure 4.4, as the spin up electrons becoming predominantly majority, the current amplification factor shoot up tremendously. This three dimensional curve has the same shape with the one we plotted in Figure 4.4 except the inclusion of holes as variable here.

In order to have full analysis of a transistor for small signal analysis, we need AC equivalent circuit models. We know emitter current is a function of emitter current and thermal voltage. In Figure 4.5, the calculated emitter resistance as function of polarization of electrons in the base is plotted.

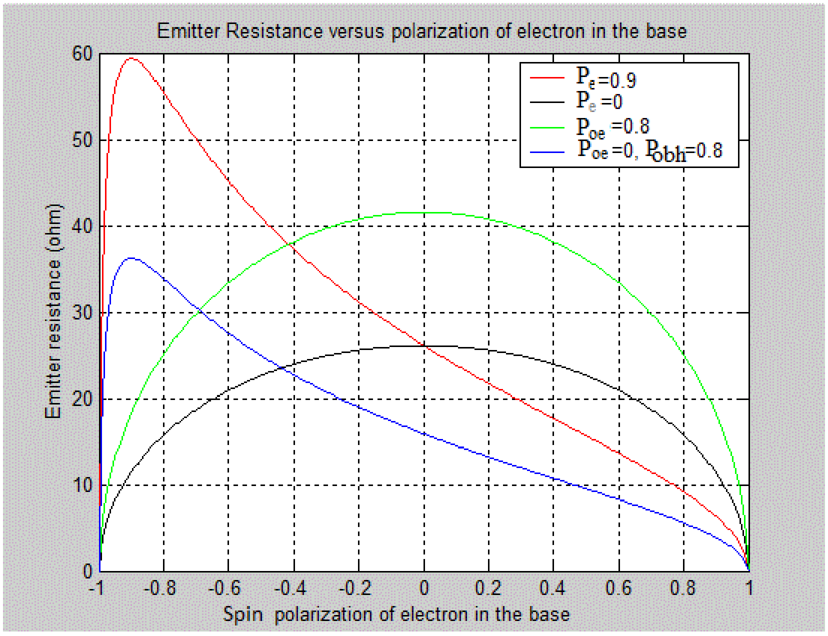

Figure 4.5: Emitter resistance versus polarization of electron in the base

In Figure 4.5,

- The red line represents when base magnetic with the spin injection of electrons in the emitter set to P_e=0.9, and only electrons are assumed spin polarized (this was done by researchers [31] when only base is magnetic).
- The black line represents when the base is magnetic, and injected spin polarized electrons are ignored P_e=0 (It means that on the conventional BJT we added only magnetic material on the base side and we didn't use additional spin injection).
- The blue line represents when base and emitter are magnetic, and electrons and holes are assumed spin polarized in the base with spin polarization of holes in the base set to P_{obh}=0.8 and spin polarization of holes in emitter set to p_{oe}=0.
- The light green line represents when base and emitter are magnetic with spin polarization of holes in the emitter set to P_{oe} =0.8, and only electrons are assumed spin polarized in the base.

From the Figure 4.5, we can see that wide range values of resistance for different polarization of electrons are obtained. In contrast to conventional transistor, where the resistance value is fixed (26 ohm- resistance value for emitter current of one milliampere which is related to zero spin polarization of electrons as shown in the figure), the emitter resistance in spin based transistor can have wide range of values. This may be a good option for applications that seek different design parameters. The emitter resistance 3D view as function of spin polarization of electrons in the base is shown Figure 4.6.

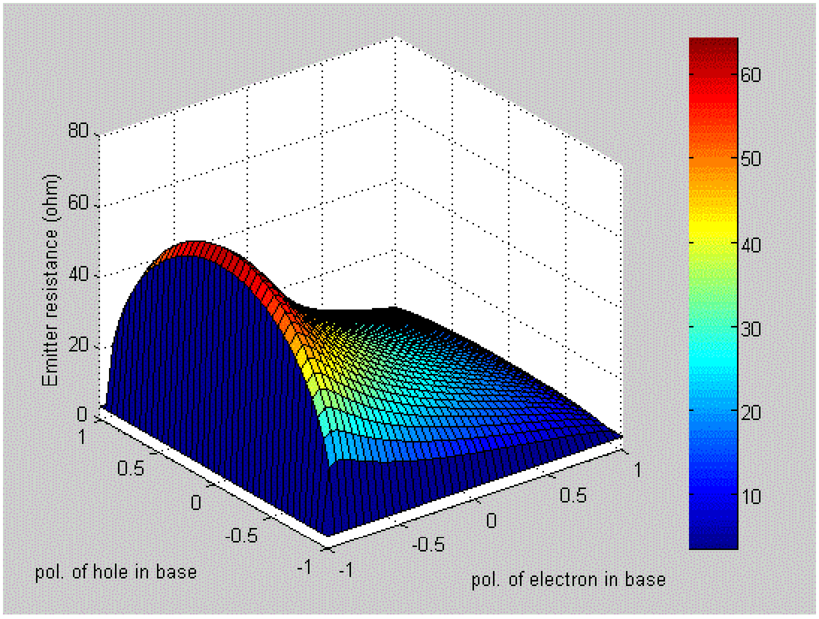

Figure 4.6: 3D view of emitter resistance

From 3D view in Figure 4.6, we can see that when both spin polarization of electrons and holes in the base are zero (the number of spin up and spin down electron are equal), we get the emitter resistance equal to 26 ohm which is a conventional transistor's emitter resistance value when the emitter current is taken at 1mA. It is clear that it is possible to find wide range of emitter resistance values by varying both polarization hole and electron or either of them.

Input impedance is another important parameter in dealing with amplifier. In Figure 4.7, the input impedance as function of polarization of electrons is plotted.

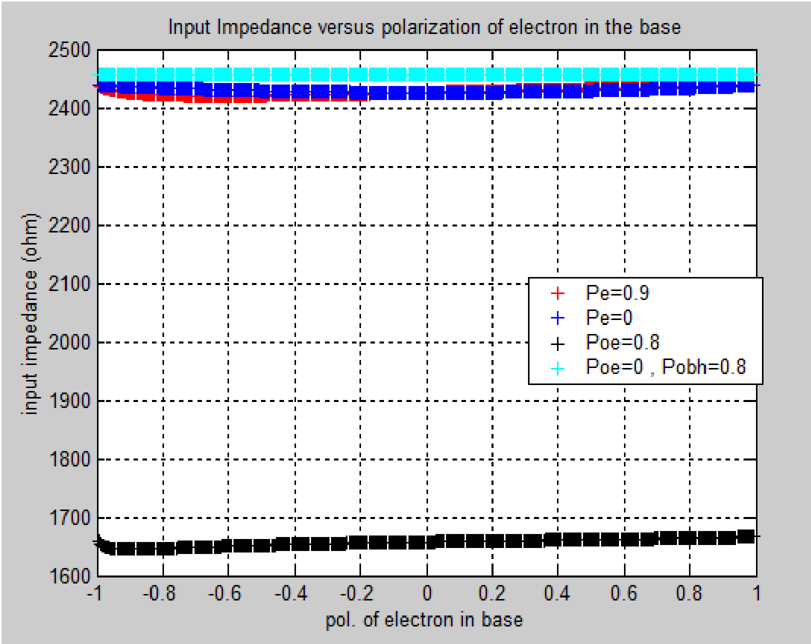

Figure 4.7: Input impedance versus polarization of electron in the base

In Figure 4.7,

- The red line represents when base magnetic with the spin injection of electrons in the emitter set to P_e=0.9, and only electrons are assumed spin polarized (this was done by researchers [31]).
- The blue line represents when base is magnetic, and injected spin polarized electrons are ignored P_e=0 (It means that on the conventional BJT we added only magnetic material on the base side and we didn't use additional spin injection).
- The light green line represents when base and emitter are magnetic, and electrons and holes are assumed spin polarized in the base with spin polarization of holes in the base set to P_{obh}=0.8 and spin polarization of holes in emitter set to p_{oe}=0.
- The black line represents when base and emitter are magnetic with spin polarization of holes in the emitter set to P_{oe} =0.8, and only electrons are assumed spin polarized in the base.

From Figure 4.7, we note that the input impedance is dependent on spin, and as a result, it is managed to obtain wide range of values of input impedance. This will help in selecting suitable input impedance that suit specific application. We can see also that the input impedance remains constant for specific value of spin polarization of holes in the base and for variable values of spin polarization of electrons in the base. The input impedance is higher in the proposed magnetic bipolar transistor model (Where base and emitter are magnetic and in addition the electrons and hole are spin polarized). This is as a result of spin polarization of holes in the base.

Figure 4.8 is plotted below for the proposed magnetic transistor (Where both base and emitter is magnetic and electrons are only assumed spin polarized) separately because of its having smaller magnitude compared to the others (Shown in figure 4.7)

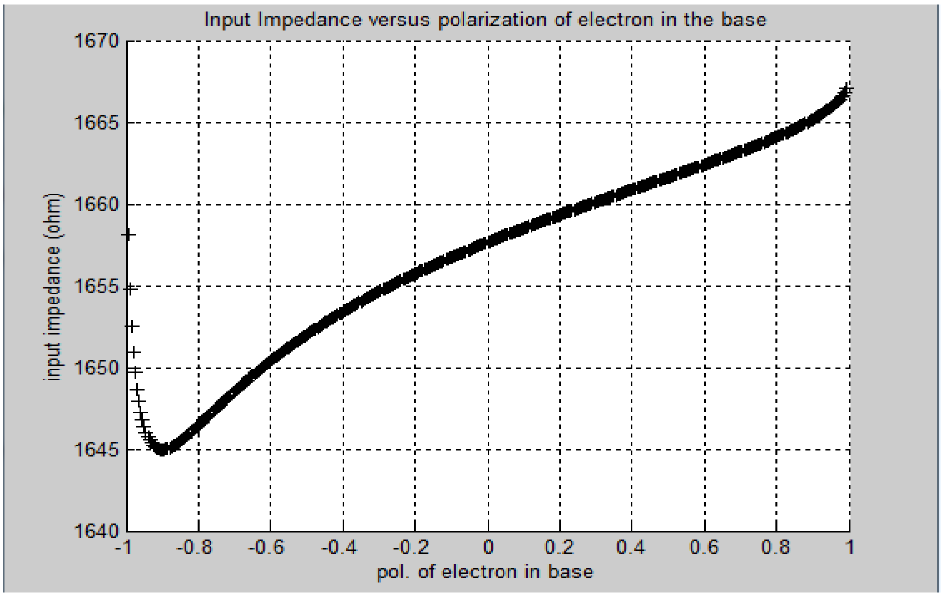

Figure 4.8: Input impedance for magnetic transistor (When both emitter and base are magnetic and only electrons are spin polarized in the base)

The input impedance of the proposed model shown in Figure 4.8, slightly lower in magnitude than the other proposed models (Shown in Figure 4.7). The reason behind this is that the current amplification factor in this proposed model has lower magnitude compared to the others. This is attributed for the presence of magnetic impurities in the emitter. Even though the higher magnitude of density holes will increase the magnitude of the emitter current, it will also boost the magnitude of the density of base current. As a result the current amplification factor is lower in magnitude.

The 3D calculated input impedance is shown in Figure 4.9 as function of spin polarization of electrons and holes in the base.

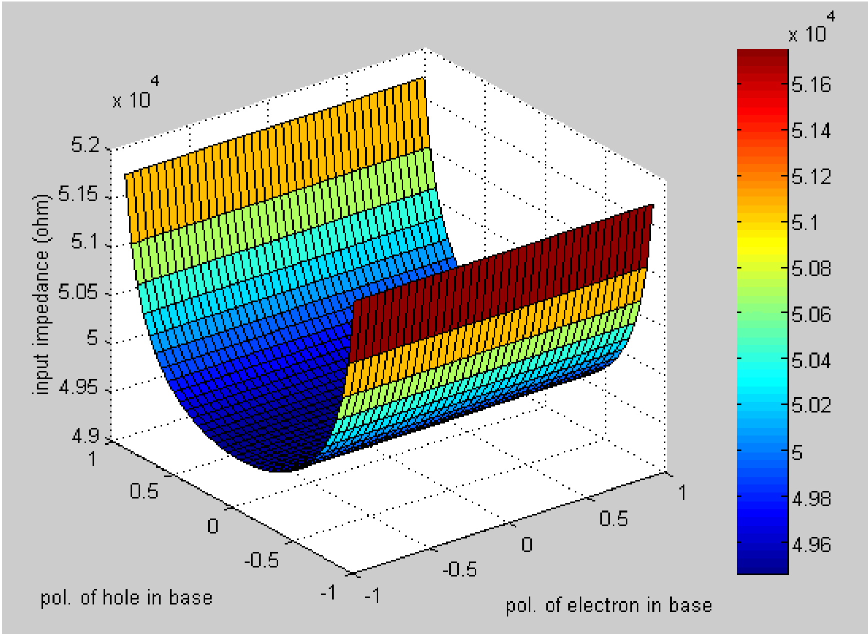

Figure 4.9: input impedance in 3D

From the Figure 4.9, we understand that for fixed values of spin polarization of holes in the base, the input impedance has constant value regardless of what values of spin polarization of electrons have. The input impedance in Figure 4.9 has the same graph plotted in 2 dimension plot in Figure 4.7. By holding the spin polarization of holes at constant value and varying the spin polarization of electrons, we can get constant input impedance in the proposed model where the base and emitter are magnetic (depicted in light green color in Figure 4.7).

The calculated voltage gain versus polarization of electrons is shown in Figure 4.10.

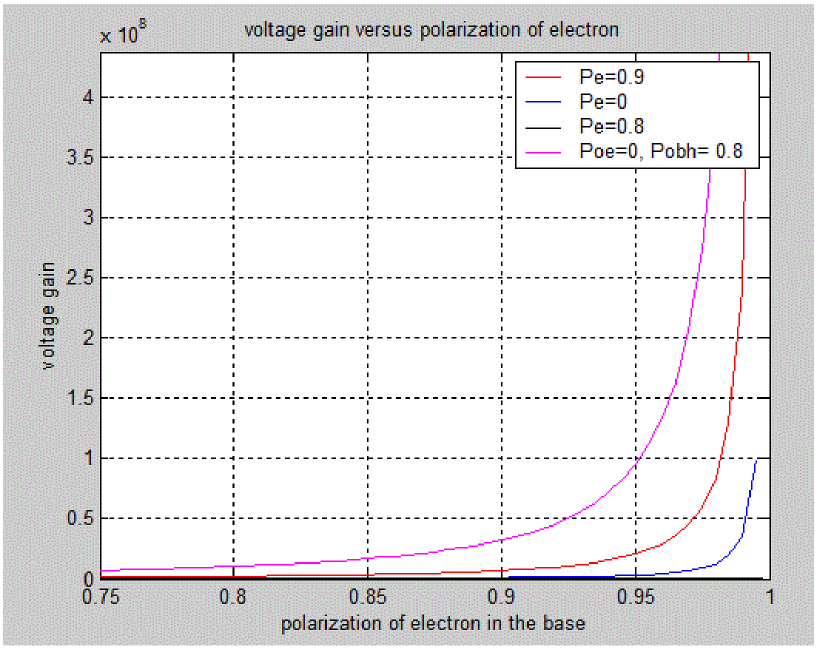

Figure 4.10: voltage gain versus polarization of equilibrium electron in the base.

In Figure 4.10,

- The red line represents when base magnetic with the spin injection of electrons in the emitter set to P_e=0.9, and only electrons are assumed spin polarized (this was done by researchers [31]).
- The blue line represents when base are magnetic, and injected spin polarized electrons are ignored P_e=0 (It means that on the conventional BJT we added only magnetic material on the base side and we didn't use additional spin injection).
- The light red (magenta) line represents when base and emitter are magnetic, and electrons and holes are assumed spin polarized in the base with spin polarization of holes in the base set to P_{obh}=0.8 and spin polarization of holes in emitter set to p_{oe}=0.
- The black line represents when base and emitter are magnetic with spin polarization of holes in the emitter set to P_{oe} =0.8, and only electrons are assumed spin polarized in the base.

The voltage gain increases comparatively when the spin is becoming dominantly spin up electrons in the model where the base and emitter is magnetic (Both electrons and holes are spin polarized). Since the current amplification factor is higher in the proposed model where the base and emitter are magnetic (depicted in light red or magenta color), the voltage gain also will increases similarly.

In Figure 4.11, the calculated current gain as function of polarization of electrons is plotted below.

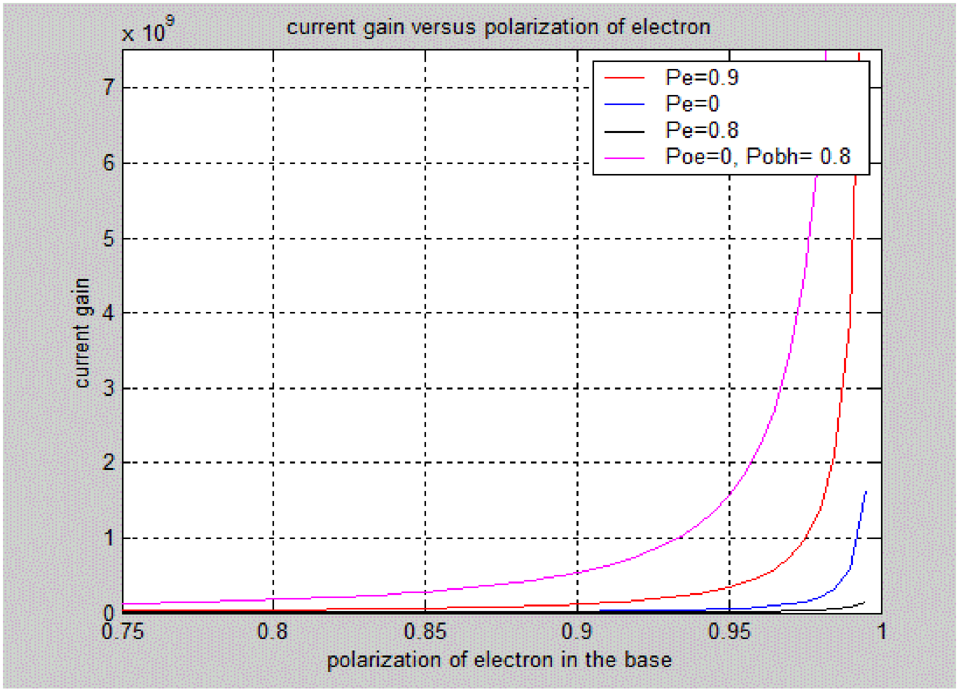

Figure 4.11: current gain versus polarization of equilibrium electron in the base.

In Figure 4.11:

- The red line represents when base magnetic with the spin injection of electrons in the emitter set to P_e=0.9, and only electrons are assumed spin polarized (this was done by researchers [31]).
- The blue line represents when base are magnetic, and injected spin polarized electrons are ignored P_e=0 (It means that on the conventional BJT we added only magnetic material on the base side and we didn't use additional spin injection).
- The light red (magenta) line represents when base and emitter are magnetic, and electrons and holes are assumed spin polarized in the base with spin polarization of holes in the base set to P_{obh}=0.8 and spin polarization of holes in emitter set to p_{oe}=0.
- The black line represents when base and emitter are magnetic with spin polarization of holes in the emitter set to P_{oe} =0.8, and only electrons are assumed spin polarized in the base.

In Figure 4.11, the current gain in both proposed models (the red line and the magenta (light red line)) show improvement in its magnitude compared to the conventional bipolar transistor's current gain (when spin polarization is zero). Current gain is approximately proportional to cube of current amplification factor. As a result the current gain we obtained is reasonable.

4.1.2 Analysis for higher frequency for small signal

In section 4.1.1, we considered the small signal for low frequency cascaded amplifier of re-model using MATLAB software. And that was done by plotting different parameters as function of spin of polarization of carriers. In this section, we will investigate the low and high frequency small signal analysis for hybrid-π model as function of frequency.

In the coming all simulations analysis, the current amplification factor β 132 represents the conventional bipolar transistor's value. This comes from the fact that using the parameters listed in section 3.3.1, the current amplification factor for the conventional bipolar transistor is evaluated first. After that, the same parameters which were used for conventional transistor are applied on the proposed magnetic bipolar transistors alongside with the injection of spin in different regions of a transistor as explained in chapter 3. And then at different spin polarization of carriers, the current amplification factors for proposed transistor are evaluated.

For small signal analysis and for low frequency, the input impedance as function of frequency is plotted in Figure 4.12:

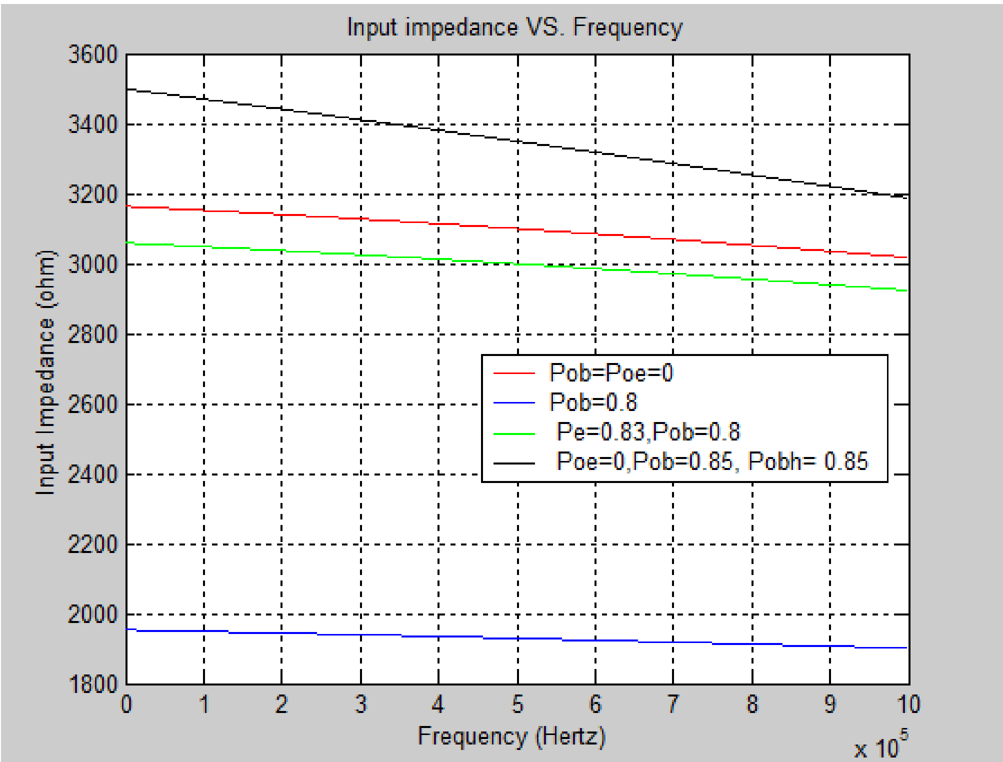

Figure 4.12: Input impedance as function of frequency for low frequency

In Figure 4.12:

The red line represents a transistor which has current amplification factor β= 132. This transistor is considered as a conventional transistor. This is because; using appropriate values we obtained the required parameters of the transistor.

The blue line represents a proposed magnetic bipolar transistor (Where the base and emitter are magnetic and only electrons are spin polarized in the emitter which is P_{oe}= 0.8) with current amplification factor β = 248.

The green line represents a proposed transistor by the researchers [31] (Where only base is magnetic material) with current amplification factor β of 378.

The black line represents a proposed transistor (Where the base and emitter are magnetic material, and both electrons and holes are spin polarized in the base with electrons are spin polarized with P_{0b}=0.85, holes spin polarized in emitter with P_{0e} = 0.83 and holes are spin polarized in the base with P_{obh}= 0.83) with current amplification factor β =826.

From Figure 4.12, the proposed transistor with current amplification factor 826 (With both base and emitter are magnetic including both electrons and holes are spin polarized) has higher magnitude of input impedance. The output responses shown in Figure 4.12 has similar trend of output responses shown in section 4.1.1 in Figure 4.7.

In Figure 4.13, the input impedance for high frequency as function of frequency is plotted.

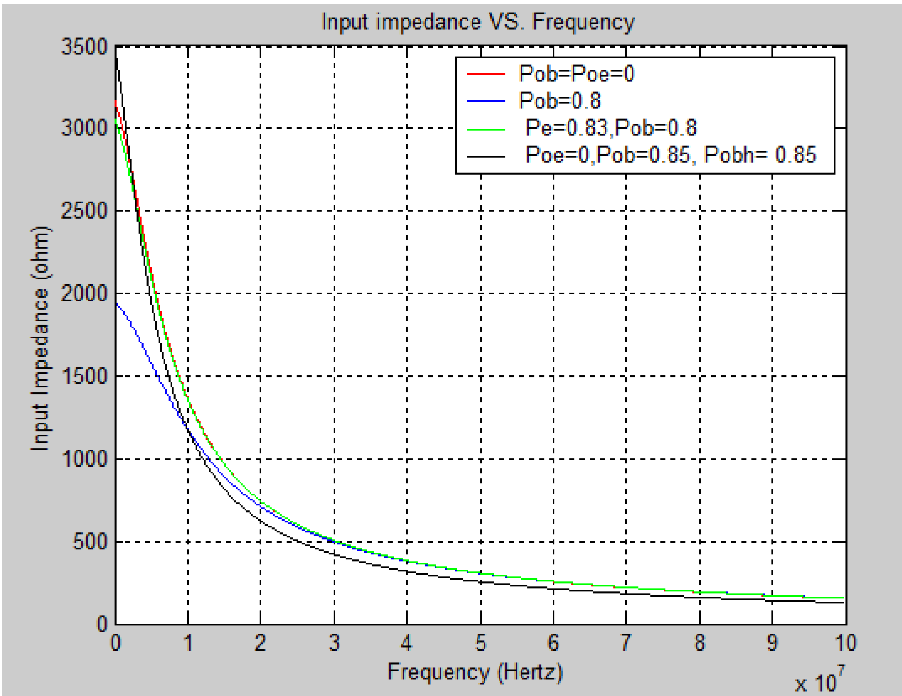

Figure 4.13: Input impedance for relatively higher frequency

In Figure 4.13:

The red line represents a transistor which has current amplification factor β =132. This transistor is considered as a conventional transistor. This is because; using appropriate values we obtained the required parameters of the transistor.

The blue line represents a proposed magnetic bipolar transistor (Where the base and emitter are magnetic and only electrons are spin polarized in the base which is P_{ob}= 0.8) with current amplification factor β = 248.

The green line represents a proposed transistor by the researchers [31] (Where only base is magnetic material) with current amplification factor β of 378.

The black line represents a proposed transistor (Where the base and emitter are magnetic material including both electrons and holes are spin polarized in the base with electrons are spin polarized with P_{0b}=0.85, holes spin polarized in emitter with P_{0e} = 0.83 and holes are spin polarized in the base with P_{obh}= 0.83) with current amplification factor β =826.

In Figure 4.13, more or less all the proposed transistors eclipsed the conventional transistor's input impedance value. We can also see that its input impedances are deteriorating at very high frequencies.

In Figure 4.14, the voltage gain for relatively high frequency is plotted.

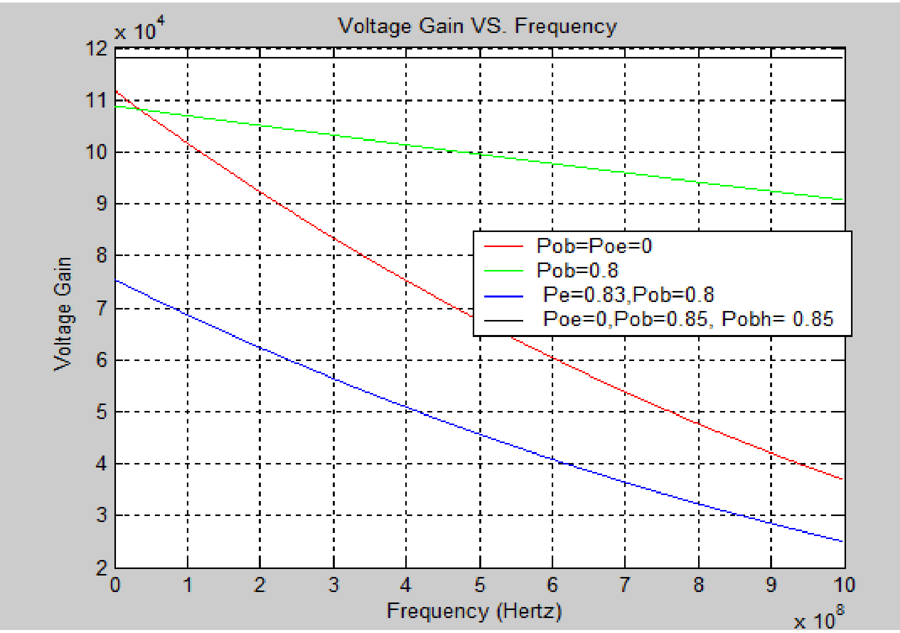

Figure 4.14: voltage gain at high frequency as function of frequency

In Figure 4.14:

The red line represents a transistor which has current amplification factor β 132. This transistor is considered as a conventional transistor. This is because; using appropriate values we obtained the required parameters of the transistor.

The blue line represents a proposed magnetic bipolar transistor (Where the base and emitter are magnetic and only electrons are spin polarized in the base which is P_{oe}= 0.8) with current amplification factor β 248.

The green line represents a proposed transistor by the researchers [31] (Where only base is magnetic material) with current amplification factor β of 378.

The black line represents a proposed transistor (Where the base and emitter are magnetic material including both electrons and holes are spin polarized in the base with electrons are spin polarized with P_{0b}=0.85, holes spin polarized in emitter with P_{0e} = 0.83 and holes are spin polarized in the base with P_{obh}= 0.83) with current amplification factor β 826.

From Figure 4.14, we note that all the spin base proposed transistors shows good performance which will agree with our analysis in Figure 4.10. But the voltage gain is not constant for certain of ranges of frequency. Something should be done to make the voltage gain constant. In addition its magnitude is deteriorating at higher frequencies.

4.2 Simulation result for cascaded amplifier using Spice software

In section 4.1, we plotted the mathematical model using MATLAB software. Next we will simulate the electrical circuit model of the system using LTspice XVII and Hspice software. LTspice is used because it is comfortable working with schematics. On the other hand Hspice is programing language based software which is explained in section 4.2.2.

4.2.1 Using LTspice XVII software

It is worth consideration that both the conventional and proposed transistors which have been dealing here have been assumed made of the same parameters except the incorporation of magnetic materials in different regions and the injection of spin injection of electrons in the emitter and collector of the proposed magnetic bipolar transistors.

In the coming all simulations analysis, the current amplification factor β = 132 represents the conventional bipolar transistor's value. This comes from the fact that using the parameters listed in section 3.3.1, the current amplification factor for the conventional bipolar transistor is evaluated first. After that, the same parameters which were used for conventional transistor are applied on the proposed magnetic bipolar transistors alongside with the injection of spin in different regions of a transistor as explained in chapter 3. And then at different spin polarization of carriers, the current amplification factors for proposed transistor are evaluated.

In order to carry out the simulation in the LTspice, we need transistor models that suits the magnetic bipolar transistors and the conventional bipolar transistor characteristics. In this way, it is possible to use parameters pertinent to each respective type of transistors. Hence it is imperative to develop transistor symbol for the proposed transistors. The transistor symbol developed using LTspice is shown in Figure 4.15. Following this, essential parameters for each developed magnetic bipolar transistors is incorporated in the developed transistors' model, and saved in the library file of the LTspice.

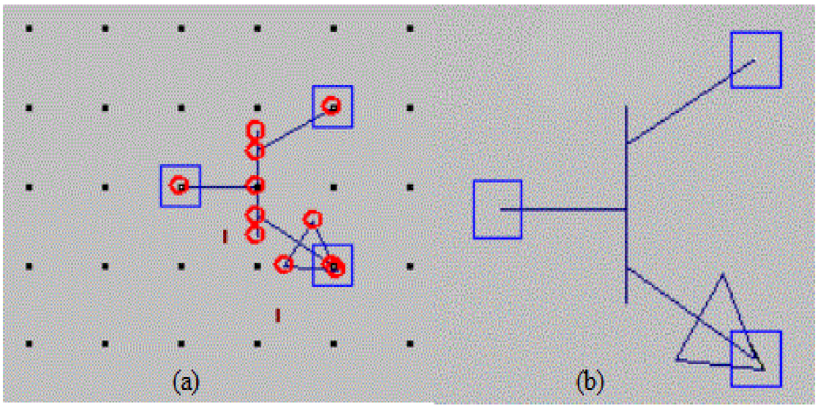

Figure 4.15: a) customizing symbol b) transistor symbol

H-parameter of the transistor is measured for current amplification factor of β=132 and β=248 using LTspice and calculated, and the result is shown in Table 4.1. At current amplification factor β =132, spin polarization of carriers is assumed zero (Conventional transistor). And for current amplification factor β = 248, the spin polarization of electrons in the base is P_{0b}= 0.83 and the spin polarization of holes in the emitter is P_{oe}= 0.8 (magnetic bipolar transistor in which the base and emitter are magnetic and in addition only electrons are spin polarized in the base).

H parameter	β =132	β =248
h_{ie}	4923	9,044
h_{re}	$2.07*10^{-4}$	$1.72*10^{-4}$
h_{fe}	114	214
h_{oe}	$2.07*10^{-4}$	$1.1*10^{-5}$

Table 4.1: H- parameters of the transistors for β=248 and β=132

From the table 4.1, we see that the input impedance is higher for proposed model (When the base and emitter are magnetic in addition electrons are only spin polarized in the base) when current amplification factor is β =248. The forward current gains have more or less closer value to the dc current amplification factors.

Figure 4.16 shows a cascaded amplifier after we customized the transistor symbol and connected in LTspice. In Figure 4.16, the cascaded amplifier is shown with created transistor model for current amplification factor of 132 with the transistor model of 2ERM132.

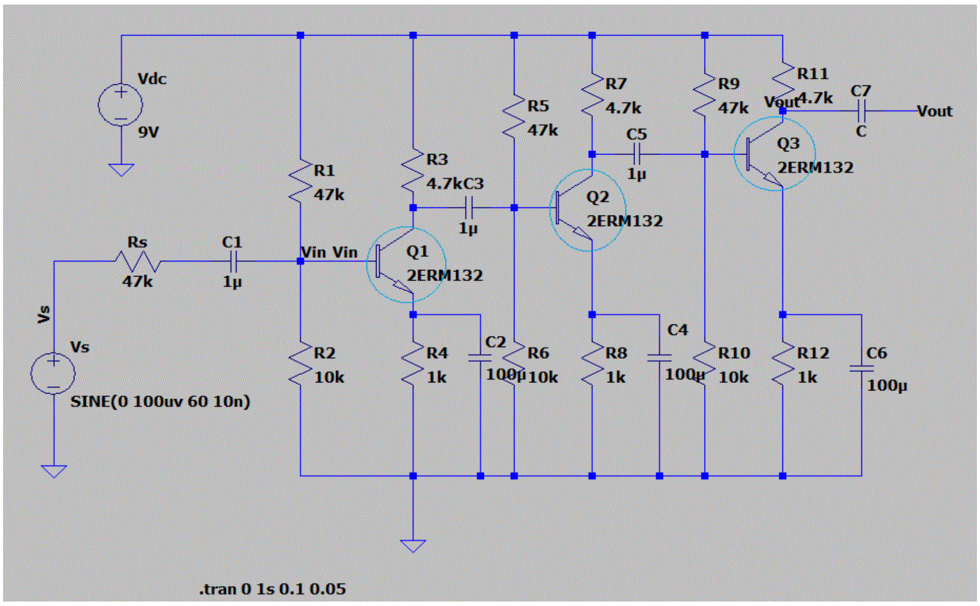

Figure 4.16: cascaded amplifier

Next, the output responses of the cascaded amplifier are simulated for different cases:

1) When the magnetic bipolar transistor is magnetic in the base and in the emitter region, including only electrons are spin polarized in the base.
2) When the magnetic bipolar transistor is magnetic in the base and in the emitter, including electrons and holes are spin polarized in the base.
3) When only the base is magnetic, and only electrons are spin polarized in the base (This is the researcher's [31] work)
4) For the conventional transistor for β=132 (Spin polarization is zero)

1- When the magnetic bipolar transistor is magnetic in the base and in the emitter region, including only electrons are spin polarized in the base.

For spin polarization of holes in the emitter P_{oe}= 0.8 and spin polarization of electrons in the base P_{ob} = 0.83 (magnetic bipolar transistor when base and emitter are magnetic and also electrons are only spin polarized in the base), different parameters calculated as [39]:

β = 248, i_c= 3.1mA, I_s= I_C exp($-V_{be}/V_t$) = 1.42* 10^{-11} A, $V_{JE}=v_t \ln N_E N_B/n_i^2$=0.757, V_{JC}= $V_t \ln(N_E N_B/n_i^2)$= 0.64, C_{JE0}=sqrt(($\epsilon_s q N_B N_E$)/(2V_{JE}(N_B +N_E)))= 5.4*10^{-12}, C_{JC}= sqrt(($\epsilon_s q N_B N_C$)/(2V_{JC}(N_B +N_C)))=1.86*10^{-12}

Simulation is also done for conventional bipolar transistor with relevant parameters calculated as:

β = 132, i_c= 1mA, I_s= I_C exp($-V_{be}/V_t$) = 4.58* 10^{-12} A, $V_{JE}=v_t \ln N_E N_B/n_i^2$=0.757, V_{JC}= $V_t \ln(N_E N_B/n_i^2)$= 0.64, C_{JE0}=sqrt(($\epsilon_s q N_B N_E$)/(2V_{JE}(N_B +N_E)))= 5.4*10^{-12}, C_{JC}= sqrt(($\epsilon_s q N_B N_C$)/(2V_{JC}(N_B +N_C)))=1.86*10^{-12}

where I_s is saturation current, V_t is thermal voltage, ϵ_s is permittivity of air, V_{JE} and V_{JC} are built in voltage across base emitter and base collector junctions respectively, C_{JEO} is capacitance due to base to emitter junction when there is no biasing and C_{JC0} is base collector junction capacitance without the presence of biasing.

Input impedance will be investigated below for different current amplification factors. Input impedance at spin polarization of holes in the emitter P_{oe}= 0.8 and spin polarization of electrons in the base P_{ob} = 0.83 (magnetic bipolar transistor when base and emitter are magnetic and also electrons are only spin polarized in the base), current amplification factor has the value of 248. Input impedance at current amplification factor β= 248 is simulated in Figure 4.17.

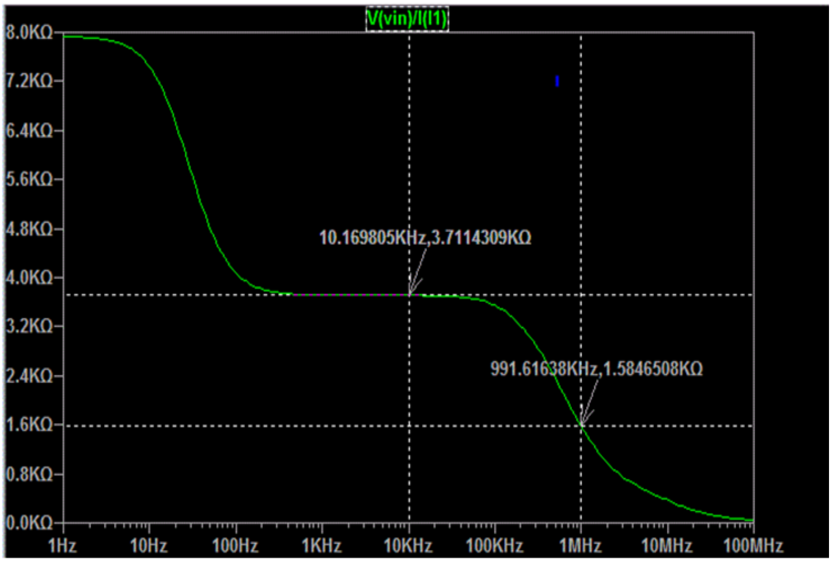

Figure 4.17: input impedance for current amplification factor of β= 248

From Figure 4.17, the input impedance count high at lower frequencies and start declining as the frequency increases.. The main reason for this trend is that at low frequencies the reactance of the capacitor become large and its contribution to the whole input impedance will be higher. At higher frequency, the capacitor will have generally very small reactance in such case it can be ignored.

In Figure 4.18, the input impedance for current amplification factor of 132 is simulated. It should be remembered that the transistor with current amplification factor of 132 is considered the conventional bipolar transistor value which we calculated using relevant data.

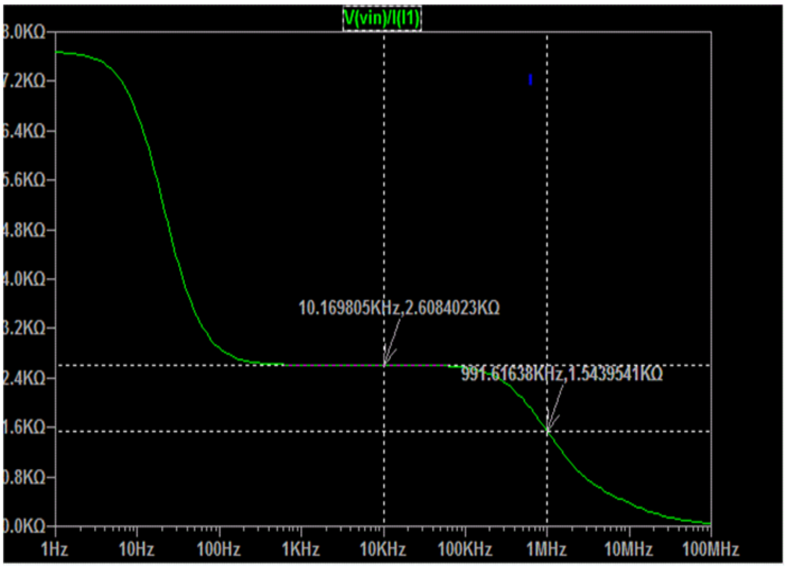

Figure 4.18: input impedance at β=132

From simulation result of Figure 4.17 and Figure 4.18, the input impedance is higher for β = 248 (when spin polarization is P_{oe} = 0.8, and p_{ob} = 0.83). In most application areas, high impedance is needed.

In Figure 4.19 and Figure 4.21, the output impedance is simulated for magnetic bipolar transistor and conventional transistor. For magnetic bipolar transistor of spin polarization of electrons P_{ob} = 0.8 and spin polarization of holes P_{oe}= 0.83, the current amplification factor is around β = 248.

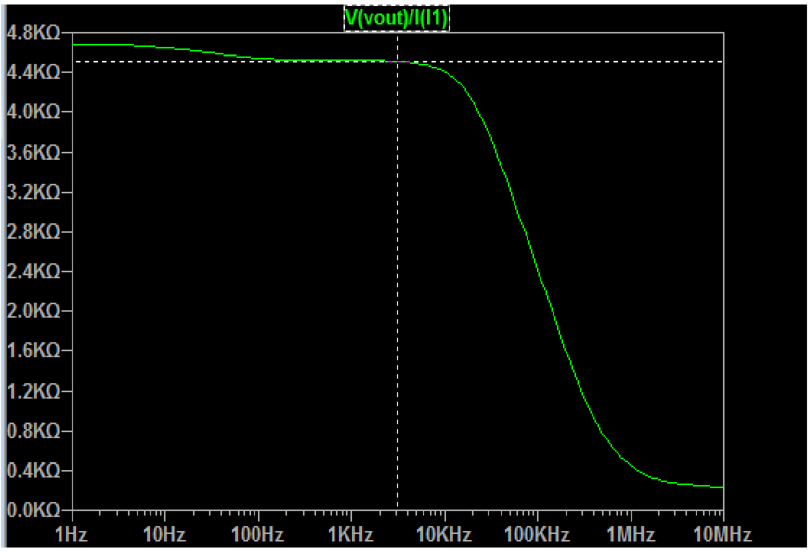

Figure 4.19: detailed measurement for output impedance at β= 248

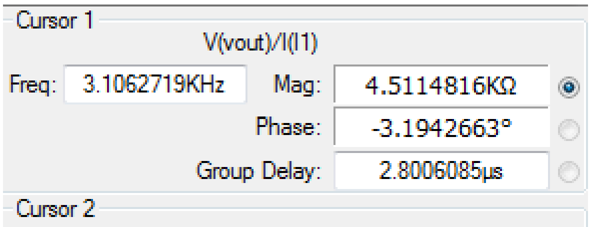

Figure 4.20: Detailed measurement of output impedance for β= 248

For the current amplification factor 132, the output impedance is simulated in Figure 4.21.

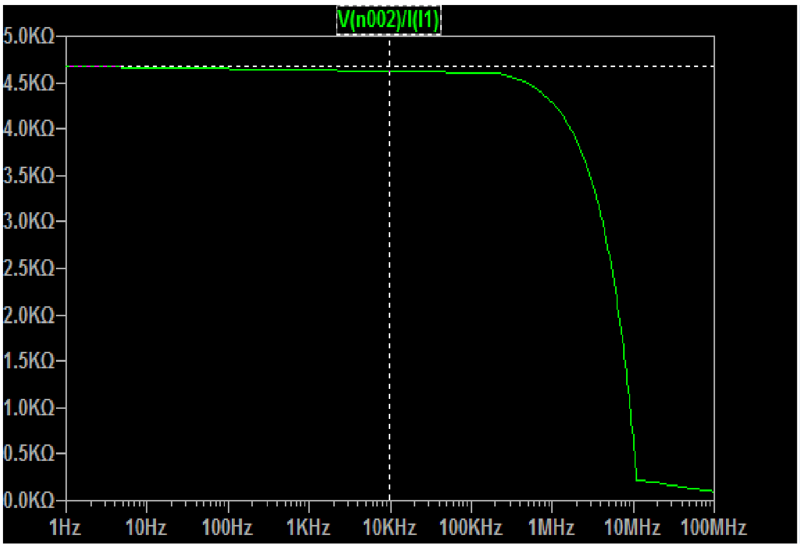

Figure 4.21: output impedance for B= 132

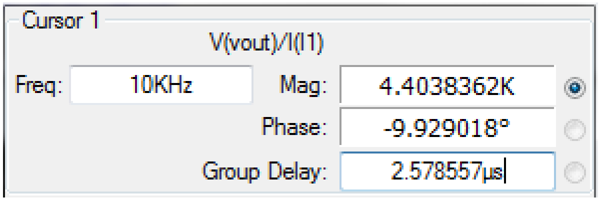

Figure 4.22: Detail measurement of output impedance for B=132

As it was predicted in section 4.1, the output impedance more or less has the same for all cases. This is because the output impedance of the third amplifier is too large, and the net output impedance rely on the collector transistor which is R_{c3}= 4.7k ohm.

In order to determine the voltage gain, the output and input waveforms simulated for different current amplification factor β which represent proposed model and the conventional bipolar transistors. In Figure 4.23 and Figure 4.25, simulations of voltage gains for current amplification factor β of 132 and current amplification factor β of 248 are presented respectively.

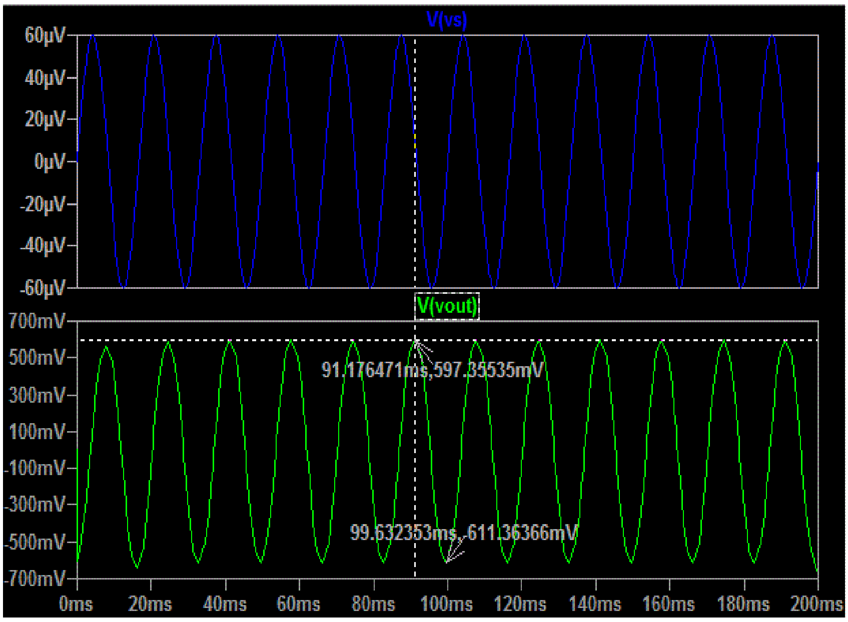

Figure 4.23: voltage wave form for B=132

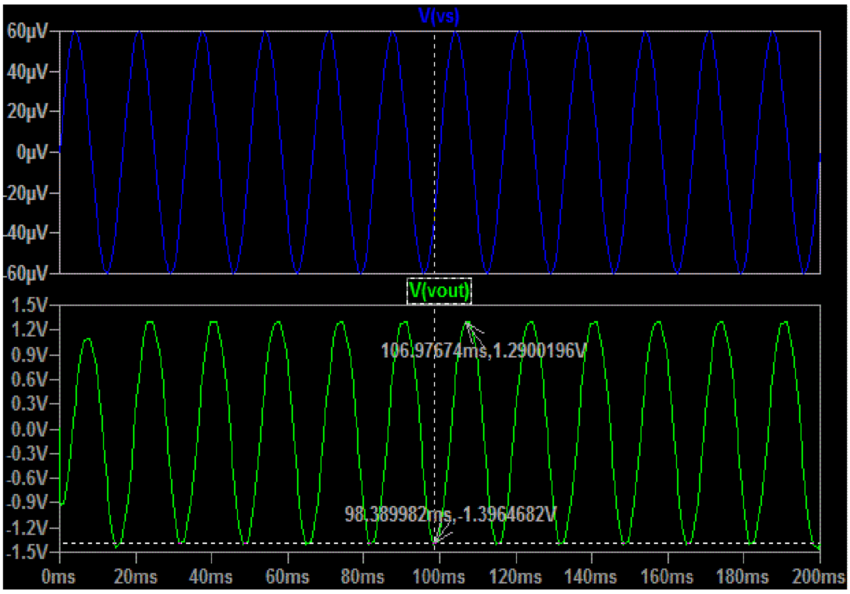

Figure 4.24: input and output voltage waveforms at β =248 to determine voltage gain

Figure 4.24, the peak to peak voltage at current amplification factor β=248 is approximately 2.68V whereas the peak to peak input voltage is 120uv. Therefore the voltage gain is A_v = $V_{out}(pp)/V_{in}(pp)$= 2.23 *10^4. From Figure 4.23, the voltage gain for current amplification factor β=132 is A_v= $V_{out}(pp)/V_{in}(pp)$ = 1.2V/120uV= 1 *10^4.

The current gain performance for different current amplification factor (Current amplification factor of 248 and 132) is simulated in Figure 4.25 and Figure 4.26 respectively.

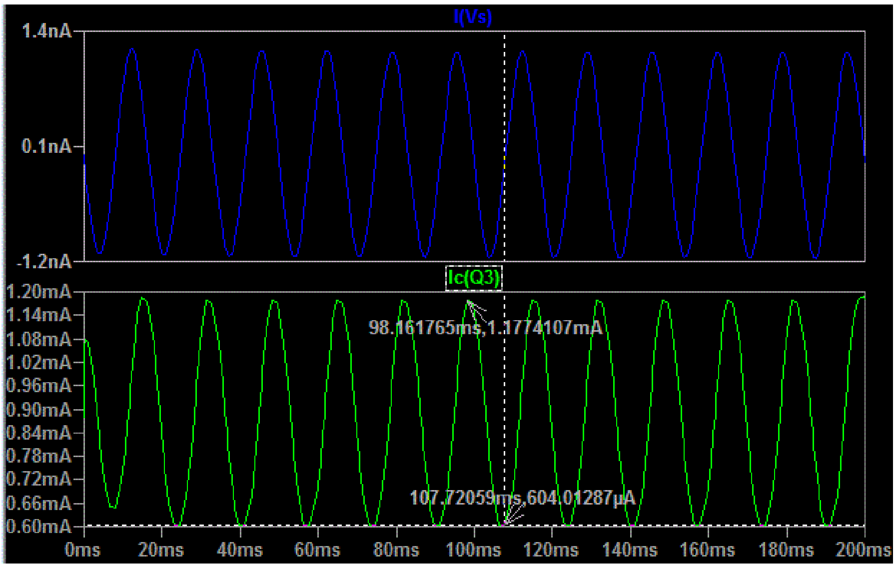

Figure 4.25: Current wave form for current amplification factor of β=248

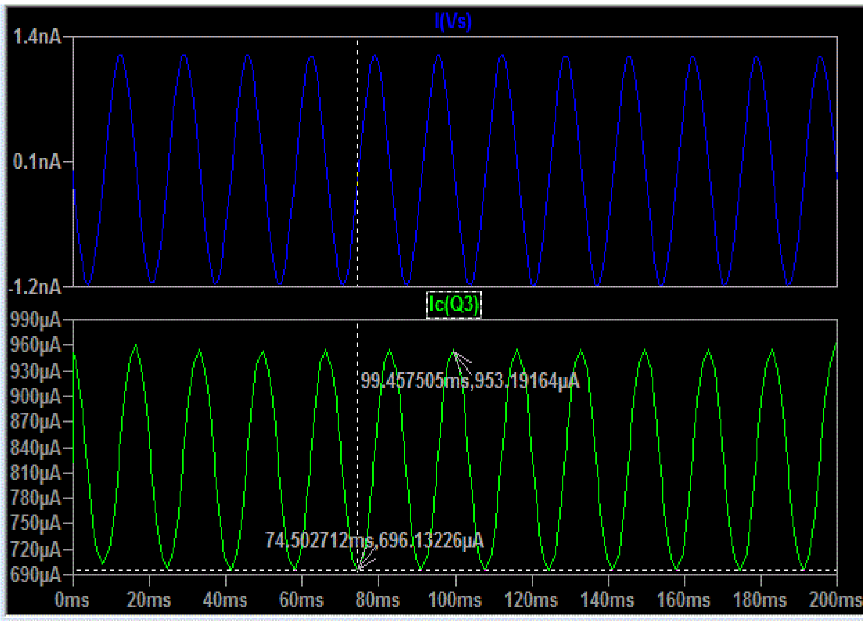

Figure 4.26: current output waveform for β =132

From Figure 4.25, the peak to peak current output for current amplification β =248 is $I_{out}(pp)$= 0.573mA and the peak to peak input current is $I_{in}(pp)$= 2.4nA. So the current gain is A_i= I_{out}/I_{in} = 1.2mA/4nA=2.38*10^5. Similarly for β = 132 in figure 4.26, the current gain is I_{out}/I_{in}= 0.257mA/2.4nA= 1.07* 10^5. And it can be concluded that the current gain is good at current amplification β =248.

2- Simulation of magnetic bipolar transistor when both base and emitter are magnetic including electrons and hole are spin polarized in the base

For spin polarization of holes in the base P_{obh}= 0.87 and spin polarization of electrons in the base P_{ob}= 0.85, the current amplification factor is around 826. Different parameters calculated as [39], [43], [44]:

β= 826, I_c=5.55mA, I_s= I_C exp(-V_{be}/V_t) = 1.13* 10^{-14} A, $V_{JE}=v_t \ln N_E N_B/n_i^2$=0.757, V_{JC}= $V_t \ln(N_E N_B/n_i^2)$= 0.64, C_{JE0}=sqrt(($\epsilon_s q N_B N_E$)/(2V_{JE}(N_B +N_E)))= 5.4*10^{-12}, C_{JC}= sqrt(($\epsilon_s q N_B N_C$)/(2V_{JC}(N_B +N_C)))=1.86*10^{-12}

where I_s is saturation current, V_t is thermal voltage, ϵ_s is permittivity of air, V_{JE} and V_{JC} are built in voltage across base emitter and base collector junctions respectively, C_{JEO} is capacitance due to base to emitter junction when there is no biasing and C_{JC0} is base collector junction capacitance without the presence of biasing.

The input impedance for a transistor with current amplification factor β=826 is simulated in Figure 4.30.

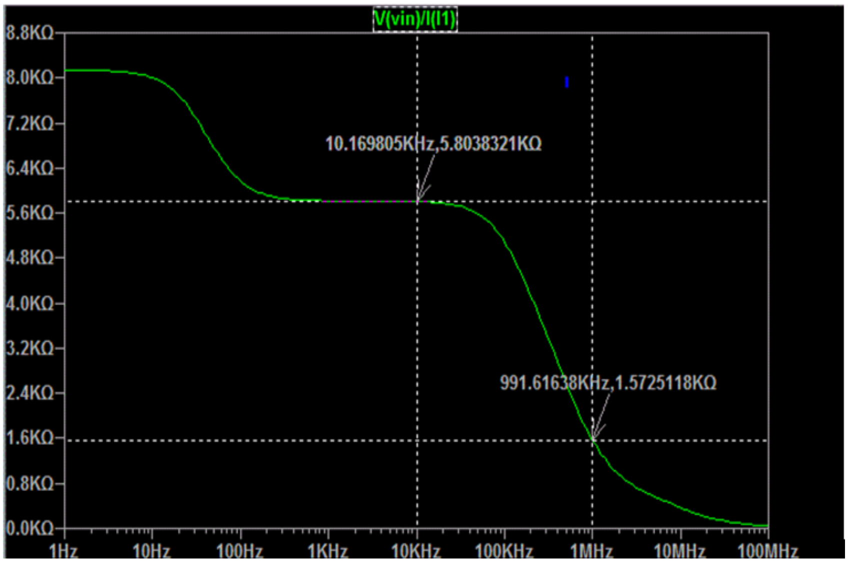

Figure 4.27: input impedance at current amplification factor β= 826

The transistor with current amplification factor β= 826, has an input impedance which deviate hugely from the input impedance of a transistor with current amplification factor β= 132. At frequency 1 kHz, the input impedance is around 5.8k ohm. On the other hand the conventional transistor with current amplification factor β= 132, the input impedance is 2.6k ohm at 1k Hz.

In Figure 4.28, the output impedance is simulated for a cascaded amplifier for for current amplification factor β= 826.

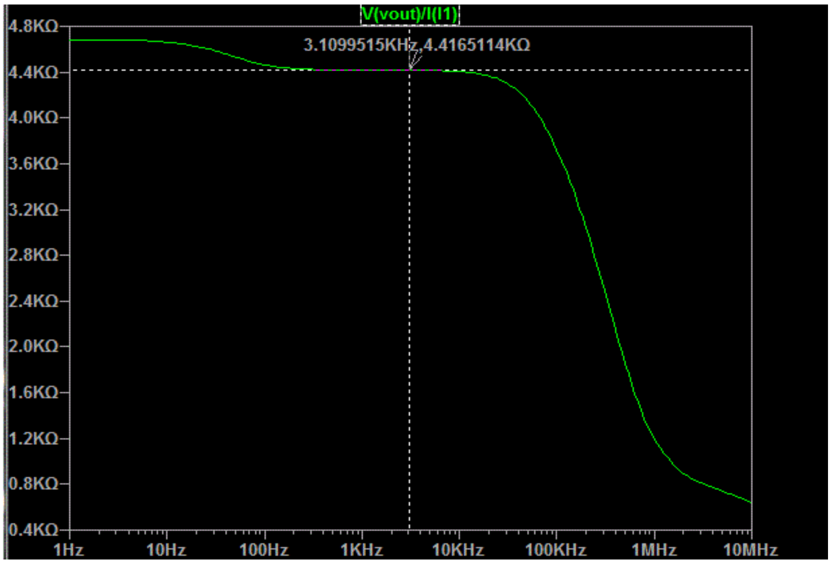

Figure 4.28: output impedance for current amplification factor of β= 826

The output impedance is more or less has similar values for all cases. This is because when the output impedance of the transistor paralleled with Rc (The transistor at the collector which is R11), the total output impedance becomes equal to approximately the value of resistance Rc.

In Figure 4.29, the voltage waveform is simulated which help us to predict the voltage gain.

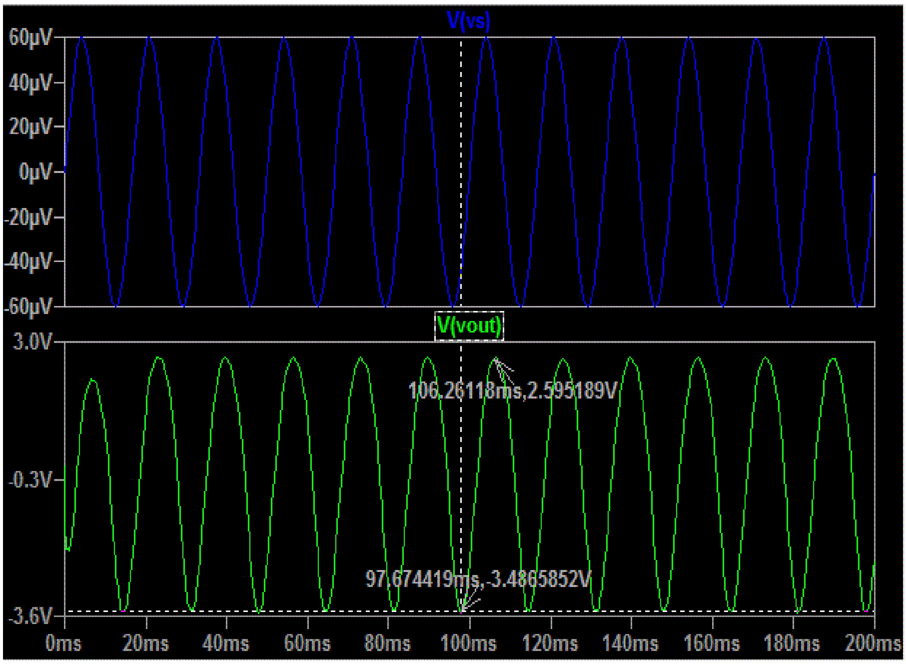

Figure 4.29: input voltage Vs and output voltage Vout waveform for B=826

From Figure 4.29, the peak to peak voltage at current amplification factor β 826 is approximately 6.07V whereas the peak to peak input voltage is 120uv. Therefore the voltage gain is $A_v = V_{out}(pp)/V_{in}(pp)= 5.06 *10^4$. For conventional transistor with current amplification factor β= 132, the voltage gain is around 10^4 which is depicted in Figure 4.23.

The current waveform which helps to calculate the current gain is depicted in figure 4.30 for current amplification factor β= 826.

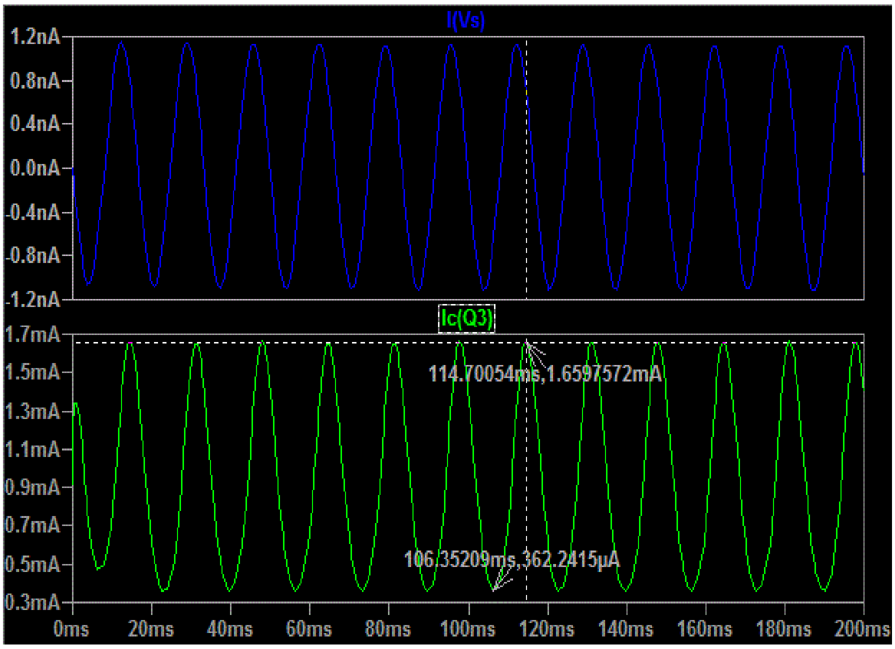

Figure 4.30: current output for B= 826

From Figure 4.30, the peak to peak current output for current amplification β =826 is I_{out}(pp)= 1.29 $*10^{-3}$A and the peak to peak input current is I_{in}(pp)= 2.4nA. So the current gain is A_i= I_{out}/I_{in} = 5.4$*10^5$. Similarly the current gain is calculated in figure 4.29 for β = 132 which is I_{out}/I_{in}= .457mA/4nA= 1.07* 10^5. As a result, the current gain is good at current amplification β =826.

3- Simulation result for the magnetic bipolar transistor when only the base is magnetic material and in addition electrons are spin polarized in the base.(This is the researchers' work [31])

At spin polarization of electrons in the base P_{ob}= 0.8, the current amplification factor for this magnetic transistor (Where only the base is magnetic material and only electrons are spin polarized in the base) is β = 378. Different parameters calculated as [39], [43], [44]:

β =378, Ic= 2.84*10-3, Is= 5.78 $*10^{-15}$, $V_{JE}=v_t \ln N_E N_B/n_i^2$=0.757, $V_{JC}= V_t \ln(N_E N_B/n_i^2)$= 0.64, C_{JE0}=sqrt(($\epsilon_s q N_B N_E$)/(2V_{JE}(N_B +N_E)))= 5.4$*10^{-12}$, C_{JC}= sqrt(($\epsilon_s q N_B N_C$)/(2V_{JC}(N_B +N_C)))=1.86$*10^{-12}$

where I_s is saturation current, V_t is thermal voltage, ϵ_s is permittivity of air, V_{JE} and V_{JC} are built in voltage across base emitter and base collector junctions respectively, C_{JEO} is capacitance due to base to emitter junction when there is no biasing and C_{JC0} is base collector junction capacitance without the presence of biasing.

The input impedance for current amplification factor β =378 is simulated in Figure 4.31.

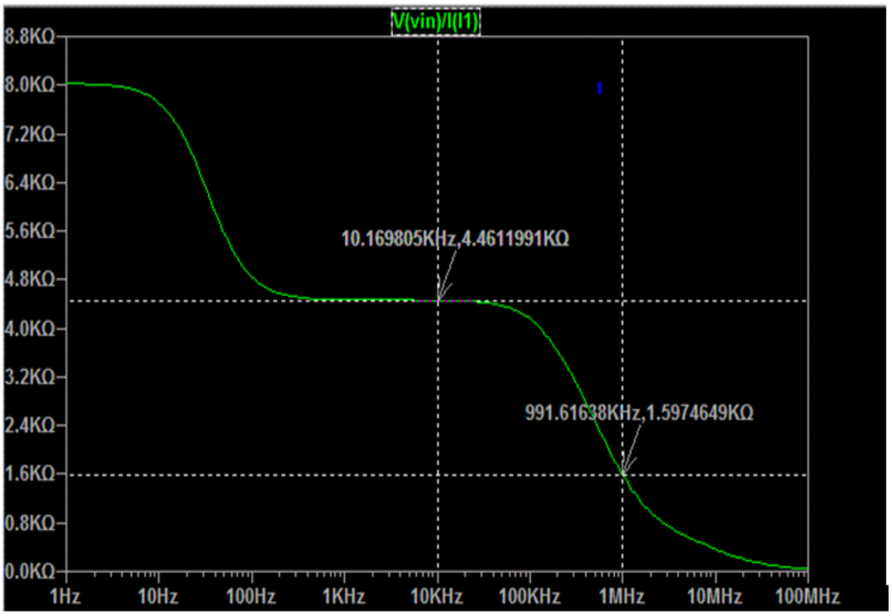

Figure 4.31: input impedance for β =378

Comparing the result obtained in Figure 4.31, Figure 4.18 and figure 4.27, the input impedance for magnetic bipolar transistor (When the base and emitter are magnetic material in addition holes and electrons are spin polarized in the base) current amplification of β =826 has the highest magnitude of 5.19k ohm at 1k Hz. The recorded output value of input impedance for β =378 is 4.46k ohm, for β =248 is 3.71k and for β =132 is 2.6k ohm respectively.

In Figure 4.32, the voltage waveform which helps us to calculate the voltage gain is simulated.

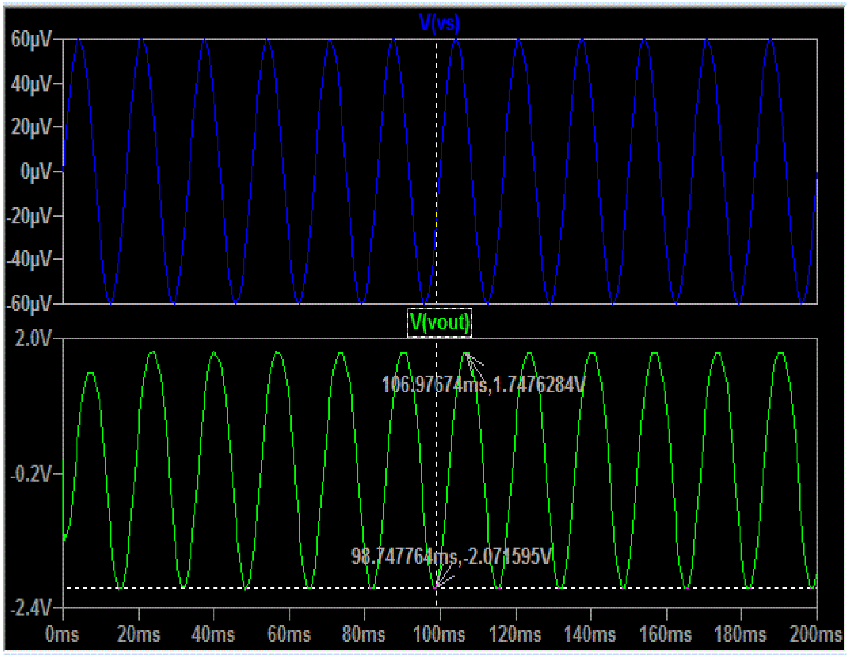

Figure 4.32: voltage waveform for β =378

From Figure 4.32, the peak to peak output voltage for β =378 is 3.81v and the voltage gain is A_v= 3.18*10^4. To generalize:

At β =378, the voltage gain A_v = 3.18 *10^4v, at β =132, A_v=1*10^4, at β = 826, A_v= 5.045 *10^4. B =248, voltage gain is Av= 2.23*10^4.

And it can be seen that all the proposed magnetic bipolar transistors show good performance.

Simulation is done for current waveform to determine the current gain in Figure 4.33.

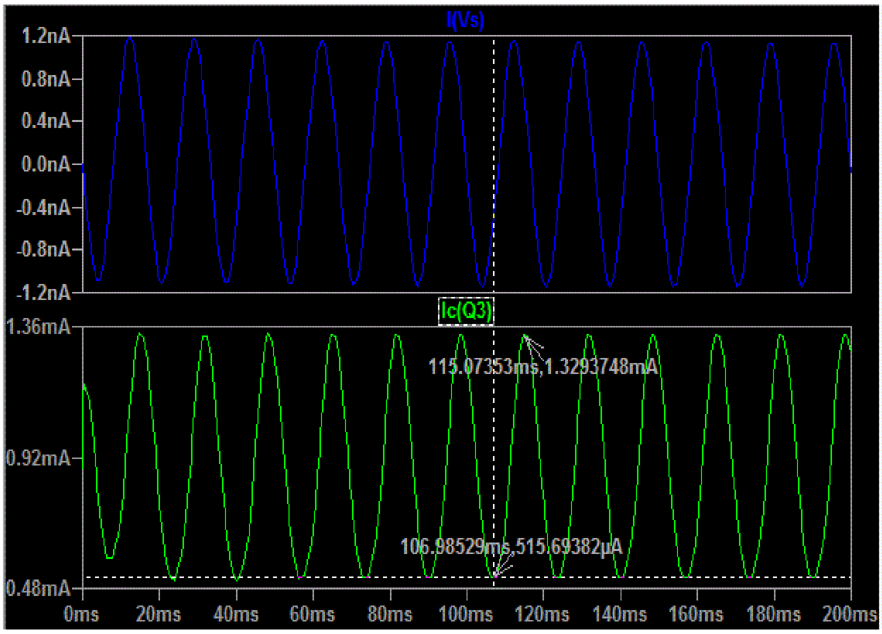

Figure 4.33: current waveform for β =378

From Figure 4.33, the peak to peak output current is 8.13*10^{-4}A and the peak to peak input current is 2.4nA. Then the current gain is 3.39 *10^5. Compared to other current gain of current amplification factors:

At β =378, A_i= 3.39 *10^5, β =248, A_i = 2.38*10^5, β =826, A_i= 5.4 *10^5, β =132, A_i= 1.07*10^5

All the proposed magnetic bipolar transistors show better performance.

4.2.2 Simulation using Hspice software

Hspice software is programming language based software which allows users to define the parameters of the models as they wish. Important parameters for simulation purpose calculated as:

V_{JE}=$v_t$lnN_EN_B/n_i^2=0.757, V_{JC}= $V_t$ln(N_EN_B/n_i^2)= 0.64, C_{JE0}=sqrt((e_sqN_BN_E)/(2V_{JE}(N_B +N_E)))= 8.4*10^{-12}, C_{JC}= sqrt(($_{es}$qN_BN_C)/(2V_{JC}(N_B +N_C)))=1.86*10^{-12} , MJC=MJE=0.4.

where V_t is thermal voltage, ϵ_s is permittivity of air, V_{JE} and V_{JC} are built in voltage across base emitter and base collector junctions respectively, C_{JEO} is capacitance due to base to emitter junction when there is no biasing and C_{JC} is base collector junction capacitance without the presence of biasing. We have also:

$\beta = 132$, $i_c = 1mA$, $I_s = I_C \exp(-V_{be}/V_t) = 2.08 * 10^{-15}A$

$\beta = 248$, $i_c = 3.1mA$, $I_s = I_C \exp(-V_{be}/V_t) = 6.43 * 10^{-15}A$

$\beta = 378$, $i_c = 2.82mA$, $I_s = I_C \exp(-V_{be}/V_t) = 5.9 * 10^{-15}A$

$\beta = 826$, $i_c = 5.55mA$, $I_s = I_C \exp(-V_{be}/V_t) = 1.14 * 10^{-14}A$

where I_s is saturation current and Ic is collector current.

In this section, the output response of the cascaded amplifier is conducted for different spin polarizations. In Figure 4.34 the voltage wave form for transistor of current amplification factors of 132, 248, 378 and 826 is simulated using Hspice software. Simulation for voltage waveforms which constitute all current amplification factors of a transistor is presented in Figure 4.34.

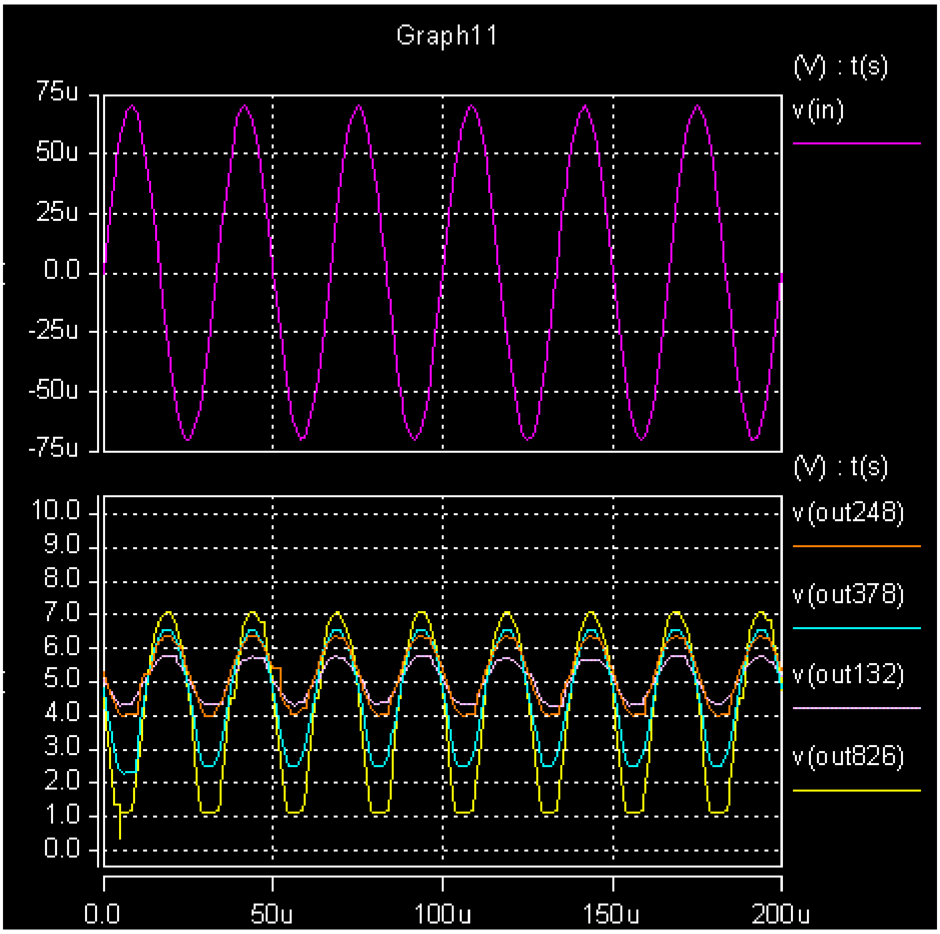

Figure 4.34: output and input voltage waveforms using Hspice software

From Figure 4.34, it is obvious that the voltage gain has good performances in all the proposed transistors. More or less, it strengthens the claim what was done using LTspice software in section 4.2.1 and MATLAB software in section 4.1.

Simulation for current waveforms which constitute all current amplification factors of a transistor is presented in Figure 4.35.

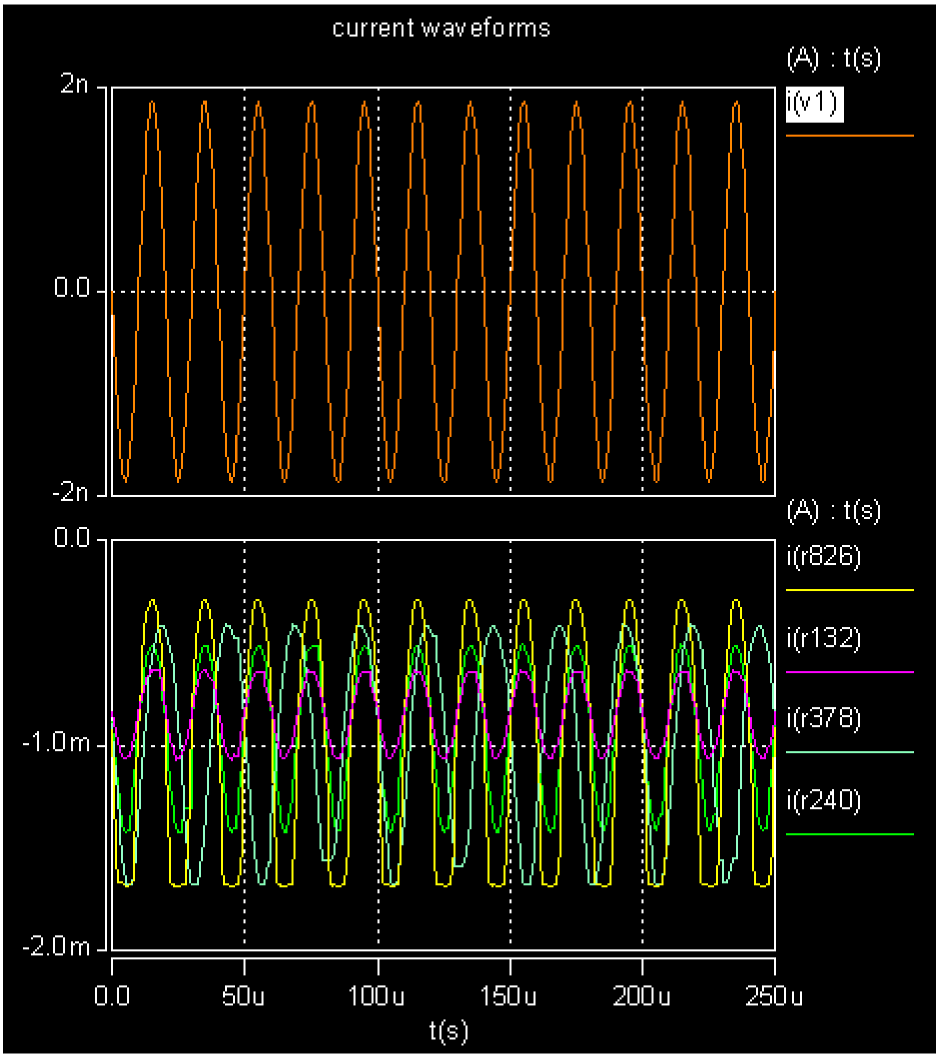

Figure 4.35: output and input current waveforms using Hspice software

Similarly, the current waveform shown in Figure 4.35 illustrates the predicted result in section 4.1 and section 4.2.

Chapter Five

Conclusion and Recommendation

5.1 Conclusion

Spintronics is a new technology, and its researches are more or less carried out theoretically and experimentally using fundamental physics concept (such as spin injection, spin filtering, or semiconductor ferromagnetism).

In the first part of this thesis, magnetic bipolar transistor models were proposed in which the spin degrees of freedom of carriers added as an additional controlling input to the existing charge based device. The strength of spin splitting in the energy bands are specifically depends on the type of magnetic material we used. By just investigating the magnitude of spin polarization of carriers, it is possible to differentiate which spin polarization matches with the specific magnetic material. Hence, the proposed magnetic bipolar transistors will works for all types of magnetic materials. As a result, from this thesis it is managed to come up with quite different types of magnetic bipolar transistors which are functions of spin of carriers. In the second part, the proposed magnetic bipolar transistors are validated by applying on application areas (Cascaded amplifier). Here three stage cascaded spin amplifier is considered, and input impedance, output impedance, voltage gain and current gain are analyzed for low and high frequency using suitable AC equivalent models. In addition, density of equilibrium electrons in the base, current amplification factor, density of electron / hole generation current and emitter current are clearly developed. Using MATLAB software, the calculated characteristics of all the aforementioned parameters investigated. In addition, simulation is performed using Spice software to investigate the performances of the voltage gain, current gain, input impedance and output impedance.

From this thesis, it is clear that incorporation of spin carriers in the device will help to boost the output responses of different parameters of the device. Further, in the proposed transistor models, it is obvious that the density of minority of carriers and the current amplification factor are tuned by spin of carriers. Contrary to the conventional cascaded amplifier, the spin amplifier's parameters have wide range of values which is a function of polarization of spin carriers. All in all, it can be concluded that spin can be a main player in controlling a device's parameters.

5.2 Recommendation

This thesis focused on one type of spin based transistor, i.e., magnetic bipolar transistor. In addition to studying on magnetic bipolar transistor, it is also possible to research on other types of spin transistors. So:

1) It is possible to develop a model by injecting polarized/ unpolarized electron on the base side.

This thesis is based on the existing bipolar transistor by injecting spins to the device to exploit the advantage of spin degree of freedom. It is also possible:

2) It is possible to work on other type of spin transistors, for example, spin valve transistor, spin-FET, and so on.
3) It is also possible to calculate the new energy bands resulting from splitting of conduction and valence bands due to presence of magnetic impurities using different techniques. In addition, recombination rate, mobility and diffusion constant can be calculated.
4) Developing small signal AC models for spin based transistor is another interesting area to study.

References

[1] Shiromani Balmukund Rahi and Priyank Rastogi, "A REVIEW REPORT FOR NEXT GENERATION OF CMOS TECHNOLOGY AS SPINTRONICS: FUNDAMENTALS, APPLICATIONS AND FUTURE," *International Journal of Advances in Engineering & Technology*, Vol. 6, Issue 2, pp. 696-702, May 2013.

[2] Vinod Kumar Joshi, "Spintronics: A contemporary review of emerging electronics devices", *Engineering Science and Technology, an International Journal*, pp. 1503–1513, 2016.

[3] T. Dietl, "Semiconductor Spintronics', in: Walter Potz, Jaroslav Fabian, Ulrich Hohenester, Eds., *Modern Aspects of Spin Physics*," Springer, 2007, pp. 1-46.

[4] Atsufumi Hirohata, Koki Takanashi, "Future perspectives for spintronic devices," *Journal of Physics D Applied Physics* 47(19):193001 • May 2014.

[5] AkritiSrivastava, ShokhiRastogi, Akshita Verma, Pooja Singh, "SPINTRONICS-A RETROSPECTIVE AND PERSPECTIVE," *International Journal of Advance Research In Science And Engineering, IJARSE*, Vol. No.4, Special Issue (01) , February 2015.

[6] Purneshwari Varshney, Hemangi Agrawal, "SPINTRONICS TECHNOLOGY: A REVIEW," *NATIONAL CONFERENCE ON ADVANCES IN TECHNOLOGY AND APPLIED SCIENCES*, Jodhpur, March 2014.

[7] Mark Lundstrom and Jing Guo S., Nanoscale Transistors: Device physics, Modeling and simulation, New York: Springer Science+Business Media, 2006.

[8] Donald A. Neamen, *Microelectronics: Circuit Analysis and Design*. Fourth Edition, McGraw-Hill, 2010.

[9] R. R. Thankalekshmi, A. C. Rastogi J., Appl. Phys. 111, 07D104, 2012.

[10] Roland K. Kawakami, Kathleen McCreary, and Yan Li, "Fundamentals of Spintronics in Metal and Semiconductor Systems", in: David J. Lockwood, eds., *Nanoelectronics and photonics from atom to materials, devices and architecture*, Springer Science Business Media, LLC, 2008, pp. 59 – 110.

[11] Datta, S., and B. Das, "Electronic analog of the electrooptic modulator," *Appl. Phys. Lett.* 56, pp. 665–667, 1990.

[12] R.R.Pelá, L.K.Teles, "Simulation of a spintronic transistor: A study of its performance," *Journal of Magnetism and Magnetic Materials*, Volume 321, Issue 8, pp. 984-989, April 2009.

[13] Gefei Wang, Zhaohao Wang, Jacques-Olivier Klein, Weisheng Zhao, "Modeling for Spin-FET and Design of Spin-FET-Based Logic Gates," *IEEE Transactions on Magnetics*, Volume: 53 , Issue: 11 , Nov. 2017.

[14] G. Zahnd, L. Vila, V. T. Pham, A. Marty, C. Beigné, C. Vergnaud & J. P. Attané," Giant magnetoresistance in lateral metallic nanostructures for spintronic applications", *Scientific Reports*, 2017, volume 7, Article number: 9553.

[15] "The Discovery of Giant Magnetoresistance." *The Class for Physics of the Royal Swedish Academy of Science*, 2007.

[16] Julien Vigroux, "Fabrication and characterization of a magnetic tunnel transistor with an epitaxial spin valve by the shadow mask technique," Ph.D. dissertation, university ̈at Regensburg, 2010.

[17] Md. Ayaz Masud, Md. Shafiqul Islam and Quazi D. M. Khosru, "Modified Ebers-Moll model of magnetic bipolar transistor," IEEE International Conference on Electron Devices and Solid-State Circuits (EDSSC), Singapore, 2015

[18] Wessels, B. W., "Bipolar magnetic junction transistors for logic applications," *Materials Science and Engineering*, pp. 435-445, 2016.

[19] Han Hsu and Sheng-Chieh Huang, "Rapid CommunicationsSimultaneous metal–half-metal and spin transition in SrCoO3under compression," *PHYSICAL REVIEW MATERIALS*, 2, 111401(R), 2018.

[20] Nguyen Thanh Tu1, Pham Nam Hai, Le Duc Anh and Masaaki Tanaka,"High-temperature ferromagnetism in heavily Fe-doped ferromagnetic semiconductor (Ga,Fe)Sb," *Appl. Phys. Lett.* 108, 192401, 2016.

[21] Jaroslav Fabian, Alex Matos-Abiague, Christian Ertler, Peter Stano and Igor Zutic, 'Semiconductor Spintronics,' *Acta Physica Slovaca*, 57, 565, 2007.

[22] M. Cahay, and Supriyo Bandyopadhyay, *IEE Proc.-Circuits Devices Syst.*, 2005, Vol. 152, No. 4.

[23] Zhao K1, Deng Z, Wang XC, Han W, Zhu JL, Li X, Liu QQ, Yu RC, Goko T, Frandsen B, Liu L, Ning F, Uemura YJ, Dabkowska H, Luke GM, Luetkens H, Morenzoni E, Dunsiger SR, Senyshyn A. and Böni P, Jin CQ, "New diluted ferromagnetic semiconductor with Curie temperature up to 180 K and isostructural to the '122' iron-based superconductors," *Nat Commun*, 2013, 4:1442.

[24] H. Ohno, A. Shen, and F. Matsukura, et al., *Appl. Phys. Lett.*, 69, 363, 1996.

[25] Igor Zutic and Jaroslav Fabian "Bipolar Spintronics," in: Sadamichi Maekawa, Eds., Concepts in Spin Electronics, OXFORD UNIVERSITY PRESS, 2006, PP. 43-86.

[26] M.I. Dyakonov, "Spintronics ?" in: S. Luryi, J. Xu, and A. Zaslavsky, eds., *Future Trends in Microelectronics. The Nano, the Giga, and the Ultra*, Wiley, 2004, pp. 157-167.

[27] R. N. Gurzhi, A. N. Kalinenko, A. I. Kopeliovich, A. V. Yanovsky, E. N. Bogachek and Uzi Landman , "A magnetic-field-effect transistor and spin transport," *Appl. Phys. Lett.*, Vol. 83, No. 22, 2003.

[28] M. E. Flatte´, Z. G. Yu, E. Johnston-Halperin and D. D. Awschalom, "Theory of semiconductor magnetic bipolar transistors," *Appl. Phys. Lett.*, 82, (26), pp.4740-4742, 2003.

[29] P.S. Anil kumar and J.C. Lodder, "The spin-valve transistor -a new magnetoelectronic device," *Appl. Phys. Lett.*, vol. 97, No. 1, 2000.

[30] Spectrum.ieee.org, "Intel Now Packs 100 Million Transistors in Each Square Millimeter," 2017. Available online at: https://spectrum.ieee.org/nanoclast/semiconductors/processors/intel-now-packs-100-million-transistors-in-each-square-millimeter [Accessed: 30- Mar- 2017].

[31] Jaroslav Fabian, Igorˇ Zuti´c and S. Das Sarma "Magnetic bipolar transistor," *Appl. Phys. Lett.*, Vol. 83, No. 22, 2004.

[32] S. Tiwari, *Compound Semiconductor Device Physics*. San Diego, Academic Press, 1992.

[33] N. Rangaraju, J. A. Peters, and B. W. Wessels, "Magnetoamplification in a Bipolar Magnetic Junction Transistor," *Phys. Rev. Lett.*, 105, 117202 , 2010.

[34] J.A. GAJ " Semimagnetic semiconductors," *ACTA PHYSICA POLONICA*, Vol. 96, No. 5, 1999.

[35] N. Lebedeva, P. Kuivalainen, "Modeling of ferromagnetic semiconductor devices for spintronics," *JOURNAL OF APPLIED PHYSICS*, VOLUME 93, NUMBER 1, 2003.

[36] Physics.udel.edu, 'Lecture 10 Perturbation theory', 2008. Available online at: http://www.physics.udel.edu/~msafrono/425-2011/Lecture%2010.pdf. [Accessed: 07-October- 2008].

[37] Sakurai, J.J., and Napolitano, J., *Modern quantum mechanics* (2nd ed.). Addison Wesley, 2011.

[38] Liboff, Richard L., *Introductory Quantum Mechanics*. Addison-Wesley, 2002.

[39] Louis Nashelsky Robert L. Boylestad, *Electronic Devices and Circuit Theory*. 10th (tenth) Edition, Prentice Hall, 2008.

[40] Neil w. Ashchroft, N. David Mermin, *Solid state physics*. Orlando, Hartcourt, 1976.

[41] R. M. White, Quantum, *Theory of Magnetism*. 3rd ed. Berlin, Springer, 2007.

[42] F. Meier and B. P. Zakharchenya (eds), Optical Orientation (North-Holand New York, 1984).

[43] Robert F.Pierret, *SEMICONDUCTOR DEVICE FUNDAMENTALS.* ADDISON WESLEY PUBLISHING COMPANY, 1996.

[44] Jacob Millman,Christos C. Halkias, *Intergerated Electronics:Anlog and Digital Circuits and systems.* McGraw-HILL KOGAKUSHA.LTD, 1977.

[45] Spintronics-info.com, ‘Spintronics history’, 2019. Available online at: https://www.spintronics-info.com/history [Accessed: 20- July- 2019]

Appendix

1 Derivation of density of minority electrons and holes

To show the density of equilibrium electron in the base as:

$$n_{ob} = \frac{n_i^2}{N_{ab}} * \cosh\frac{q\psi_c}{kT}\cosh\frac{q\psi_v}{kT}$$

(When electron and hole are considered spin polarized, both conduction and valence energy bands split)

Starting with the following equations [25], [32]:

$$n\lambda = \frac{Nc}{2}\exp(\frac{-(Ec\lambda-\mu_{n\lambda})}{kT})) \quad \text{(B1)}$$

$$p\lambda = \frac{Nv}{2}\exp(\frac{-(\mu_{p\lambda}-Ev\lambda)}{kT})) \quad \text{(B2)}$$

Where,

$$Ec\lambda = E_o - q\Phi - \lambda q\psi_c$$

$$E_{v\lambda} = E_{vo} - q\Phi - \lambda q\psi_v$$

λ represents $\uparrow$ *or* $\downarrow$

$$n\lambda = \frac{Nc}{2}\exp(\frac{-(E_o-q\Phi-\lambda q\psi_c-\mu_n\lambda)}{kT}))$$

$$n\uparrow = \frac{Nc}{2}\exp(\frac{-(E_o-q\Phi-\uparrow q\psi_c-\mu_n\uparrow)}{kT})) \quad \text{(B1a)}$$

$$n\downarrow = \frac{Nc}{2}\exp(\frac{-(E_o-q\Phi-\downarrow q\psi_c-\mu_n\downarrow)}{kT})) \quad \text{(B2a)}$$

And remembering $n=n_\uparrow+n_\downarrow$, [25], it follows:

$$n=n\uparrow + n\downarrow = \frac{Nc}{2}\exp(\frac{-(E_o-q\Phi-\uparrow q\psi_c-\mu_n\uparrow)}{kT}) + \frac{Nc}{2}\exp(\frac{-(E_o-q\Phi-\downarrow q\psi_c-\mu_n\downarrow)}{kT})$$

$$= \frac{Nc}{2}\exp(\frac{-(E_o-q\Phi)}{kT})\ [\exp(\frac{-(-\uparrow q\psi_c-\mu_n\uparrow)}{kT}) + \exp(\frac{-(-\downarrow q\psi_c-\mu_n\downarrow)}{kT})\ ]$$

$$= N_c\exp(\frac{-(E_{vo}-q\Phi)}{kT})\cosh\frac{(q\psi_c+\mu_n)}{kT}) \quad \text{(B3)}$$

$$s=n\uparrow - n\downarrow = \frac{Nc}{2}\exp(\frac{-(E_o-q\Phi-\uparrow q\psi_c-\mu_n\uparrow)}{kT}) - \frac{Nc}{2}\exp(\frac{-(E_o-q\Phi-\downarrow q\psi_c-\mu_n\downarrow)}{kT})$$

$$= \frac{Nc}{2}\exp(\frac{-(E_o-q\Phi)}{kT})\ [\exp(\frac{-(-\uparrow q\psi_c-\mu m\uparrow)}{kT}) - \exp(\frac{-(-\downarrow q\psi_c-\mu_n\downarrow)}{kT})\ ]$$

$$= \quad N_c \exp(\frac{-(E_{vo}-q\Phi)}{\mathrm{kT}}) \sinh \frac{(q\psi_c+\mu_n)}{\mathrm{kT}}) \qquad \text{(B4)}$$

Similarly for holes:

$$p\lambda = \frac{\mathrm{Nv}}{2}\exp(\frac{-(\mu p\lambda-(E_{vo}-q\Phi-\lambda q\psi_v)}{\mathrm{kT}})$$

$$p\uparrow = \frac{\mathrm{Nv}}{2}\exp(\frac{-(\mu p\uparrow-E_{vo}+q\Phi+\uparrow q\psi_v)}{\mathrm{kT}})$$

$$p\downarrow = \frac{\mathrm{Nv}}{2}\exp(\frac{-(\mu_p\downarrow-E_{vo}+q\Phi+\downarrow q\psi_v)}{\mathrm{kT}})$$

$$p = p_\uparrow + p_\downarrow = \frac{\mathrm{Nv}}{2}\exp(\frac{-(\mu_p\uparrow-E_{vo}+q\Phi+\uparrow q\psi_c)}{\mathrm{kT}}) + \frac{\mathrm{Nv}}{2}\exp(\frac{-(\mu_p\downarrow-E_{vo}+q\Phi+\downarrow q\psi_v)}{\mathrm{kT}})$$

$$= \quad \frac{\mathrm{Nv}}{2}\exp(\frac{-(-E_{vo}+q\Phi)}{\mathrm{kT}}) \left[\ \exp(\frac{-(\mu_p\uparrow+\uparrow q\psi_v)}{\mathrm{kT}}) + \exp(\frac{-(\mu_p\downarrow+\downarrow q\psi_v)}{\mathrm{kT}}\ \right]$$

$$= \quad \exp(\frac{-(-E_{vo}+q\Phi)}{\mathrm{kT}}) \ \cosh(\frac{(\mu_p+q\psi_v)}{\mathrm{kT}})$$

$$\mathrm{np} = \ (N_c \exp(\frac{-(E_o-q\Phi)}{\mathrm{kT}}) \cosh\frac{(q\psi_c+\mu_n)}{\mathrm{kT}})*(\mathrm{N_v}\exp(\frac{-(-E_{vo}+q\Phi)}{\mathrm{kT}}) \cosh(\frac{(\mu_p+q\psi_v)}{\mathrm{kT}}))$$

$$= \mathrm{NvNc}\exp(\frac{-(E_o-E_{vo})}{\mathrm{kT}} \cosh\frac{(q\psi_c+\mu_n)}{\mathrm{kT}} \cosh(\frac{(\mu_p+q\psi_v)}{\mathrm{kT}}))$$

$$= n_i^2 \cosh\frac{(q\psi_c+\mu_n)}{\mathrm{kT}} \cosh(\frac{(\mu_p+q\psi_v)}{\mathrm{kT}}))$$

If the spin down and spin up of μ_p and μ_n are spin independent and equal, then:

$$\mathrm{np} = n_i^2 \cosh\frac{q\psi_c}{\mathrm{kT}} \cosh\frac{q\psi_v}{\mathrm{kT}}$$

Using the usual equation [40] of concentration of holes and electron in the p type semiconductor for conventional transistor: $n_{ob} \approx \frac{(n_i^2)}{N_{ap}}$

$$n_0 = \frac{(n_i^2)}{N_{ap}} \ \cosh\frac{q\psi_c}{kT} \cosh\frac{q\psi_v}{kT} \qquad \text{(B5)}$$

Analogous equation can be made for equilibrium holes in the emitter. In case when conduction energy bands are only considering splitting, one can set $\psi_v = 0$. The same could be applied to valence energy bands. In this case, for instance, when electrons are only considered polarized in the base, the density is given by:

$$n_0 = \frac{(n_i^2)}{N_{ab}} \cosh\frac{q\psi_c}{\mathrm{kT}} \qquad \text{(B6)}$$

And when holes are only considered spin polarized in the emitter, the density of holes in the emitter is:

$$p_0 = (\frac{n_i^2}{N_{De}}\cosh\frac{q\psi_v}{\mathrm{kT}}) \quad \text{(B7)}$$

Polarization of equilibrium electron and hole is given by:

$$P_{ob} = \tanh\frac{q\psi_c}{\mathrm{kT}} \quad \text{(B7.1)}$$

$$P_{oe} = \tanh\frac{q\psi_v}{\mathrm{kT}} \quad \text{(B7.2)}$$

To prove equation (B7.1), the definition of spin polarization [25] is used. This is:

$$P = \frac{(n\uparrow - n\downarrow)}{(n\uparrow + n\downarrow)} \quad \text{(B8)}$$

Using equation (B3), (B4) and (B8)

$$n\uparrow + n\downarrow = N_c\exp(\frac{-(E_{vo} - q\Phi)}{\mathrm{kT}})\cosh\frac{(q\psi_c + \mu m)}{\mathrm{kT}})$$

$$n\uparrow - n\downarrow = N_c\exp(\frac{-(E_{vo} - q\Phi)}{\mathrm{kT}})\sinh\frac{(q\psi_c + \mu m)}{\mathrm{kT}})$$

If the chemical potential μ_n is spin independent, then:

$$P_{ob} = \tanh\frac{q\psi_c}{kT}$$

2 Derivation of polarization

Polarization of non-equilibrium electron density is:

$$P = \frac{tanh\frac{(\delta\mu\_)}{\mathrm{kT}} + P_{ob}}{1 + P_{ob}\, tanh\frac{(\delta\mu\_)}{\mathrm{kT}})} \quad \text{(3.1.7)}$$

The derivation will proceed below. The density of electron in the emitter base junction is given by:

$$n_{be} = n = n_{ob}\, exp(\frac{(qV_{be})}{kT}) \quad \text{(B9)}$$

Or alternatively, we can write [25]:

$$n_\lambda = n_{\lambda ob}\, exp(\frac{(q(\delta\Phi) + \delta\mu_{n\lambda})}{kT}) \quad \text{(B10)}$$

$$n_\uparrow = n_{ob\uparrow}\exp(\frac{(q(\delta\Phi) + \delta\mu_{n\uparrow})}{\mathrm{kT}}) \quad \text{(B11)}$$

$$n\downarrow = n_{ob}\downarrow\exp(\frac{q(\delta\Phi) + \delta\mu_{n\downarrow}}{\mathrm{kT}}) \quad \text{(B12)}$$

$$n = n\uparrow + n\downarrow = \quad n_{ob}\uparrow\exp(\frac{(q(\delta\Phi) + \delta\mu_{n\uparrow})}{\mathrm{kT}}) + n_{ob}\downarrow\exp(\frac{(q(\delta\Phi) + \delta\mu_{n\downarrow})}{\mathrm{kT}})$$

$$= \quad \exp(\frac{(q(\delta\Phi))}{\mathrm{kT}})\,[n_{ob}\uparrow\exp(\frac{(\delta\mu_{n\uparrow})}{\mathrm{kT}}) + n_{ob}\downarrow\exp(\frac{(\delta\mu_{n\downarrow})}{\mathrm{kT}}] \quad \text{(B13)}$$

Density of spin electron is:

$$s = n_{\uparrow} - n_{\downarrow} = \exp(\frac{(q(\delta\phi))}{kT}) [n_{ob\uparrow}\exp(\frac{(\delta\mu_{n\uparrow})}{kT}) - n_{ob\downarrow}\exp(\frac{(\delta\mu_{n\downarrow})}{kT})] \quad (B14)$$

And equilibrium electron and spin can be given respectively as:

$$n_0 = n_{ob\uparrow} + n_{ob\downarrow} \quad (B15)$$

$$s_0 = n_{0b\uparrow} - n_{0b\downarrow} \quad (B16)$$

$$n_{0b\uparrow} = (n_0 + s_0)/2 \quad (B17)$$

$$n_{0b\downarrow} = (n_0 - s_0)/2 \quad (B18)$$

Substituting equations (B17) and (B18) into equations (B13), one can get:

$$n = n_{\uparrow} + n_{\downarrow} = \exp(\frac{(q(\delta\phi))}{kT}) [(n_0 + s_0)/2\exp(\frac{(\delta\mu_{n\uparrow})}{kT}) + (n_0 - s_0)/2 \exp(\frac{(\delta\mu_{n\downarrow})}{kT})]$$

$$= \exp(\frac{(q(\delta\phi))}{kT})\{ n_0/2 [(\exp(\frac{(\delta\mu_{n\uparrow})}{kT}) + \exp(\frac{(\delta\mu_{n\downarrow})}{kT})] + s_0/2 [(\exp(\frac{(\delta\mu_{n\uparrow})}{kT}) - \exp(\frac{(\delta\mu_{n\downarrow})}{kT})]\}$$

And taking

$$\mu_{\pm} = (\mu_{n\uparrow} \pm \mu_{n\downarrow})/2$$

$$n = \exp(\frac{(q(\delta\phi))}{kT}) \{n_0/2[(\exp(\frac{(\delta(\mu_+ + \mu_-))}{kT}) + \exp(\frac{(\delta(\mu_+ - \mu_-))}{kT})] + s_0/2 [(\exp(\frac{(\delta(\mu_+ + \mu_-))}{kT}) - \exp(\frac{(\delta(\mu_+ - \mu_-))}{kT})]\}$$

$$n = \exp(\frac{(q(\delta\phi) + \mu_+)}{kT}) [n_0 \cosh (\frac{(\delta\mu_-)}{kT}) + s_0 \sinh (\frac{(\delta\mu_-)}{kT})] \quad (B19)$$

Similarly it is possible to show the spin carrier as;

$$s = \exp(\frac{(q(\delta\phi) + \mu_+)}{kT}) [n_0 \sinh (\frac{(\delta\mu_-)}{kT}) + s_0 \cosh (\frac{(\delta\mu_-)}{kT})] \quad (B20)$$

Evaluating polarization of electron is straight forward. Using equation (B19) and (B20):

$$P = s/n = \frac{\tanh\frac{(\delta\mu_-)}{kT} + P_{ob}}{1 + P_{ob}\tanh\frac{(\delta\mu_-)}{kT}} \quad (3.1.7)$$

where P_{0b} is polarization of equilibrium electron in the base.

3 Derivation of density of electrons and spins in the base emitter junction

The density of electron in the base-emitter junction when electron in the base and hole in the emitter is considered polarized is given by:

$$n_{be} = n_{ob}(1 + \frac{P_{ob} - P_{oe}}{1 - P_e P_{oe}} P_e) \exp\frac{v_{be}}{kT} \quad (3.1.10)$$

Multiplying equation (B19) both the denominator and numerator of the right hand side of the equation by n_0 cosh $(\frac{(\delta\mu_-)}{kT}$,

$$n = n_0 \cosh (\frac{(\delta\mu_-)}{kT} \exp(\frac{(q\delta\phi + \delta\mu_+)}{kT}) \; [1 + s_{0/n0} \tanh (\frac{(\delta\mu_-)}{kT})]$$

$$= n_{0/2}\, exp\frac{(q\delta\phi)}{kT} \; [\exp (\frac{((\delta\mu_+) + \delta\mu_-)}{kT} + \exp\frac{\delta\mu_+ - (\delta\mu_-)}{kT}] \; [1 + s_0/n_0 \tanh (\frac{(\delta\mu_-)}{kT})]$$

$$= n_{0/2}\, exp\frac{(q\delta\phi)}{kT} \; [\exp \frac{(q\delta\phi + \delta\mu\uparrow)}{kT} + \exp\frac{(q\delta\phi + \delta\mu\downarrow)}{kT}] \; [1 + s_0/n_0 \tanh (\frac{(\delta\mu_-)}{kT})] \qquad \text{(B19a)}$$

If the discrepancies between $\delta\mu\uparrow$ and $\delta\mu\downarrow$ is considered small compared to $\delta\phi$, it can be set: $\delta\mu\uparrow = \delta\mu\downarrow$. And as a result:

$$n = n_0 \exp \frac{(q\delta\phi + \delta\mu)}{kT} \; [1 + P_{0bR} \tanh (\frac{(\delta\mu_-)}{kT}]$$

$$n = n_0 \exp \frac{v_{bc}}{kT} \; [1 + P_{0BR} \tanh (\frac{(\delta\mu_-)}{kT})] \qquad \text{(B19b)}$$

From equation (4.1.9)

$$\tanh \frac{(\delta\mu_-)}{kT} = \frac{P - P_{0b}}{1 - P(P_{0b})} = \text{constant} \qquad \text{(B21)}$$

The chemical potential μ assumed constant in the depletion layer and hence it will help connect the polarization at the right and left depletion layer.

Combining equation (B19b) with equation ((B21) give us:

$$n = n_0 \exp \frac{v_{be}}{kT} \; [1 + P_{0bL} (\frac{(P_{0R} - P_{0R})}{1 - P_{obR}P_R})] \qquad \text{(B19c)}$$

When the emitter region is considered magnetic, P_{0R}=P_{0e}. And when the emitter considered nonmagnetic, P_{0R}= 0. And P_R = P_e (spin polarization of injected electrons in the emitter)

The density of spin carriers in the base emitter region is calculated as:

$$s^* = \exp(\frac{(q\delta\phi + \mu_{n+})}{kT}) \; [n_0 \sinh (\frac{(\delta\mu_{n-})}{kT}) + s_0 \cosh (\frac{(\delta\mu_{n-})}{kT})]$$

Dividing the right side with n_0 cos $\frac{(\delta\mu_{n-})}{kT}$, the density of spin is:

$$s^* = n_0\, cosh\, \frac{(\delta\mu_{n-})}{kT} \exp(\frac{(q\delta\phi + \mu_{n+})}{kT}) \; [\tanh (\frac{(\delta\mu_{n-})}{kT}) + P_{0b}]$$

Using the relation listed in equation (B21):

$$s_{bc} = n_0\, cosh\, \frac{(\delta\mu_{n-})}{kT} \exp(\frac{(q\delta\phi + \mu_{n+})}{kT}) \; [\frac{(P_{0R} - P_{0R})}{1 - P_{obR}P_R} + P_{0b}]$$

If the discrepancies between $\delta\mu\uparrow$ and $\delta\mu\downarrow$ is considered small compared to $\delta\phi$, it can be set: $\delta\mu\uparrow = \delta\mu\downarrow$. And as a result:

$$S_{bc}=n_0 \exp \frac{v_{be}}{kT} \left[\frac{(P_{0R}-P_{0R})}{1-P_{obR}P_R}+P_{0b}\right]$$

4 Derivation of density of holes in the base collector region

Density of minority holes in the collector is calculated similar to what we did for density of holes in emitter.

$$n_{\lambda c}=\frac{\mathrm{Nc}}{2}\exp\left(\frac{-(Ec\lambda-\mu_n\lambda)}{\mathrm{kT}}\right)$$

$$p_{\lambda c}=\frac{\mathrm{Nv}}{2}\exp\left(\frac{-(\mu_p\lambda-Ev\lambda)}{\mathrm{kT}}\right)$$

Since holes are assumed spin polarized in the collector, only valence band split. Following similar steps like before, one can obtain:

$$np = \left(N_c N_v \exp\frac{-(E_o-E_{vo})}{\mathrm{kT}}\cosh\left(\frac{(\mu_p+q\psi_v)}{\mathrm{kT}}\right)\right)$$

$$p_{oc} = \left(\frac{n_i^2}{N_{De}}\cosh\left(\frac{(\mu_p+q\psi_v)}{\mathrm{kT}}\right)\right)$$

$$n_{bc}= n_{ob}\left(1+\frac{P_{ob}-P_{oc}}{1-P_eP_{oc}}P_c\right) \tag{B22}$$

$$n_{bc}= n^*= n_{ob}\exp\left(\frac{(qV_{bc})}{\mathrm{kT}}\right) \tag{B23}$$

Following similar steps from (B18) to (B17):

$$n^* = \exp\left(\frac{(q\delta\phi+\mu_{n+})}{\mathrm{kT}}\right)\left[n_0\cosh\left(\frac{(\delta\mu_{n-})}{\mathrm{kT}}\right)+s_0\sinh\left(\frac{(\delta\mu_{n-})}{\mathrm{kT}}\right)\right]$$

$$s^*= \exp\left(\frac{(q\delta\phi+\mu_{n+})}{\mathrm{kT}}\right)\left[n_0\sinh\left(\frac{(\delta\mu_{n-})}{\mathrm{kT}}\right)+s_0\cosh\left(\frac{(\delta\mu_{n-})}{\mathrm{kT}}\right)\right]$$

$$n^*= n_{0/2}\left[\exp\frac{(q\delta\phi+\delta\mu\uparrow)}{\mathrm{kT}}+\exp\frac{(q\delta\phi+\delta\mu\downarrow)}{\mathrm{kT}}\right]\left[1+s_0/n_0\tanh\left(\frac{(\delta\mu_{n-})}{\mathrm{kT}}\right)\right]$$

But,

$$P^* = s^*/n^* = \frac{\tanh\frac{(\delta\mu_{n-})}{\mathrm{kT}}+P_{0b}}{1+P_{0b}\tanh\frac{(\delta\mu_{n-})}{\mathrm{kT}}},$$

And:

$$\tanh\frac{(\delta\mu_{n-})}{\mathrm{kT}}=\frac{P-P_{0b}}{1-\mathrm{P}(P_{0b})}=\text{constant} \tag{B24}$$

The density of electron in the base-collector junction (when electron in the base and hole in the collector is considered polarized) is given by:

$$n_{bc}= n_{0/2}\ [\exp\frac{(q\delta\phi+\delta\mu\uparrow)}{kT}+\exp\frac{(q\delta\phi+\delta\mu\downarrow)}{kT}]\ [1+ s_0/n_0 \tanh\frac{(\delta\mu_{n-})}{kT}]$$

The chemical potential μ assumed constant in the depletion layer and hence it will help connect the polarization at the right and left depletion layer.

$$n_{bc}= n_{0/2}\ [\exp\frac{(q\delta\phi+\delta\mu\uparrow)}{kT}+\exp\frac{(q\delta\phi+\delta\mu\downarrow)}{kT}]\ [1+ s_{0/n0}\frac{P-P_{0b}}{1-\mathrm{P}(P_{0b})}]$$

Combining equation (B17b) with equation ((B19) density of electron in the right hand side of base collector is:

$$n_R= n_{0/2}\ [\exp\frac{(q\delta\phi+\delta\mu\uparrow)}{kT}+\exp\frac{(q\delta\phi+\delta\mu\downarrow)}{kT}]\ [1+ P_{0BR}\ (\frac{(P_L-P_{0L})}{1-P_{obL}P_L})]$$

When the collector region is considered magnetic, P_{oL}=P_{oc}. And when the collector considered nonmagnetic, P_{0L}= 0. And P_L = P_c (spin polarization of injected electron in the emitter from collector to the base). Hence,

$$n_{bc}= n_{0/2}\ [\exp\frac{(q\delta\phi+\delta\mu\uparrow)}{kT}+\exp\frac{(q\delta\phi+\delta\mu\downarrow)}{kT}]\ [1+ P_{0BR}\ (\frac{(P_c-P_{oc})}{1-P_{oc}P_c})]$$

If the δμ considered spin independent, we can set: δμ↑ = δμ↓. And as result:

$$n_{bc}= n_0 \exp\frac{(q\delta\phi+\delta\mu)}{kT}\ [1+ P_{0bR}\ (\frac{P_c-P_{oc}}{1-P_{oc}P_c})]$$

$$= \frac{(n_i^2)}{N_{ab}}\cosh\frac{q\psi_c}{kT}\exp\frac{v_{bc}}{kT}\ [1+ P_{0BR}\ (\frac{P_c-P_{oc}}{1-P_{oc}P_c})] \qquad \text{(B25)}$$

The equation in (B25) represent when all regions are doped with magnetic impurities. If the collector region is made of semiconductor material, the density of electron in the base collector region will reduced to:

$$n_{bc}= n_0 \exp\frac{v_{bc}}{kT} = \frac{(n_i^2)}{N_{ab}}\cosh\frac{q\psi_c}{kT}\exp\frac{v_{bc}}{kT}$$

The density of spin carriers in the base collector region is calculated as:

$$s^*= \exp(\frac{(q\delta\phi+\mu_{n+})}{kT})\ \ [n_0 \sinh(\frac{(\delta\mu_{n-})}{kT}) + s_0 \cosh(\frac{(\delta\mu_{n-})}{kT})]$$

Dividing the right side with $n_0 \cos\frac{(\delta\mu_{n-})}{kT}$:

$$s^*= n_0 \cosh\frac{(\delta\mu_{n-})}{kT}\exp(\frac{(q\delta\phi+\mu_{n+})}{kT})\ \ [\tanh(\frac{(\delta\mu_{n-})}{kT}) + P_{0b}]$$

Using the relation listed in equation (B24):

$$s_{bc} = n_0 \cosh \frac{(\delta\mu_{n-})}{\mathrm{kT}} \exp(\frac{(q\delta\phi + \mu_{n+})}{\mathrm{kT}}) \ [\frac{P_c - P_{oc}}{1 - P_{oc}P_c} + P_{0b}]$$

If δμ considered spin independent, we can set: δμ↑ = δμ↓. And as result:

$$S_{bc} = n_0 \exp \frac{v_{bc}}{kT} [\frac{P_c - P_{oc}}{1 - P_{oc}P_c} + P_{0b}]$$

5 calculations of emitter and collector currents

In order to calculate the currents, it is necessary to evaluate the densities of electrons in the junction due to diffusion of minority carriers. The non-equilibrium electron in the base resulted from diffusion is given by [25], [32]:

$$\frac{d^2n}{dx^2} = \frac{\mathrm{n}}{L_n{}^2} \tag{B26}$$

The solution to the above differential equation is:

$$n(x) = A \sinh (\frac{w_b - x}{L_n}) + B \sinh(\frac{x}{L_n})$$

With boundary conditions:

$n(0) = n_{be}$, $n(w_b) = n_{bc}$

$$n(x) = n_{be} \frac{(\sinh\frac{w_b - x}{L_n})}{\sinh\frac{w_b}{L_n}} + n_{bc} \frac{(\sinh\frac{w_b}{L_n})}{\sinh\frac{w_b}{L_n}} \tag{B27}$$

Then the current is:

$$\frac{dj(x)}{dx} = -qD_n \frac{dn(x)}{dx}$$

$$j^n(x) = \frac{qDn}{Ln} [n_{be} \frac{(\cosh\frac{wn - x}{Ln})}{\sinh\frac{wn}{Ln}} - n_{bc} \frac{(\cosh\frac{x}{Ln})}{\sinh\frac{wn}{Ln}}] \tag{B28}$$

At $x=0$, $j^n(0) = j^n{}_{be}$

$$j^n{}_{be} = \frac{qDn}{Ln} [n_{be} \frac{\cosh\frac{wn}{Ln}}{\sinh\frac{wn}{Ln}} - n_{bc} \frac{1}{\sinh\frac{wn}{Ln}}] \tag{B29}$$

At $x = w_b$, $j^n(w_b) = j^n{}_{bc}$

$$j^n{}_{bc} = \frac{qDp}{Ln} [(n_{be}) \frac{1}{\sinh\frac{wn}{Ln}} - n_{bc} \frac{(\cosh\frac{wn}{Ln})}{\sinh\frac{wn}{Ln}}] \tag{B30}$$

Similarly, the minority hole carrier can be calculated with simpler boundary conditions.

In the base emitter junction, the minority hole carrier can be calculated as:

$$p_e(x) = A(\sinh(\frac{x}{L_p}) + B(\sinh\frac{(w_e - x)}{L_p})$$

The boundary conditions are:

p(0)= 0, (at the contact electrode , the density of electron reduces to zero.)

And at the junction, $p\ (w_e) = p_{be}$ .Therefore,

$$p_e(x) = p_{be}\,\frac{(\sinh\frac{x}{L_p}))}{\sinh\frac{w_n}{L_p}} \qquad \text{(B31)}$$

In the collector base junction, the solution for density of hole carrier is:

$$p_c(x) = A(\sinh\frac{w_c - x}{L_p}) + B(\sinh\frac{x}{L_p})$$

With boundary conditions:

At base collector junction x = 0, p(0) = p_{bc}. And in at contact electrode x= w_c, p(w_c) = 0.

$$_c(x) = p_{bc}\,\frac{(\sinh\frac{w_c - x}{L_p}))}{\sinh\frac{w_c}{L_p}} \qquad \text{(B32)}$$

And therefore the hole emitter current is calculated as:

$$J_p = \frac{qDp}{Lp}\,\frac{dp(x)}{dx} \qquad \text{(B33)}$$

$$J^p{}_{be} = \frac{qDp}{Lp}p_{be}\,\frac{(\cosh\frac{we}{Lp}))}{\sinh\frac{we}{Lp}} \qquad \text{(B34)}$$

$$J^p{}_{bc} = -\frac{qDp}{Lp}\,p_{bc}\,\frac{(\cosh\frac{w_c}{L_p}))}{\sinh\frac{w_c}{L_p}} \qquad \text{(B35)}$$

Therefore the emitter current and collector currents are:

$$J_e = j^e{}_{be} + j^p{}_{be}$$

$$= \frac{qD_n}{L_n}\,[n_{be}\frac{(\cosh\frac{w_b}{L_n}))}{\sinh\frac{w_b}{L_n}} - n_{bc}\sinh(\frac{w_b}{L_n})] + [\frac{qD_p}{L_p}\,(p_{be})\,\frac{(\cosh\frac{w_e}{L_p}))}{\sinh\frac{w_e}{L_p}}] \qquad \text{(B36)}$$

$$J_c = j^e{}_{bc} + j^p{}_{bc}$$

$$= \frac{qD_n}{L_n}[n_{be}\,\frac{1}{\sinh\frac{w_b}{L_n}} - n_{bc}(\frac{((\cosh\frac{w_b}{L_n}))}{\sinh\frac{w_c}{L_p}})] - [\frac{qD_p}{L_p}\,p_{bc}\,\frac{(\cosh\frac{w_c}{L_p}))}{\sinh\frac{w_c}{L_p}}] \qquad \text{(B37)}$$

$$j_b = j_e - j_c$$

And current amplification factor β is:

$$\beta = \frac{j_c}{j_b} = \frac{\frac{D_n}{L_n}[\frac{n_{be}}{\sinh\frac{w_b}{L_n}} - \frac{n_{bc}}{\tanh\frac{w_b}{L_n}}] - \frac{D_p}{L_p}(\coth\frac{w_c}{L_p}) * pc}{\frac{D_n(n_{be}+n_{bc})}{L_n}[\frac{1}{\tanh\frac{w_b}{L_n}} - \frac{1}{\sinh\frac{w_b}{L_n}}] + \frac{D_p}{L_p}(\coth\frac{w_e}{L_p}) * pe + \frac{D_p}{L_p} * pc} \qquad \text{(B38)}$$

6 Energy band edges in magnetic bipolar transistor is approximated using ordinary 1st and 2nd order perturbation theory.

<u>For non-degenerate energy states</u>

First order perturbation equation [37]:

$$E_n^{(1)} = \langle (n^0)\, |H_1\, |n^0\rangle$$

where H_1 is the Hamiltonian describing perturbed eigenvalue and n^0 is unperturbed eigenstate.

And H^1 is given by [35], [34]:

$$H^1 = -V/2N \sum_R \int M_{exch}\, \delta(r - R)\, \{S^+_R\, \psi^\dagger\downarrow(r)\, \psi\uparrow(r) \;+ S^-_R\, \psi^\dagger\uparrow (r)\, \psi\downarrow(r) + (S^z_R - \langle S^z\rangle)\, [\psi^\dagger\uparrow (r)\, \psi\uparrow(r) - \psi^\dagger\downarrow (r)\, \psi\downarrow(r)\,]\, \}dr$$

where $S^+_R = S^x + S^y,\ S^-_R = S^x - S^y$

$$\psi^\dagger_\lambda (r) = 1/\sqrt{V} \sum_n a^\dagger_{n\lambda} \exp(- inr)|\lambda\rangle$$

$$\psi_\lambda (r) = 1/\sqrt{V} \sum_n a_{n\lambda} \exp(inr)|\, \lambda\rangle$$

V is the volume of a unit cell and their total number is N, λ is $\uparrow$ or $\downarrow$, $a^\dagger_n$ and a_n are creation and annihilation operator of charge carrier respectively.

And eigenstate is defined as:

$$|n\lambda\rangle = 1/\sqrt{V} \exp(inr)\, |\lambda\rangle$$

M_{exch} is exchange interaction between carrier spin and local magnetic spin varies over unit cell, $\langle S^z\rangle$ is the average spin polarization of magnetic subsystems, SR is spin operator of magnetic atom at lattice site R.

The first order correction to the band energy is:

$$E_n^{(1)} = -1/2N \int \exp(inr) * \exp(-inr)\{\int \sum_R M_{exch}\delta(r - R)\, [(S^+_R\, \psi^\dagger\downarrow(r)\, \psi\uparrow(r) \;+ S^-_R\, \psi^\dagger\uparrow (r)\, \psi\downarrow (r) \;+ (S^z_R - \langle S^z\rangle)[\psi^\dagger\uparrow(r)\, \psi\uparrow(r) \;- \psi^\dagger\downarrow (r)\, \psi\downarrow(r)\,)]\, dr\}dr$$

Using the commutation relation [41], [38] of:

$$a^\dagger_{n\uparrow}(r)\, a_{n\downarrow}(r) = ½\, \sigma^+(r)$$

$$a^\dagger_{n\downarrow}(r)\, a_{n\uparrow} (r) = ½\, \sigma^- (r)$$

$$n_{n\lambda} (r) = a^\dagger_{n\lambda}(r)\, a_{n\lambda}(r)$$

where σ is pauli spin matrice.

$\sigma^+ \;= \sigma^x + \sigma^y$ is spin raising Pauli matrice and $\sigma^- \;= \sigma^x - \sigma^y$ is spin lowering Pauli matrices

$$E_n^{(1)} = -1/(2NV) \int [\int \sum_R M_{exch}(r - R)\, \delta(r - R)\, [(S^+_R \sum_n (½\, \sigma^+) + S^-_R \sum_n (½\, \sigma^-) + (S^z_R - \langle S^z \rangle) \sum_n (n_n\uparrow - n_n\downarrow)]\, \}dr]dr$$

$$= -1/(2NV)\ [\int M_{exch} [(S^+_R \sum_n (½\, \sigma^+) + S^-_R \sum_n (½\, \sigma^-) + (S^z_R - \langle S^z \rangle) \sum_n (n_n\uparrow - n_n\downarrow)]\ \}]dr$$

$$= -R/(2NV)\ [\ M_{exch} [(S^+_R \sum_n (½\, \sigma^+) + S^-_R \sum_n (½\, \sigma^-) + (S^z_R - \langle S^z \rangle)\ (N_n\uparrow - N_n\downarrow)]\ \}$$

Using Pauli spin matrices [38]:

$$S_x = \hbar/2 \begin{pmatrix} 0 & 1 \\ 1 & 0 \end{pmatrix},\ S_y = \hbar/2 \begin{pmatrix} 0 & -i \\ i & 0 \end{pmatrix},\ S_z = \hbar/2 \begin{pmatrix} 1 & 0 \\ 0 & -1 \end{pmatrix}$$

$$\sigma^x = \begin{pmatrix} 0 & 1 \\ 1 & 0 \end{pmatrix},\ \sigma^y = \begin{pmatrix} 0 & -i \\ i & 0 \end{pmatrix},\ \sigma^z = \begin{pmatrix} 1 & 0 \\ 0 & -1 \end{pmatrix}$$

$$\sigma^- = \sigma^x - \sigma^y,\ \sigma^+ = \sigma^x + \sigma^y$$

$$S^+_R = S^{x+} S^y = \hbar/2 \begin{pmatrix} 0 & 1 \\ 1 & 0 \end{pmatrix} + \hbar/2 \begin{pmatrix} 0 & -i \\ i & 0 \end{pmatrix} = \hbar/2 \begin{pmatrix} 0 & 1-i \\ 1+i & 0 \end{pmatrix}$$

$$(S^+_R\, \sigma^-) = \hbar/2 \begin{pmatrix} 0 & 1-i \\ 1+i & 0 \end{pmatrix} [\begin{pmatrix} 0 & 1 \\ 1 & 0 \end{pmatrix} - \begin{pmatrix} 0 & -i \\ i & 0 \end{pmatrix}] = \hbar \begin{pmatrix} -i & 0 \\ 0 & i \end{pmatrix}$$

$$S^-_R\, \sigma^+\ \hbar \begin{pmatrix} -i & 0 \\ 0 & i \end{pmatrix} = -\hbar/2\, [\begin{pmatrix} 0 & 1 \\ 1 & 0 \end{pmatrix} - \begin{pmatrix} 0 & -i \\ i & 0 \end{pmatrix}]\, [\begin{pmatrix} 0 & 1 \\ 1 & 0 \end{pmatrix} + \begin{pmatrix} 0 & -i \\ i & 0 \end{pmatrix}]$$

$$= -\hbar \begin{pmatrix} i & 0 \\ 0 & -i \end{pmatrix}$$

$$(S^+_R\, ½\, \sigma^- + S^-_R\, (½\, \sigma^+) = \hbar^2 \begin{pmatrix} -i & 0 \\ 0 & i \end{pmatrix} + \begin{pmatrix} i & 0 \\ 0 & -i \end{pmatrix} = 0$$

$$E_n^{(1)} = -R/(2NV)\ [\ M_{exch} [(S^z_R - \langle S^z \rangle)\ (N_n\uparrow - N_n\downarrow)]$$

Hence the first the energy with first order correction is:

$$E = E_0 + \hbar^2 k^2/2m^* + E_n^{(1)}$$

The second order correction method calculated below.

The equation for second order correction is [37]:

$$E_n^{(2)} = \sum_{m\neq n} |\langle m^o|H_1|n^o\rangle|^2/(E^0_n - E^0_m) = \sum_{m\neq n} |\int m^o H_1 n^o)dr|^2/(E^0_n - E^0_m)$$

$$= \sum_{m\neq n} |\int \exp(-imr) \exp(inr)\, H_1)dr|^2/(E^0_n - E^0_m)$$

$$= VM^2_{exch}/2N(E^0_n - E^0_m) \sum\ |\{ \int \exp(i(n-m)r) \int \delta(r - R)\, [\, (S^+_R\, \psi^\dagger\downarrow(r)\, \psi\uparrow(r)\ + S^-_R\, \psi^\dagger\uparrow(r)\, \psi\downarrow(r) + (S^z_R - \langle S^z \rangle)[\psi^\dagger\uparrow(r)\, \psi\uparrow(r)\ + (S^z_R - \langle S^z \rangle)[\psi^\dagger\downarrow(r)\, \psi\downarrow(r)\ )]\, dr\}dr|^2$$

$$= VM^2_{exch}/2N(E^0_n - E^0_m) \sum\ |\{ \int \exp(i(n-m)r) \int \delta(r - R)\, [\, (S^+_R\, a^\dagger\downarrow(r)\, a\uparrow(r)\ + S^-_R\, a^\dagger\uparrow(r)\, a\downarrow(r)\ + (S^z_R - \langle S^z \rangle)[\, a^\dagger\uparrow(r)\, a\uparrow(r)\ - (S^z_R - \langle S^z \rangle)[a^\dagger\downarrow(r)\, a\downarrow(r))\,]\, dr\}dr|^2$$

$$= (V/2N)(E^0{}_n - E^0{}_m) \sum |\{ \int \exp(i(n\text{-}m)r) \int M_{exch} (r - R)\delta(r - R) [(S^+{}_R \tfrac{1}{2} \sigma^- + S^-{}_R (\tfrac{1}{2} \sigma^+) + (S^z{}_R - \langle S^z \rangle)[n\uparrow - n\downarrow] dr\}dr|^2$$

$$= (V/(2N(E^0{}_n - E^0{}_m))) M_{exch} \sum |\{\int \exp(i(n\text{-}m)r)[(S^+{}_R \tfrac{1}{2} \sigma^- + S^-{}_R (\tfrac{1}{2} \sigma^+) + (S^z{}_R - \langle S^z \rangle)[n\uparrow - n\downarrow\}dr|^2$$

$$= (V/(2N(E^0{}_n - E^0{}_m))) M_{exch} \sum_{m\neq n} |\{\delta(n - m) [(S^+{}_R \tfrac{1}{2} \sigma^- + S^-{}_R (\tfrac{1}{2} \sigma^+) + (S^z{}_R - \langle S^z \rangle)[n\uparrow - n\downarrow]\}|^2$$

$$= (V/(2N(E^0{}_n - E^0{}_m))) M_{exch} \sum_{m\neq n} \delta(n - m)[(S^z{}_R - \langle S^z \rangle)(n\uparrow - n\downarrow)]^2$$

$$= M^2{}_{exch}R/4(VN)^2 (E^0{}_n - E^0{}_m) \sum_n [(S^z{}_R - \langle S^z \rangle)]^2\delta(n - m) [n^2\uparrow - 2 n\uparrow n\downarrow + n^2\downarrow)]$$

$$S^z{}_R = x \langle S^z{}_{\mathbf{R}} \rangle = xSBs(y))$$

$\hbar$ is planck constant, $B_s(y)$ is Brillouin function and S is spin quantum number

$$y = gL\mu_B SB/kT,$$

where g is g factor of electron, μ_B is bohr magneton, k is boltzman constant and T is temperature.

Therefore the energy band with perturbed state is:

$$E = Eo + \hbar^2k^2/2m^* + E_n{}^{(1)} + E_n{}^{(2)}$$

where m* is effective mass

<u>For degenerate energy states</u>

First perturbation correction for two folds degeneracy:

The formula for first perturbation correction [36], [37], [34] is:

$$E^1{}_{\pm} = \tfrac{1}{2} [W_{aa} + W_{bb} \pm \sqrt{\{(W_{aa} - W_{bb})^2 + 4|W_{ab}|^2\}}]$$

where $W_{aa} = \langle \phi_a|H^1|\phi_a \rangle$, $W_{bb} = \langle \phi_b|H^1|\phi_b \rangle$, $W_{ab} = \langle \phi_a|H^1|\phi_b \rangle$, $H^1 = -V/2N \sum_R \int M_{exch}\, \delta(r - R)^* \{S^+{}_R\, \psi^\dagger\downarrow(r)\, \psi\uparrow(r) + S^-{}_R\, \psi^\dagger\uparrow (r)\, \psi\downarrow(r) + (S^z{}_R - \langle S^z \rangle)[\psi^\dagger\uparrow (r)\, \psi\uparrow(r) + \psi^\dagger\downarrow (r)\, \psi\downarrow(r)] \}dr$

$$W_{aa} = (1/2N) M_{exch}(\int(\exp(iar) * \exp(-iar)) \sum_R \int \delta(r - R) \{S^+{}_R\, \psi^\dagger\downarrow(r)\, \psi\uparrow (r) + S^-{}_R\, \psi^\dagger\uparrow (r)\, \psi\downarrow(r) + (S^z{}_R - \langle S^z \rangle)[\psi^\dagger\uparrow (r)\, \psi\uparrow(r) + \psi^\dagger\downarrow (r)\, \psi\downarrow(r)]\}dr)$$

$$= (1/2N) M_{exch}(\int_R dr \int \delta(r - R) \{S^+{}_R\, \psi^\dagger\downarrow(r)\, \psi\uparrow(r) + S^-{}_R\, \psi^\dagger\uparrow (r)\, \psi\downarrow(r) + (S^z{}_R - \langle S^z \rangle)[\psi^\dagger\uparrow (r) * \psi\uparrow(r) - \psi^\dagger\downarrow (r)\, \psi\downarrow (r)]\}dr)$$

In the non-degenerate case, it was obtained:

$$(S^+{}_R \tfrac{1}{2} \sigma^- + S^-{}_R (\tfrac{1}{2} \sigma^+) = 0$$

And using the commutation relation [41], [38]:

$$a^{\dagger}_{n\uparrow}(r_\alpha)\, a_{n\downarrow}(r_\alpha) = \tfrac{1}{2}\, \sigma^{+}(r_\alpha)$$

$$a^{\dagger}_{n\downarrow}(r_\alpha)\, a_{n\uparrow}(r_\alpha) = \tfrac{1}{2}\, \sigma^{-}(r_\alpha)$$

$$n_{n\lambda}(r_\alpha) = a^{\dagger}_{n\lambda}(r_\alpha)\, a_{n\lambda}(r_\alpha)$$

$$W_{aa} = (1/(2N))\, M_{exch}(\int_R dr \int \delta(r - R)\ (S^z_R - \langle S^z\rangle)[\psi^{\dagger}\uparrow (r)\, \psi\uparrow + \psi^{\dagger}\downarrow (r)\, \psi\downarrow]\, dr)$$

$$= (1/(2VN))\, M_{exch}(\int_R dr \int \delta(r - R)\ (S^z_R - \langle S^z\rangle)[a^{\dagger}\uparrow (r)\, a\uparrow - a^{\dagger}\downarrow (r)\, a\downarrow]\, dr)$$

$$= (R/(2VN))\, M_{exch}(\ (S^z_R - \langle S^z\rangle)[n_a\uparrow - n_a\downarrow]\ )$$

Similarly W_{bb} and W_{ab} are:

$$W_{bb} = (R/(2VN))\, M_{exch}\, (S^z_R - \langle S^z\rangle)[n_b\uparrow - n_b\downarrow]$$

$$W_{ab} = (1/(2N))\, (\int\{(\exp(-iar)\exp(ibr)) \sum_R \int M_{exch}\,(r - R)\delta(r - R)dr\, (S^z_R - \langle S^z\rangle)\, [\, a_a^{\dagger}\uparrow(r)\, a_a\uparrow - a_b^{\dagger}\downarrow (r)\, a_a\downarrow]\, \}dr$$

$$= (1/2N)\, (\int\{(\exp(-iar) * \exp(ibr))\sum_R \int M_{exch}\, \delta(r - R)\, (S^z_R - \langle S^z\rangle)[n_{a,}\uparrow - n_a\downarrow])\, dr\}dr$$

$$= (1/(2VN))\, M_{exch}\, \delta(b\text{-}a)\, (S^z_R - \langle S^z\rangle)[n_{a,}\uparrow - n_a\downarrow]$$

$$W_{aa} + W_{bb} = (R/(2VN))\, M_{exch}(\ (S^z_R - \langle S^z\rangle)\{[n_a\uparrow - n_a\downarrow] + [n_b\uparrow - n_b\downarrow]\}$$

$$(W_{aa} - W_{bb})^2 = [(R/(2VN))\, M_{exch}]^2(\ (S^z_R - \langle S^z\rangle)^2[(n_a\uparrow - n_a\downarrow) - (n_b\uparrow - n_b\downarrow)]^2$$

$$= [(R/(2VN))\, M_{exch}]^2\, (\ (S^z_R - \langle S^z\rangle)^2\, \{n^2{}_a\uparrow + n^2{}_b\uparrow + n^2{}_a\downarrow + n^2{}_b\downarrow - n_{a,b}\uparrow - n_{a,b}\downarrow\}$$

$$E^1{}_\pm = [(R/(2VN))\, M_{exch}]\, (S^z_R - \langle S^z\rangle)\, \{[n_a\uparrow - n_a\downarrow] + [n_b\uparrow - n_b\downarrow] \pm \sqrt{}(n^2{}_a\uparrow - n^2{}_b\uparrow + n^2{}_a\downarrow - n^2{}_b\downarrow - n_{a,b}\uparrow - n_{a,b}\downarrow) + 2\delta(b\text{-}a)\, [n^2{}_{a,}\uparrow + n^2{}_a\downarrow + 2n_{a,}\uparrow\, n_a\downarrow]\}$$

Thus the energy with correction is:

$$E = Eo + \hbar^2 k^2/2m^* + E^{(1)}{}_\pm$$

7. Parameters inserted into equations in section 3.3

1. Resistors values

R4 = R8 = R12 =1k ohm

R1= R5 = R9 = Rs= 47k ohm

R2 = R6 = R10 =10k ohm

R3 = R7 = R11= 4.7 k ohm

2. Input voltage

$$V_s = 100uv$$

3. Transistor's doping concentration content

To calculate the emitter current, the cross-sectional area of emitter is taken as 17um and

$L_p = L_s = 10um$, $L_n = 30um$, $\alpha_{ob} = 0.9$, $W_e = W_c = 2um$, $W_b = 1.5um$, $n_i = 1.5 * 10^{10}\ cm^3$, $N_e = 10^{17}\ cm^3$, $N_b = 10^{16}\ cm^3$, $N_c = 10^{16}\ cm^3$, D_n=100, $D_p = 10cm^2/s$, $V_{be} = 0.5\ v$, $V_{bc} = 0\ v$